INTERNATIONAL ATOMIC ENERGY AGENCY
UNITED NATIONS EDUCATIONAL, SCIENTIFIC AND CULTURAL ORGANIZATION
INTERNATIONAL CENTRE FOR THEORETICAL PHYSICS
I.C.T.P., P.O. BOX 586, 34100 TRIESTE, ITALY, CABLE CENTRATOM TRIESTE

H4.SMR/453-26

TRAINING COLLEGE ON PHYSICS AND CHARACTERIZATION OF LASERS AND OPTICAL FIBRES

(5 February - 2 March 1990)

OPTOGALVANIC SPECTROSCOPY

A. Sasso

Università di Napoli
Dipartimento di Scienze Fisiche
80125 Napoli

IL NUOVO CIMENTO

rivista internazionale di fisica

fondata a Pisa nel 1855 da C. MATTEUCCI e R. PIRIA
dal 1897 Organo della Società Italiana di Fisica

pubblicata
sotto gli auspici del Consiglio Nazionale delle Ricerche

a cura del Direttore
RENATO ANGELO RICCI
Presidente della Società

e dei Vicedirettori
R. R. GATTO e P. PICCHI

La collaborazione alla *Rivista del Nuovo Cimento* è esclusivamente su invito. I lavori possono essere scritti in francese, inglese, italiano, spagnolo o tedesco.

Si prega vivamente d'inviare i lavori destinati alla pubblicazione, in duplice copia, direttamente al **Direttore del Nuovo Cimento, via degli Andalò, 2 - 40124 Bologna**. Ciascuna copia, scritta a macchina su un solo lato del foglio, deve essere corredata di disegni, fotografie e bibliografia con i nomi e le iniziali di tutti gli autori; una serie di disegni originali in inchiostro di China su carta da lucidi deve essere allegata alle copie del lavoro; le eventuali fotografie devono essere stampate su carta bianca lucida pesante. Non si accettano manoscritti in una sola copia od incompleti. I manoscritti non si restituiscono.

Di regola le bozze sono inviate agli autori una sola volta, salvo che siano state esplicitamente richieste seconde bozze.

Gli autori non hanno spese di pubblicazione, salvo quelle per le correzioni dovute ad insufficienze del manoscritto inviato per la pubblicazione, modifiche del testo originario, modifiche o rifacimenti di figure, ecc.

Gli estratti (eventualmente con copertine stampate e montate apposta) possono essere forniti a richiesta secondo la tariffa che la Redazione comunicherà agl'interessati. L'importo degli estratti assieme a quello per le correzioni straordinarie sarà fatturato dall'**Editrice Compositori, via Stalingrado, 97/2 - 40128 Bologna**.

Norme più dettagliate si trovano nella «Guida per gli Autori», che viene inviata dietro versamento di L. 1.000.

Contribution to *Rivista del Nuovo Cimento* is by invitation only. Papers may be written in English, French, German, Italian or Spanish.

Manuscripts submitted for publication should be sent in triplicate and only to **The Director of Il Nuovo Cimento, via degli Andalò, 2 - I 40124 Bologna (Italy)**. Each copy, typewritten on one side of the sheets only, must be complete with drawings, photographs and references with the names and initials of all the authors; a set of original drawings in India ink on tracing paper must be enclosed with the copies of the manuscript; photographs must be on heavy-weight glossy white paper. Manuscripts either in single copies or incomplete will not be accepted. Manuscripts will not be returned.

Proofs will be sent only once unless second proofs are specifically requested for by the author.

Authors will be charged only for corrections due to lack of clarity of the manuscript submitted, modifications to the original text, modifications or remaking of figures, etc.

Reprints as well as covers printed to order may be supplied on payment. The Editorial Office will give the corresponding prices on request. The cost of the reprints and the charges for corrections will be invoiced by **Editrice Compositori, via Stalingrado, 97/2 - I 40128 Bologna (Italy)**.

Further details are contained in the «Guide for the Authors», which will be sent against payment of US $ 1.00.

Direzione e Redazione **Via degli Andalò, 2 40124 Bologna**

K. ERNST and M. INGUSCIO

Unconventional Techniques in Laser Spectroscopy.

Unconventional Techniques in Laser Spectroscopy.

K. ERNST

Institute of Experimental Physics, Warsaw University - Warsaw, Poland

M. INGUSCIO

Dipartimento di Scienze Fisiche, Università di Napoli 80125, Napoli, Italy

(ricevuto il 21 Luglio 1986)

1. – Conventional and unconventional techniques.

The subject and the aim of the present work are in a way summarized in fig. 1, where the same region of the spectrum of excited neon atoms, but obtained using three different detection techniques, is shown. The first spectrum (*a*)) is

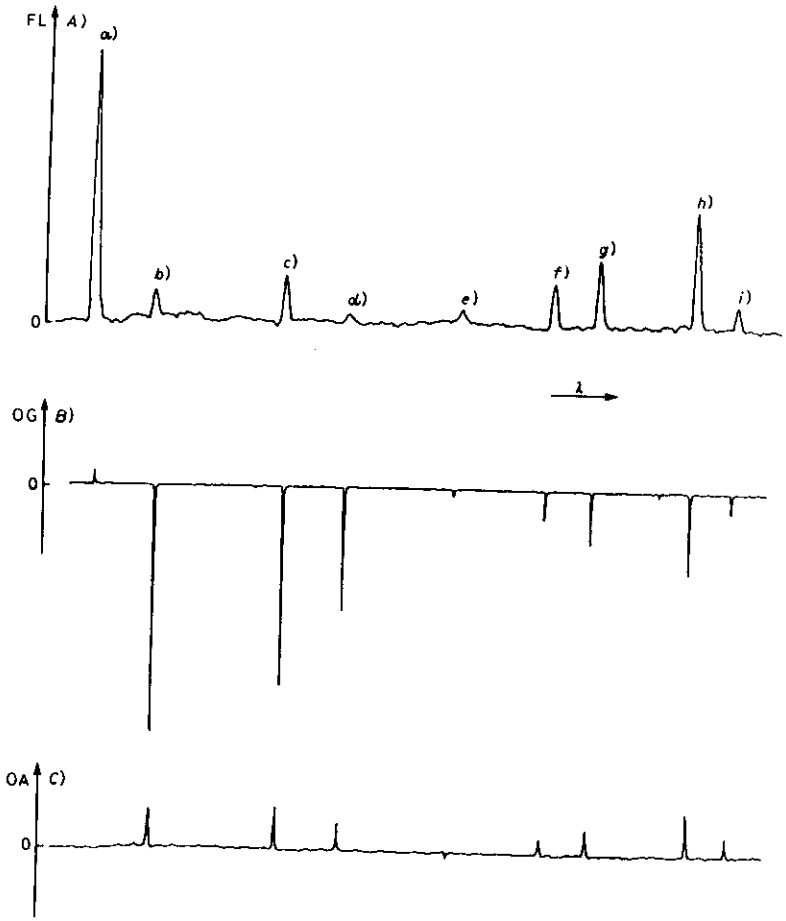

Fig. 1. – Transitions in neon from 560 to 620 nm. The atomic gas at pressure of 2 Torr is excited in a d.c. discharge ($i = 3$ mA). The fluorescence spectrum is recorded in *A*). When the discarge is irradiated by a tunable laser source, the spectral lines are recorded as changes in the current (*B*)) and by detecting acoustic signal (*C*)). Wavelengths corresponding to observed transitions are: *a*) 585.2, *b*) 588.2, *c*) 594.5, *d*) 597.6, *e*) 603.0, *f*) 607.4, *g*) 609.6, *h*) 614.3, *i*) 616.4 nm. *A*) and *B*) recordings are from [1], and *C*) recording is from [2].

obtained as usual by detecting the emitted photons, while the others two are recorded by means of optoacoustic (*b*)) and optogalvanic (*c*)) techniques. In the case of the emission spectrum, the whole information on the interaction between radiation and matter is obtained through the observation of fluorescence radiation. A slightly different experimental configuration could be used replacing the detection of the emitted light by detection of either transmitted or scattered light, hence providing various spectroscopic information about atoms and molecules. The feature commom to these techniques is that all we learn about atomic and molecular systems comes from the observed radiation. This detection method has dominated in spectroscopy from its very beginning and we shall refer to it as «conventional».

Comparing spectra recorded by means of optoacoustic and optogalvanic techniques with conventional ones, one can note that they are identical as far as positions of lines corresponding to different atomic transitions are concerned. On the other hand, some other features, as for example relative intensities and signs, are different. That is due to completely different physical effects leading to each of the recorded signals. The optoacoustic (OA), also called photoacoustic, and optogalvanic (OG) techniques conceptually differ from conventional techniques in that, in principle, no radiation detection devices are necessary and the detection system has to be quite different. This is one of the reasons why we shall call those techniques unconventional ones. In both of them, *microscopic processes* as atom-photon and molecule-photon interactions are revealed by means of *macroscopic* changes in the reaction of the system, as a whole. Instead of measuring the intensity of radiation interacting with the system, we measure now macroscopic physical quantities such as pressure, temperature and current.

The idea of investigating the interaction with radiation by looking at macroscopic changes in the matter is not new and not only limited to spectroscopic studies. For instance, the absorption of circuarly polarized photons by a magnetic-resonance experiment was early investigated in Pisa [3] using the sample itself as a detector. In fact, the macroscopic couple of force acting on the sample causes its torsional oscillations.

The unconventional name used for the OA and OG detection techniques has also historical reasons. Both the effects have been known for many decades but nobody thought about their applications in the period of pre-laser spectroscopy. Only when combined with laser sources, these two formerly abandoned techniques re-appeared as new and powerful tools for spectroscopy. Hundreds of papers on their applications have been published in the past years and a large variety of problems has been investigated.

The goal of the present paper is to describe the mechanisms of both OA and OG effects and to show how they can be successfully applied to many different problems in laser spectroscopy and related topics. We will also discuss both unconventional detection techniques from the point of view of their advantages and limitations with respect to other techniques.

2. – Optoacoustic effect.

The optoacoustic effect was observed for the first time more than one century ago [4-6]. In those experiments, acoustic waves were generated by absorption of incoming electromagnetic radiation. In the first optoacoustic experiments, a chopped sunlight was absorbed by a sample contained in a cell. Resulting periodic heating of the sample generated an acoustic wave at chopping frequency and the sound could be heard through the listening tube mounted on the cell [4] or using a cautchouc tube inserted in the ear [5]. Bell called his new device «photophone» and using its sophisticated version he was also able to distinguish words and sentences spoken into the transmitter. He concludes his paper [4] with the following prediction: «I anticipate that it has a wide and independent field of usefulness in the investigation of absorption spectra in the ultra-red». Now we can verify how accurate and foreseeing was this prediction declared one hundred years ago.

By measuring the acoustic disturbance, various information about absorbing sample can be obtained. There is, however, a fundamental condition which has to be satisfied: at least a part of energy absorbed by a sample has to be transferred into heat through collisional relaxation processes.

The optoacoustic effect was observed in solids, liquids and gases but in the present paper we will limit our considerations to the application of the OA technique to gas phase only. If we compare the output (acoustic) energy and input (radiation) energy, the conversion factor determined by their ratio turns out to be very low. The effect is then very weak. However, due to the high sensitivity of microphones used as acoustic detectors and due to spectral brightness and tunability of lasers used as light sources the optoacoustic technique became a very powerful spectroscopic tool. Three monographs [7-9] and several review papers [10-15] were devoted to the optoacoustic technique and its application to spectroscopy. It has been also the subject of three conferences [16-18].

In the following, we will recall the physical model and discuss the most significant spectroscopic applications of the OA effect.

2·1. *The physical model.* – The detection of absorption by means of a microphone can be understood as a sequence of processes as schematically shown in fig. 2.

Optical absorption is the first step. Let us consider an experimental situation in which a sinusoidally amplitude-modulated light beam propagates along the axis of a cylindrical cell containing an absorbing gas. As mentioned before, in order to observe the optoacoustic effect the energy absorbed by a gas sample has to be transferred through collisions into heat. Such a process can occur for molecular gases only due to V-T collisional relaxations. We assume then a molecular gas system and consider low absorption corresponding to the optical

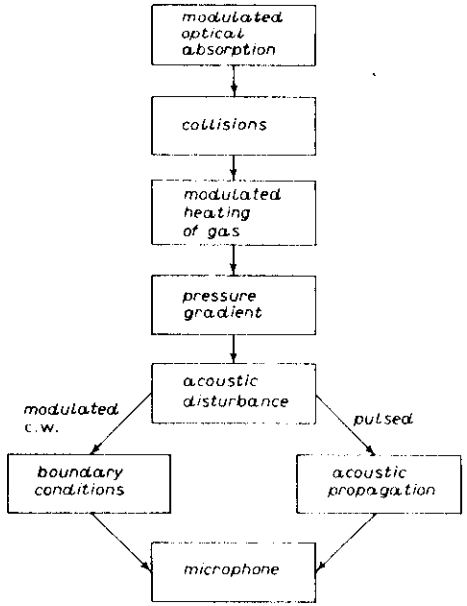

Fig. 2. – Schematical model of physical processes involved in the generation of acoustic signals originated by absorption of radiation in gases.

transition between levels of energies E_1 and E_2. That means that population of higher-level E_2 is small with respect to the lower, say, the ground state. For this situation, the rate equation for the level excited by radiation can be simply written [14]

$$\frac{\mathrm{d}N_2}{\mathrm{d}t} = N_1 R_e - N_2(A_r + A_c)\,, \tag{1}$$

where N_1 and N_2 are the concentrations corresponding to lower and higher-energy levels, respectively, R_e is the excitation rate.

The second term on the right takes into account two possible mechanisms of de-excitation of the upper level: radiative with a rate constant A_r and collisional with a rate constant A_c. The latter is responsible for the transfer of absorbed energy into translational energy of molecules.

In the simplest case, when the modulation frequency of the incident light is low with respect to the decay rate of the excited state, we can solve eq. (1) for steady-state conditions, what gives for N_2

$$N_2(r, t) = \frac{N_1 R_e}{A_r + A_c} = \frac{N_1 \varphi(r, t)\sigma}{A_r + A_c}\,, \tag{2}$$

where K_c is expressed as the product of the photon flux φ which depends on position r and time t, and absorption cross-section σ. The collisional energy transfer leads to the heat production at a rate (energy per unit time)

$$H(r, t) = N_2(r, t) A_c E . \tag{3}$$

Using eq. (2) we have

$$H(r, t) = \frac{N_1 \varphi(r, t) \sigma A_c E}{A_r + A_c}, \tag{4}$$

where E is the energy released due to collisional relaxation of molecules. For a molecule relaxing nonradiatively to the initial state, E is simply equal to $E_2 - E_1$. The heat generated in a gas sample is then proportional to the molecular concentration (gas pressure), photon flux (light intensity), absorption cross-section, collisional decay rate and energy released through nonradiative channel. It is worthwhile to note that temporal dependence of the released heat follows exactly that of the light intensity.

If the modulation frequency does not satisfy the condition of being low with respect to the decay rate of the excited state, the temporal dependence of φ must be taken into account to solve eq. (1). Assuming a sinusoidally modulated photon flux

$$\varphi = \varphi_0 [1 + \exp[i\omega t]], \tag{5}$$

we have as a solution of eq. (1)

$$N_2 = \frac{N_1 \varphi_0 \sigma}{(A_r + A_c)(1 + \omega^2 t^2)^{1/2}} \exp[i(\omega t - \psi)], \tag{6}$$

where $\psi = \mathrm{tg}^{-1}(\omega \tau)$ is the phase lag of N_2 with respect to φ. The heat produced is given now by substituting (6) in (3)

$$H(r, t) = \frac{N_1 \varphi_0 \sigma A_c E}{(A_r + A_c)(1 + \omega^2 t^2)^{1/2}} \exp[i(\omega t - \psi)]. \tag{7}$$

As a next step of our scheme we have to consider the expansion of the heated volume due to the radial temperature gradient created in the gas. As a consequence, a pressure wave propagates outwardly from the axis of the cell. This results in an acoustic disturbance which propagates in the gas medium. Two different cases must be distinguished: c.w. modulated excitation and pulsed excitation. The propagation process may be described by the inhomogeneous

wave equation which for the cylindrical symmetry has the following form:

$$\frac{\partial^2 p}{\partial t^2} - c^2 \left(\frac{\partial^2 p}{\partial r^2} + \frac{1}{r} \frac{\partial p}{\partial r} \right) = (\gamma - 1) \frac{\partial H}{\partial t}. \tag{8}$$

H represents the heat source, p the pressure, c is the speed of sound and γ is the ratio of specific heats for the gas. Equation (8) can be derived from the equation of mass, momentum and energy conservation neglecting molecular-diffusion effect.

The procedure for the solution of this equation is presented by Tam in [14]. The final solution depends on boundary conditions and is obtained under the assumption of optically thin absorbing medium, leading to purely radial propagation. The OA signal for the modulated c.w. excitation is larger for larger value of γ, larger light absorption power and smaller cell volume.

Let us consider now the case of the OA signal generation by pulsed excitation. In almost all experimental situations the time of pulse duration Δt is much shorter than collisional decay times of excited states and excitation process may be considered as an instantaneous deposition of energy ($\Delta t = 0$). On the other hand, the time of heat releasing, being directly dependent on collisional decay time, is generally shorter than time in which the generated acoustic disturbance reaches the microphone.

An example of the microphone output shown in fig. 3 demonstrates the complexity of the pulsed OA signal. If we then measure only the first OA signal peak (connected to the acoustic disturbance coming directly from the illuminated volume), we can neglect all secondary processes as resonances, reflections and interferences which means that boundary conditions are unimportant. Neglecting also the process of heat diffusion, which is much slower than the process of collisional relaxation of the excited state, we have for temporal evolution of the released heat [14]

$$H_p(t) = \frac{W A_c E}{A_c + A_r} \left[1 - \exp\left[-\frac{t}{\tau} \right] \right], \tag{9}$$

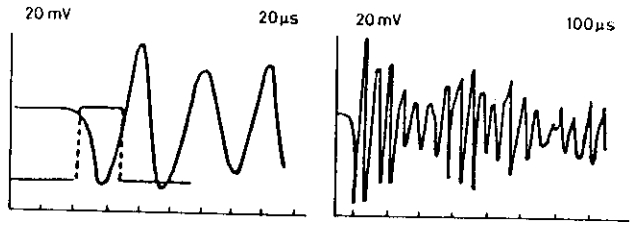

Fig. 3. – Typical oscilloscope trace of the OA signal for a single laser pulse. From [66].

W is the number of photons absorbed during the pulse, τ is the lifetime of the excited state equal to $(A_r + A_c)^{-1}$and H_p is now expressed in energy units.

The expansion of irradiated volume V of gas leads to the pressure increase $p(t)$ which can be calculated from the ideal-gas law

$$p(t) = \frac{H_p(t)R}{MC_V V}, \tag{10}$$

where R is the gas constant, M is the molecular weight and C_V the specific heat at constant volume.

We can also estimate [19] how the first OA peak depends on the radius of the illuminated cylindrical volume and on its distance from the microphone. The volume V to be considered determined by the radius R_b of the laser beam and the length L of the cell is equal to $\pi R_b^2 L$. The absorption of the laser pulse and the subsequent heat (H_p) release lead to the rise of temperature

$$\Delta T = \frac{H_p}{\rho V C_p} \tag{11}$$

and to the isobarical expansion of the illuminated volume described by equation

$$\pi(R_b + \Delta R_b)^2 L - \pi R_b^2 L = \beta V \Delta T. \tag{12}$$

ρ is the density of gas, C_p the specific heat at constant pressure, β the expansion coefficient and ΔR_b the increase of the radius of the illuminated volume.

Assuming that all absorbed energy is transferred into heat we have

$$H_p = E_l \alpha L, \tag{13}$$

where E_l is the laser pulse energy and α the absorption coefficient.

Equations (11)-(13) and the assumption $\Delta R_b \ll R_b$ lead to the following form for ΔR_b:

$$\Delta R_b = \frac{\beta E_l \alpha}{2\pi R_b \rho C_p}. \tag{14}$$

Because of the conservation of acoustic energy, the peak displacement $U(r)$ measured at distance r and for a cylindrical acoustic wave propagating perpendicularly to its axis may be expressed as follows:

$$U(r) = \Delta R_b \left(\frac{R_b}{r}\right)^{1/2}. \tag{15}$$

Using the relation between the peak acoustic pressure $p(r)$ and the peak

displacement $U(r)$ [19]

$$p(r) = c\rho U(r)/\tau_l, \tag{16}$$

we get

$$p(r) = \frac{\beta c E_l \alpha}{2\pi R_b^{1/2} C_p r^{1/2} \tau_l}, \tag{17}$$

where c is the speed of sound and τ_l the laser pulse width. Equation (17) is valid only for sufficiently small R_b values in order to justify our assumption that illuminated volume expands isobarically immediately after the laser pulse. This condition is satisfied for $R_b < c\tau_l$. In the opposite case ($R_b > c\tau_l$), the pressure increase at the heated cylinder surface takes place after absorption of the laser pulse and the peak acoustic pressure measured at distance r is given by [19]

$$p'(r) = \frac{\beta c^2 E_l \alpha}{\pi R_b^{3/2} C_p r^{1/2}}. \tag{18}$$

As we can see from eqs. (17) and (18) in both cases (small and big radius of the heated volume) the measured acoustic peak pressure p is proportional to the laser pulse energy. Since the acoustic energy is proportional to p^2, the efficiency η of OA detection techniques defined as a ratio of output to input energy has a linear dependence on E_l

$$\eta = \frac{E_{ac}}{E_l} \sim \frac{E_l^2}{E_l} \sim E_l. \tag{19}$$

All above calculations in the case of pulsed OA signals were limited to the usual techniques of choosing the first signal peak which is only a small part of the total «ringing» signal arising from multiple reflections, resonances, absorption by the cell windows etc. Chin *et al.* [20] discuss the origin of complex pulsed OA signal showing also in a simple qualitative way the proportionality of the first peak OA signal to the absorbed energy.

Instead of the first peak, the envelope of the total ringing signal can be also used as a measure of the absorption.

Let us conclude our theoretical analysis with some remarks concerning general features of both c.w. and pulsed OA techniques. Because of the spectral characteristics (linewidth) of laser sources, the modulated c.w. excitation is mostly used when spectral resolution is required. On the other hand, when we need high-temporal resolution, the pulsed OA method is usually applied. Especially in the case of fast processes real-time measurements have several advantages over the phase shift measurements. Due to higher-conversion efficiency into acoustic energy, the pulsed technique gives usually higher

detection sensitivity at the same average power of exciting source and may have considerable advantage over c.w. technique in particular for weakly absorbing sample. Another advantage of the pulsed technique is that it can be widely applied to nonlinear processes requiring high light intensity.

2·2. *Experimental arrangement.* – Any experimental arrangement built for optoacoustic measurements consists of three fundamental sections: *a*) light source (including modulator in the case of c.w. radiation), *b*) optoacoustic cell (including microphone), *c*) electronic channel for signal processing. A detailed description of OA detection systems is given in [13-15]. We would like to present here some chosen aspects which may be useful for further discussion concerning the applications of the OA technique.

Lasers offer many advantages over conventional light sources. First of all, their spectral brightness can be several orders of magnitude higher than that obtainable with systems combining lamps and monochromators. The cylindrical symmetry of laser beam is in perfect accord with radial propagation of acoustic waves in cylindrical cells typically used in OA experiments. Due to the high degree of directionality, the output light may be easily focused producing high-power densities. This is of particular importance when nonlinear effects have to be measured. Lasers offer also possibility of generation of very short light pulses allowing to perform OA measurements even in picosecond domain [21]. Finally, the tunability of lasers, even if limited to certain spectral ranges is of great importance in all spectroscopic studies. The laser sources typically used in infrared region are CO_2 lasers (close to 10 μm) having many lines coinciding with absorption lines of various molecules, and spin flip Raman laser (close to 5 μm) pumped by a CO laser. In the visible range tunable dye lasers are mainly used.

Another advantage offered by lasers is that the intracavity technique may be applied to measure very weak absorptions [22-25]. Recently, a broad-band investigation of trace amounts throughout the mid-infrared region was performed using solid-state lead salt diode lasers [26].

The light coming from a c.w. laser has to be modulated before reaching an OA cell. Mechanical choppers operating easily up to frequencies of several kHz and giving 100% amplitude modulation depth satisfy generally all the requirements and are commonly used. The only pratical disadvantage of amplitude modulation is a background signal due to windows absorption generated at the same frequency. This inconvenience can be overcome by using frequency modulation as it was successfully demonstrated by Kreuzer and Patel [27].

Modulated or pulsed laser light passing through absorbing gas sample generates time-dependent temperature changes and subsequently pressure waves propagating outwardly from the heated volume. The gas is contained in the OA cell with a built-in microphone in order to detect the acoustic signal. For

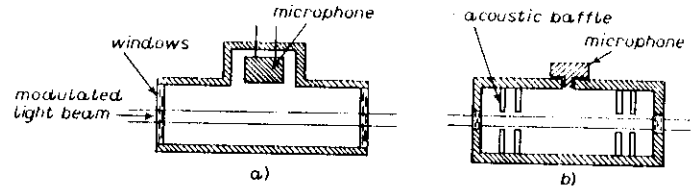

Fig. 4. – Two types of OA cells for measurements in gases. The simplest scheme is presented in *a*), while in *b*) «acoustic baffles» have been introduced in order to minimize windows absorption effect. From [14].

measuring strong absorptions the simplest cell construction as shown in fig. 4*a*) is completely satisfactory.

However, dealing with low absorptions, particular care has to be taken in order to minimize background signals. In most cases, those signals arise from absorption by cell windows. A subsequent increase of their temperature is transferred to the gas sample producing an additional acoustic signal. This «window» effect may be substantially reduced by introducing in the cell the so-called acoustic buffles as proposed in [28] and shown in fig. 4*b*). The laser beam can pass undisturbed through small apertures but acoustic waves generated by windows are strongly dumped. Any imperfection of window surface (dirt, scratch) produces also scattered light which can hit directly the microphone or the cell surface very close to it. The buffles made of absorbing material eliminate such a signal by cutting off the scattered light. Another construction [29] consists of adding two buffer sphere volumes near the Brewster windows. They are very effective in isolating the laser noise at the windows and allow a tenfold decrease of the background signal.

Particular care has to be taken in preparing cells used for intracavity measurements. This technique applied for very weak absorptions requires samples introducing very small losses into the laser cavity. High-quality Brewster windows are then necessary. It is also possible to operate the resonant cell with no windows at all [30, 31]. Absence of windows certainly solves the insertion loss and the window-heating problem but it degrades the quality factor of acoustic cavity resonance and increases the ambient acoustic noise.

One way to improve the performances of the OA cell consists then in minimizing all background signals. Another way leading to higher signal/noise ratio is to increase the signal itself. One of the solutions consists in multipass arrangement in which focused laser radiation travels across the cell several times after being reflected by two spherical mirrors placed outside the cell [32]. Absorption by a gas sample is ruoghly proportional to the number of passes of laser pulse through the cell.

In a typical geometry with laser beam along the cylinder axis, microphone is placed in such a way to receive the signal propagating perpendicularly to the axis

of the cell. «Inverted» cylindrical configuration was also investigated [33]. The laser beam perpendicular to the cell axis was reflected many times due to opportune coating of the side walls and the microphone detected the signal propagating along the cylinder axis.

The second way leading to the increase of sensitivity of the OA systems is the resonant enhancement of the signal by choosing properly modulation frequency for given dimensions of the cell. In the cylindrical symmetry with the laser beam propagating along the axis of the cell and without the temperature gradient along this axis (weak absorption) only radial resonance modes may be strongly excited. On the other hand, the configuration with laser beam perpendicular to the axis of the cell allows longitudinal modes to be excited. Detailed discussion on advantages of both resonant and nonresonant techniques may be found elsewere [14].

Microphones typically used for detecting the OA signal may be divided into two classes. Pressure variations can lead to the change of capacitance between a diaphragm being in contact with a gas and fixed metal plate, and to subsequent voltage signal. This is the principle of operation of condenser microphones. A different mechanism is used for producing electric signals in electret microphones. In this case a change in polarization of the electret material is responsible for transforming pressure waves into a measured voltage signal. Both types of microphones have been successfully and widely used in OA measurements. In order to enhance the signal, several microphones can be mounted into the cell and a partial output can be electronically summed [34]. Due

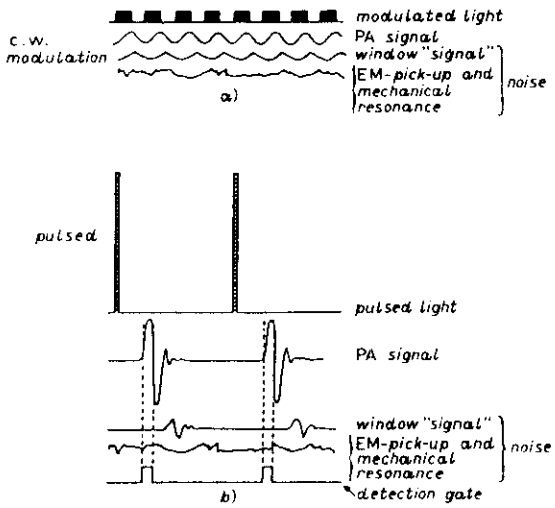

Fig. 5. – Schematic comparison of the c.w.-modulated OA method (*a*)) and the pulsed OA method (*b*)). From [19].

to their miniature size the electret microphones are particularly suited for such a sensitivity enhancement of the OA cell.

Finally, we would like to mention the electronic-signal processing channel being the third section of a typical OA set-up. In the c.w.-modulated technique OA signals produced inside the cell are detected by a lock-in amplifier. Their intensities are proportional to the absorption by gas, while the phase-lag may provide information about collisional relaxation rates.

In the pulsed case, the OA signal is detected by a box-car integrator, wave form eductor or transient digitizer. Properly chosen delay and width of the detection gate allow to select the OA signal due to absorption by gas and to discriminate background signals coming from window absorption and multiple reflection having different delay times. Figure 5 summarizes qualitatively the difference between c.w.-modulated and pulsed OA techniques as for signal and noise production and handling.

3. – High-sensitivity optoacoustic spectroscopy.

3·1. *Weak absorptions.* – Development of high-power tunable lasers and advances in the OA cell design have made possible the measurements of extremely weak absorption transitions. One of the earliest applications of the OA spectroscopy which has proven to be a highly sensitive detection method was the identification and measurements of trace constituents in gas mixtures and in particular measurements of air pollution [27, 36, 37].

The main problem of detection of pollutants by conventional absorption measurements is that for typical pollutant concentrations of 1 p.p.m. or less at atmospheric pressure, the absorption is too small to be measured by direct determination of transmission through reasonable path length. The minimum detectable concentration varies for different atmospheric pollutants depending on absorption coefficient of molecular transitions as well as on the intensity of available laser line overlapping with that transition. Data on detectable sensitivities for various molecular gases are given in [13]. The OA technique is sensitive to detect a concentration of less than 1 p.p.b. in air samples as it was measured for SF_6 [13], SO_2 [37], NO_2 [35].

Besides very low absorption, another problem arises in relation to the selectivity of this method. A sufficient resolution of the laser source is required in order to distinguish between pollutant absorption and interfering absorption. When measuring trace amounts of pollutants the absorption is due to the gas at extremely low partial pressure. The generated acoustic disturbance is detectable because it propagates in a high-pressure medium (atmosphere).

A very spectacular experiment was performed by Patel [38] who measured the stratospheric concentration of NO using the OA technique with a spin-flip Raman laser as a source of tunable infrared radiation. Monitoring of NO

concentration is one of the very important objectives for the stratospheric reduction of ozone and the subsequent increase in the UV radiation reaching the Earth. NO is produced either due to photodissociation of NO_2 or by reaction of NO_2 with atomic oxygen. Both reactions require then UV radiation and NO concentration should depend on solar operation. The experimental set-up consisting of SFR laser, CO pump laser, OA absorption cell, associated electronics and minicomputer controlling the experiment was mounted inside the flight vessel and transported by a balloon at the altitude of 28 km. SFRL tuned to one of the NO absorbing lines close to 1827 cm^{-1} allowed to measure the OA signal due to absorption by NO molecules. Its pre-sunrise concentration as low as $(1.5 \cdot 10^8)$ mol/cm^3 corresponding to volumetric mixing ratio of 0.02 p.p.b. could be detected. Moreover, real-time evolution of NO concentration could be measured.

3·2. *Excited states.* – The OA technique, being very convenient for trace detection of absorbing gases, can be also used for spectroscopic measurements of excited states which can be considered trace amounts in a gas system. Excited states may be populated by electric discharge [39], optical absorption [34] or collisional energy transfer [40]. It is worth noting that population originating from Boltzmannian distribution at room temperature can be sufficient to produce significant optoacoustic signals from levels separated by a few thousand cm^{-1} from the ground state.

The technique which involves molecular vibrational energy transfer was applied to the study of $v = 1 \rightarrow v = 2$ vibration-rotational transitions of ^{15}NO. The technique uses a coincidence of one of the CO-laser lines with one of the vibration-rotational transitions of ^{14}NO leading to excitation to the first vibrational level. In a mixture containing ^{14}NO and ^{15}NO the excitation is then collisionally transferred to ^{15}NO molecules. No other suitable and selective technique is available to populate the $v = 1$ state of ^{15}NO molecule. This method of preparing excited molecular states is quite efficient, since the mismatch of energy levels involved may be even as large as several times kT. Measurements of absorbing transitions from excited vibrational level $v = 1$ may be performed for both ^{14}NO and ^{15}NO molecules using two collinear beams of CO laser (exciting ^{14}NO molecules to $v = 1$ level) and CO laser pumped tunable SFR laser (exciting transitions from $v = 1$ level for both isotopic species). The OA signal due to absorption by ^{15}NO molecules can be easily distinguished, since it disappears when the cell contains ^{14}NO only.

3·3. *Overtone spectroscopy.* – Another example of weak absorption successfully observed by means of OA technique is the spectroscopy of overtone transitions. Experimentally, the «forbidden» nature of high-overtone and combination band transitions in gas phase usually restricts spectroscopic studies to very high pressures. Information about isolated molecule dynamics is then

lost, since line shapes and overall band contours are determined primarily by intermolecular interactions. Intracavity c.w. dye laser technique combined with optoacoustic detection method allowed to measure gas phase overtone absorption spectra of several molecules.

Measurements performed for C_6H_6 and its deuterated analogues [23, 24] gave the overtone spectrum for CH stretch excitation up to $\Delta v = 9$ transition. Analysis of the line-shapes is very important to understand the nature and the dynamics of highly vibrational excited molecules. Due to rapid (subpicosecond) intramolecular interactions overtone linewidths are very broad ($\approx 100\,cm^{-1}$). On the other hand, the overtone spectra od HCl [22] exhibit sharp lines since no intramolecular interactions are possible for diatomic molecules. This allowed to observe the rotational structure, for each of $\Delta v = 5, 6, 7$ of vibrational structure.

Stella *et al.* [25] applied the OA detection to the observation of overtone transitions of CH_4 and NH_3 and pointed out that, using essentially the same pressure, they obtained a high-quality spectrum with an effective path length of less than 10 cm. That, compared with the 400 m length required by conventional method, means that they needed 5000 times less of absorbing material.

As we have shown so far the OA technique allowing to measure very weak absorptions has been widely applied in various spectroscopic measurements due to its high sensitivity.

4. – High-resolution optoacoustic spectroscopy.

So far we have discussed the sensitivity of the OA technique. This feature has been stimulating many attempts of combining sophisticated conventional laser techniques with OA detection. The Doppler broadening of spectral lines has been overcome in order to take advantage of the very narrow instrumental linewidth of laser sources.

4·1. *Saturation* OA *spectroscopy.* – The optacoustic signal, being proportional to the energy absorbed by the gas sample, is then proportional to the number of molecules excited per unit time. That allows to observe directly saturation effects of OA signal and to follow signal variations as a function of experimental parameters such as laser intensity and gas pressure.

As is well known, in an atomic or molecular system interacting with two counterpropagating beams of the same frequency, one can observe the effect of the hole burning in the Doppler-broadened absorption profile. The direct manifestation of that phenomenon in the form of Lamb-dip by using OA technique was observed in vibrational transitions of CH_3OH excited by a CO_2 laser, as an evidence of the physical origin of saturation effects observed in three-level optically pumped laser [41]. Figure 6 displays the Lamb-dips OA

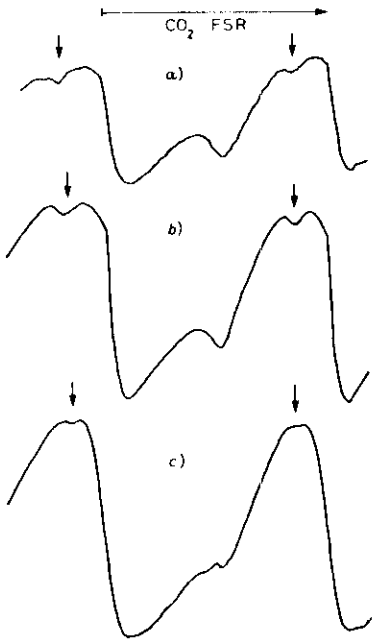

Fig. 6. – OA recordings of Lamb dips observed on a vibrational transition of CH_3OH interacting with two counter-propagating CO_2 laser beams. The gas pressures are: *a*) 24 mTorr, *b*) 65 mTorr, *c*) 300 mTorr. From [41].

recorded in CH_3OH. The CO_2-laser power was about 1 W, almost equally divided between the two counterpropagating beams. The observation of the dip is critical on the pressure value and an important saturation broadening is also present [42].

4·2. *Intermodulated* OA *spectroscopy.* – The signal-to-noise ratio obtained in the Lamb-dip measurements can be substantially improved using the intermodulation technique [43]. This method, successfully introduced for detecting the fluorescence light from the absorbing sample, turned out to be very effective for sub-Doppler OA spectroscopy. When the highly monochromatic light beam at frequency ν_l close to the frequency ν_0 of the absorption line centre is incident on a gas sample then only a small velocity group of atoms (molecules) can be excited. Their velocity components parallel to the light beam have to be equal to $(\nu_l - \nu_0)c/\nu_0$.

If the sample is subjected to two oppositely directed laser beams of the same frequency they will interact with different velocity groups unless $\nu_l = \nu_0$. If laser beams are strong enough and saturation of the transition takes place, a decrease in absorption and subsequently in the intensity of the emitted light is observed

when laser frequency ν_l is tuned at ν_0. If the two counterpropagating laser beams are amplitude modulated at two different frequencies, say f_1 and f_2, since under saturation the response of the sample is nonlinear, the «dip» effect can be recorded using the sum $f_1 + f_2$ frequency reference for a lock-in amplifier. An accurate analysis of the lineshape of the nonlinear component of the fluorescence in intermodulated spectroscopy can be found in [44].

In principale, the intermodulated scheme allows the detection of the saturation dip in the absence of any background. Instead of monitoring-emitted radiation by means of a photomultiplier a microphone may be used to measure directly absorption changes. Such experiments of intermodulated optoacoustic spectroscopy (IMOAS) were performed in visible for the 11-0 band of I_2 molecules excited by a dye laser [45] as well as in the infrared for vibrational transitions of CH_3OH and other molecules [29, 46] excited by a CO_2 laser, and for HCN molecules excited by a colour centre laser [47].

The application of the OA method to high-resolution sub-Doppler spectroscopy is made difficult by strong decrease in sensitivity at low gas pressures. Tonelli *et al.* [29] observed OA saturation signal for CH_3OH at a pressure as low as 20 mTorr with the modified construction of the OA cell allowing substantial decrease of the background signal caused by window

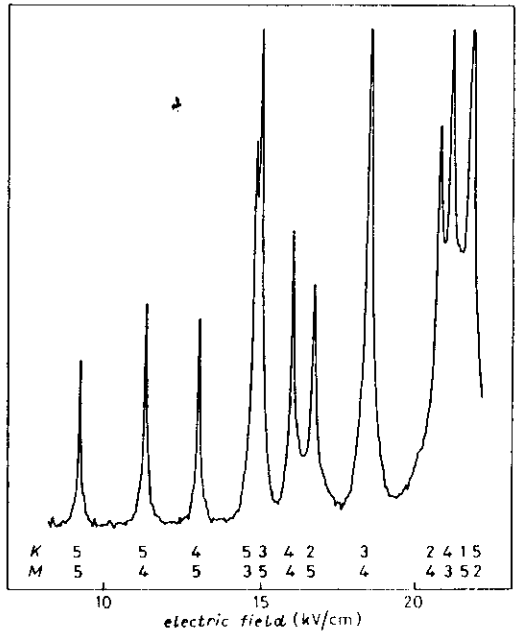

Fig. 7. – OA laser Stark spectrum of NH_3 recorded with intermodulated detection. Pressure in the cell is 100 mTorr. From [48].

absorption. It is worthwhile noting that at the low pressures required in order to avoid collisional broadening, the saturation broadening increases, which has to be taken into consideration.

At this point let us indicate a difference between OA measurements performed in visible and infrared region. In the former case, the OA detection technique could be replaced by fluorescence measurements possibly allowing even higher resolution. In the IR region, where fluorescence is hardly detectable there is no alternative to OA detection. A typical OA intermodulated spectroscopy recording at 10 μm is shown in fig. 7.

The sharp Doppler-free lines are sometimes recorded over a broad pedestal. Elastic-velocity–changing collisions are in general assumed as the main causes of the presence of this pedestal in intermodulated spectroscopy, as we discuss later in subsect. 4·2.

Recently a careful analysis of the line shape in intermodulated OA spectroscopy has been reported by Minguzzi *et al.* [49]. They extended to OA detection the model developed in [44] for fluorescence detection. In addition, they treated the effect of the actual Gaussian transversal energy distribution in the laser beam, yielding spatial inhomogeneity of the saturation parameter. Using this extended model, they could fit the experimental lineshapes better than simply using a single Lorentzian curve.

4·3. *Two-photon* OA *sub-Doppler spectroscopy.* – Two-photon transitions [50] can be induced in atoms at optical frequencies thanks to the powerfulness of laser sources. Two-photon spectroscopy is interesting and useful for several reasons. High-energy transitions become accessible to laser sources and highly excited levels can be reached from the ground state. Selection rules for two photon are different from those for single photon transitions and different atomic or molecular states can be investigated. If the two photons come from opposite directions, the first-order Doppler shifts cancel [51].

The OA technique was applied in [52] to two-photon spectroscopy for detecting Doppler-free resonances in the ν_2 band of NH_3, as shown in fig. 8. The two counterpropagating photons were from two different CO_2-laser transitions (P(18)) and (P(32)). As a consequence, the Doppler shifts were not exactly compensated, but there was not the broad background originated in spectroscopy with photons of equal energy by two-photon absorptions from the same direction.

In the two-photon spectroscopy measurements, the precise tuning of the difference between initial and final energy levels of the polar molecule to the sum of the photons energy was accomplished by means of Stark effect, using an external electric field.

This is an advantage of the OA technique related to the small interaction volume. Such an experimental arrangement allows to apply easily an external homogeneous field and to assure its uniformity over the whole gas sample.

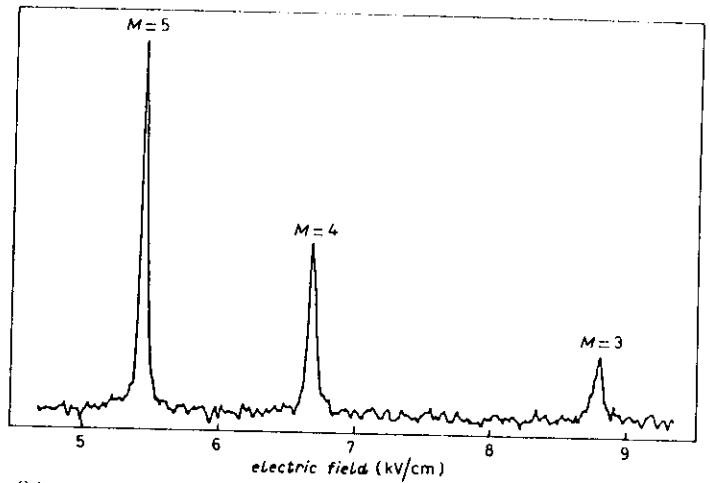

Fig. 8. – OA recording of the two-photon transitions observed with $P(18)$ and $P(32)$ CO_2 laser lines in NH_3. From [52].

A series of OA measurements performed by applying uniform and weak electric fields to various molecular samples allowed to explain the effect of the electric field on the efficiency of optically pumped FIR lasers [53]. The effect was understood as a nonlinear Hanle effect (NLHE), as we discuss after. Let us simply stress here that the OA technique allowed the investigation of the phenomenon for a large variety of transitions, gas pressures and laser intensities. Using conventional absorption spectroscopy and the same volume of gas multipass or intracavity configurations should have been necessary.

Another demonstration of the usefulness of small optoacoustic cells was given by optoacoustic laser-Stark spectroscopy. In this technique molecular transitions which are close to fixed laser frequencies are brought into resonance by means of Stark effect. The OA detection was used in ref. [54, 55] to investigate absorptions around CO_2-laser lines.

4·4. *Nonlinear Hanle effect.* – Besides the developement of new nonlinear techniques, like those described so far, the use of intense laser sources has opened the possibility of observing the nonlinear version of effects already known from linear spectroscopy. Among these we have the Hanle effect, discovered more than sixty years ago [56], which consists in a change of the polarization of the resonance radiation when an external (magnetic) field removes the degeneracy between the Zeeman sublevels.

The nonlinear version of the Hanle effect (NLHE) manifests itself as an increase of the laser-saturated absorption when the degeneracy is removed due to the Zeeman or Stark effect [57]. The physical origin of the effect is in the

different saturation of the different components of a resonance line (in the presence or not of an external field) caused by coherences induced between the Zeeman sublevels through the optical transition.

A theoretical analysis of the NLHE based on the density matrix formalism was introduced in [58], while a rate equation model has been successfully applied to provide a quantitative analysis of experimental results in [59, 60].

As anticipated in the previous subsection, the OA technique was used to detect the NLHE in the interaction between saturating infrared laser beams and resonant vibrational transitions of polar molecules. A typical experimental recording is shown in fig. 9. Here the molecular sample was normal methyl alcohol and the saturating radiation from a CO_2 laser was resonant with a transition of the CO stretching band. The application of an external electric field orthogonal to the laser polarization caused the Stark effect [61], hence the removal of the degeneracy, leading to the increase of the absorption. As already mentioned, these increases in the absorption, investigated by OA technique, allowed the understanding of the behaviour of optically pumped molecular lasers in the presence of external fields [53, 62].

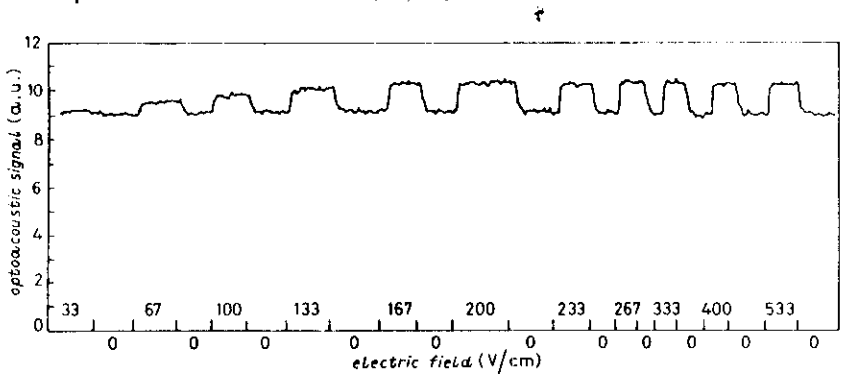

Fig. 9. – Absorption increase originated by NLHE recorded with OA method for various electric-field intensities. From [53]. CH_3OH, $p = 200$ mTorr, CO_2 9-$P(34)$, $\Delta M = \pm 1$.

4·5. OA *Raman spectroscopy*. – The OA detection, combined with nonlinear coherent Raman scattering, has become recently a very interesting and promising spectroscopic method. The principles of PARS (photoacoustic Raman spectroscopy) technique may be simply explained following the scheme in fig. 10. A molecular gas system contained in a cell interacts with two incident laser beams (one of them is tunable) of frequencies ω_S and ω_p, and intensities I_S and I_p. When the difference frequency ω_p-ω_S is equal to the Raman active frequency of the medium determined by the energy states $|a\rangle$ and $|b\rangle$ the nonlinear interaction occurs resulting in the amplification of I_S (Stokes beam) and attenuation of I_p (pump beam). In such a way, for each process of Stokes photon

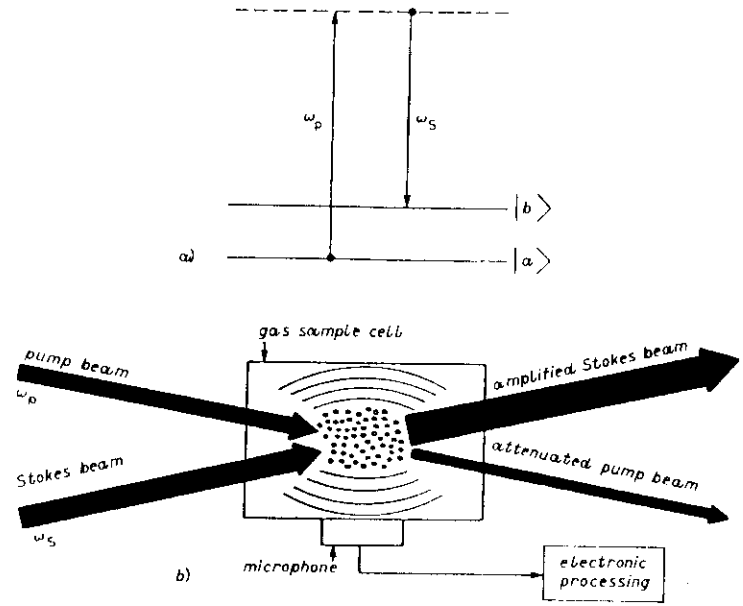

Fig. 10. – Schematic representation of the PARS process. From [13].

generation one molecule is transferred from level $|a\rangle$ to level $|b\rangle$. Subsequent collisional relaxation leads to the heating of the illuminated region and to the generation of pressure wave detected by a microphone. The expression for the pressure increase due to nonlinear interaction process is given by Barret and Heller [63] and has the following form:

$$\Delta p = [(\gamma - 1) I_S(0) g_S Z A_S T \omega_0 / \omega_S] / V , \tag{20}$$

γ is the specific-heat ratio, $I_S(0)$ is the initial intensity of the Stokes beam, g_S is the Stokes gain coefficient, Z is the interaction length, A_S is the cross-section area of the Stokes beam, T the interaction time of two laser beams, ω_0 is the Raman transition frequency and V is the interaction volume. It is assumed that both beams are of uniform intensities over their cross-sectional plane and that they overlap both spatially and temporally.

PARS measurements were performed for both c.w. [64] and pulsed [65] laser excitation. In the latter case, the amount of energy deposited in a gas sample is greater by several orders of magnitude. An example of PARS spectrum of CH_4 is shown on fig. 11. The peak powers of two dye lasers used for the pump and Stokes beams were 1.2 and 0.5 MW, respectively.

PARS technique can also be applied for identifying and quantifying trace

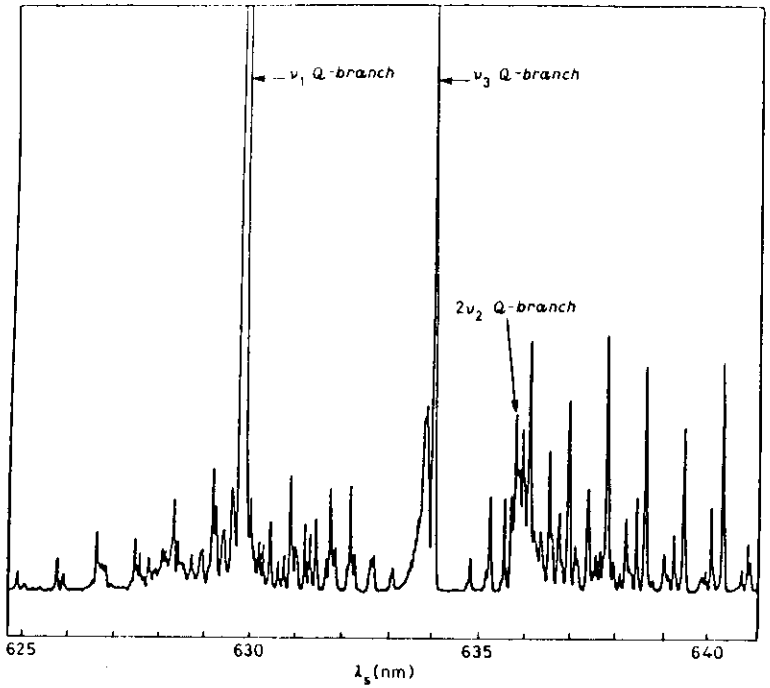

Fig. 11. – Vibrational PARS spectrum of CH_4 at a pressure of 50 Torr. From [13].

constituents in gaseous mixtures. Sensitivity limits for several gases in air were determined by Siebert *et al.* [32].

As we see again, the main advantage of the OA technique is that it provides a direct way for detecting the energy deposited in the sample, while other techniques are based on measurements of small changes in the energy of intense radiation passing through the cell.

4·6. *Multiphoton* OA *spectroscopy.* – High intensity is essential to observe nonlinear interactions of radiation with matter; in many cases, however, high-sensitivity detection is also required. Multiphoton absorption is a typical example. The OA method turned out to be a very convenient way for measuring multiphoton absorptions for both vibrational [66, 67] and electronic [13] transitions. It allowed also to observe sublinear variations of the absorption coefficient with incident power in the OCS gas [68].

The dependence of the optoacoustic signal on laser intensity provides a direct information on number of photons involved in nonlinear interaction. Since the OA technique allows us to measure the absolute value of absorbed energy, a

determination of the number of photons absorbed per molecule is also possible [69]. Such an information is of considerable importance for studying multiple-absorption processes in polyatomic molecules [70].

4·7. *Time-dependent* OA *measurements.* – The acoustic signal detected by a microphone is always delayed with respect to the optical excitation of a gas sample. This delay time is strictly related to the mechanism itself of the optoacoustic effect. As a first step the internal energy of a gas has to be transferred into heat and the time needed for that (t_1) depends on the V-T relaxation rate. The generated pressure disturbance reaches the microphone after the time t_2 depending on the sound velocity (c) in the medium. For a given gas sample t_1 depends on the gas pressure, while t_2 on the distance d between the illuminated region and microphone. Such a simple technique of measuring the c-value as a slope of the t_2 (d) dependence was used by Chin *et al.* [20]. However, measurements of collisional decay rates are not so straighforward and they need particular care in the interpretation of signal shape.

Detailed discussion of the acoustic-wave generation by laser excitation as well as considerations on how the microphone signal reflects the V-R, T relaxation of gas were given by Smith *et al.* [71]. They applied their model to measure the collisional probabilities for relaxation of the lowest vibrational modes of OCS and CF_4 by several collision partners.

Interesting results on picosecond time-resolved optoacoustic measurements have been recently reported [21]. The technique consists in detecting the total OA impulse produced by two ultrashort optical pulses with variable time delay between them. Optoacoustic detection by itself, of course, cannot achieve picosecond time resolution. However, by observing the integrated optoacoustic response generated by two picosecond pulses with varying time delay, one can measure fast relaxation processes with time resolution limited only by the optical pulse width, even though the optoacoustic detection mechanism is very much slower. Measurements were performed for organic dye molecules in solution but the technique itself appears to be of wide and general application.

4·8. *Photothermal effects.* – Optical heating of the medium, being the result of the dissipation of incident energy within the material can be converted into sound and detected with a microphone. There are, however, other techniques allowing to measure the warming effect of the incident radiation on a sample. They are called photothermal techniques and are based on the influence of the temperature on the index of refraction of the heated medium.

There are two different approaches to photothermal detection spectroscopy. In both of them, the refractive-index gradient is created and optically detected within the medium of interest. Laser used as a source of light can provide both a means for high-energy delivery to the sample and a means for extremely sensitive detection of the resultant heating of the sample.

One of the methods called «photothermal deflection spectroscopy» [72, 73] or initially detection by the «mirage effect» [74] relies on detection of the deflection of a probe beam in the vicinity of a pulsed or intensity-modulated excitation beam which produces a temperature gradient and subsequently a refractive-index gradient in the sample. The amplitude and phase of the periodic deflection can be measured with a position sensor.

Photothermal deflection spectroscopy provides a simple means for the measurements of very weak absorptions which can be determined from the deflection of the probe beam by varying the wavelength of the pump beam. By intersecting the probe and pump beams in space, *in situ*, real time measurements can be performed. The method has been recently applied to monitor a heat release that can be ascribed to photochemical particulation [75].

Another technique used to monitor changes in the refractive index of the sample is called «thermal lensing detection» [76] and it is schematically shown on fig. 12. When the absorption of light leads to the temperature change within the exciting light beam, the radial density and refractive index profiles reproduce the shape of the beam. Using a laser source, a Gaussian intensity profile with an extremum on the laser axis is obtained.

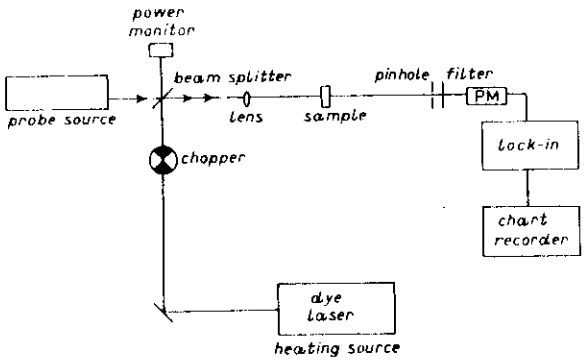

Fig. 12. – Schematic diagram of the thermal lensing detection. From [80].

The refractive index distribution acts as a lens to a probe beam sent through the sample collinear with the pump beam. With a negative value of dn/dt, the refractive-index profile very closely approximates that of a diverging lens. As a consequence, any change of temperature induced by a pump beam is manifested as a signal variation from phototube which measures the intensity at the centre of the probe beam.

Laser-induced time-dependent thermal lensing was used in the study of vibrational relaxation phenomena in various gaseous systems [77]. The technique

was also succesfully applied to the study of a gas phase multiphoton spectra [78, 79].

Details and applications concerning the thermal-lensing detection technique can be found in the review paper by Fang and Swofford [80].

4·9. *Future and discussion.* – Many other applications of optoacoustic technique could be mentioned. We do not intend, however, to give a complete and exhaustive description of the subject. Our goal was rather to point out the versatility of this unconventional detection method. The applications we have being discussing should be also useful for our concluding remarks concerning advantages, prospectives and limitations of the OA technique.

First of all, the OA method is relatively simple and does not require sophisticated and expensive devices. At the same time its very high sensitivity allows to measure extremely weak absorptions corresponding to cross-sections as low as 10^{-23}cm^2. In conventional absorption spectroscopy it would require absorption lenght of the order of 10^6 m [12]. It is worth noting that such a high sensitivity can be obtained in spite of very low conversion ratio of output (acoustic) to input (radiative) energy. The response of the OA spectrometer is linear over several orders of magnitude. It has also a flat characteristic over the whole frequency spectrum, while sensitivity of radiation detectors generally depends strongly on frequency. Moreover, there are frequency ranges of electromagnetic radiation where sensitive detectors of radiation are not available.

Certainly, the OA technique has also several limitations. The fundamental condition which has to be satisfied results from the principle of the OA effect which requires that at least a part of the absorbed energy is transferred into heat. It eliminates the OA detection for all systems irradiating the whole absorbed energy. Chin *et al.* [20] discuss pressure limits of the pulsed OA technique. The upper limit of the pressure range is governed by absorption in the entrance volume causing that first acoustic-peak vanishes. It depends on the absorption coefficient of the gas. The lower pressure limit is encountered when the V-T relaxation time is so large that the first peak does not occur before the contributions from other sources arrive at microphone.

As far as high resolution is concerned, applications of the OA technique are drastically limited. It seems quite obvious since requirements for high resolution are contradictory to principles of the OA effect itself. In fact, high-resolution measurements have to be performed in such experimental conditions to minimize collisional interaction (pressure broadening), while, on the other hand, collisions are essential for generating the acoustic signal. Borde [81] considered various aspects of optical and optoacoustic detection and showed that OA technique being highly competitive at high pressures (low resolution) and for weak absorption, is not suitable for low-pressure and high-resolution experiments.

In conclusion we would like to point out how accurate and foreseeing was the Bell prediction anticipating of one hundred years the application of his invention.

5. – Optogalvanic effect.

The optogalvanic effect is approximately twice younger than the optoacoustic effect, since it was observed for the first time in 1928 by Penning [82]. He noticed that the discharge current of a Ne tube changed when illuminated by another Ne tube. This phenomenon did not offer any particular application until combined with tunable-laser sources by Green *et al.* in 1976 [83]. Since then, the optogalvanic spectroscopy has developed rapidly and hundreds of papers have been devoted to its various aspects. The subject has been partially covered by reviews [84, 12] and by an international conference [85].

The basic physics of the optogalvanic effect is the change in the discharge current (or voltage drop) caused by illuminating the discharge with radiation being in resonance with an atomic or molecular transition. This change in the current can be conveniently monitored, which offers a very simple and sensitive unconventional absorption detector.

As we discussed in the beginning of this paper, an unconventional detection technique requires an interaction-induced microscopic modification in the matter, which is «amplified» and then evidenced as a macroscopic process. In the optoacoustic technique, the microscopical process was the collisional-energy transfer to kinetic energy, while the macroscopic process was an overall change in the gas pressure evidenced as an acoustic wave.

Another «microscopic» effect in the matter, after its interaction with radiation, can be a change in some electrical property of the single atom or molecule. For instance, after photon or photons absorption, the atom can be brought closer to ionization, and in fact techniques have been developed in which the atomic transition is investigated by detecting the electron released after ionization. Resonant ionization spectroscopy (RIS) [86] is a well-representative example of this and, thanks to the extraordinary sensitivity, made possible the detection of even a single atom.

The situation is a bit complicated by the collisions for *in situ* measurements, like for the detection of atomic or molecular species in flames. However, conceptually, it is still the same physics, since the ionization of the atom is detected collecting the electrons by means of an applied voltage and measuring the changes in the current. Here, again, a microscopic process is «amplified» and detected as a modification in a macroscopic property of matter, here its electrical conductivity.

Discharges provide a physical example in which the electric current is essential to the production of excited levels and ionized states. We could say that the whole discharge is at the same time the sample to be investigated and the macroscopic property (its current) to be detected.

The scheme of a typical experimental arrangement for measuring the OG signal is shown in fig 13. Absorption of resonant photons causes a change in the discharge impedance (the effect was also called impedance effect). If the

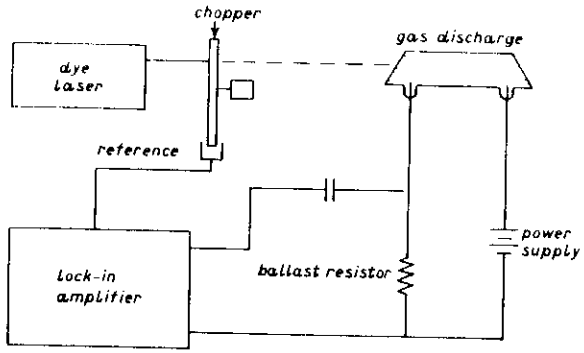

Fig. 13. – Typical experimental arrangement for measuring the OG signal. From [84].

discharge is direct current (DC), this change can be measured as a change of the voltage drop on the resistor R connected in series with the discharge tube. For other types of discharge, the logic scheme is the same, but slightly different technical solutions must be adopted.

5·1. *The physical model.* – As a first approximation the effect can be explained by a simple model which takes into consideration the difference between the ionization cross-sections σ_i for the two states involved in the optical transition. Such an explanation is useful due to its simplicity, but it can be applied only to very few experimental situations. Such a simple (practically the simplest) model explains the fact that the optical transition leads to the change of number of charges (electrons and ions) which causes the change of the discharge impedance.

The complexity of all the phenomena involved in the processes following the excitation and finally leading to the ionization (for instance, associative ionization, Penning ionization) prevents from developing a general quantitative theory. In fact several parameters, strongly dependent on the particular type of discharge, have to be taken into account.

5·1.1. Neon-positive column. A satisfactory theory of the OG effect for the 594.5 nm transition in the Ne-positive column was developed by Daughty and Lawler [87]. In spite of being applicable only to few transitions and particular types of discharges, this theory seems to be very useful in understanding how the various radiative and collisional processes are involved in producing OG signals.

The quantitative analysis of the OG effect in an atomic discharge requires the knowledge of the collisional processes which determine the density of ions and electrons and the distribution of excited atoms. Laser excitation modifies the

distribution of atomic populations and subsequently the number of charges in the discharge, leading to the change of the conductance.

The OG effect can be positive if absorption of the radiation leads to the increase of the discharge current and negative when a decrease of the current is observed. The latter situation takes place, for instance, when the laser excites atoms to a level with smaller probability of ionization.

Transitions starting from metastable levels and involving short-living upper levels are typical examples.

Let us consider a Ne discharge as an example of weakly ionized gas. The energy levels of Ne which are taken into account in our considerations are shown in fig. 14. All of them are divided into four groups. The mechanisms responsible for ionization are the following:

1) one-step ionization by electron impact

$$\mathrm{Ne} + \mathrm{e} \rightarrow \mathrm{Ne}^{+} + 2\mathrm{e} \; ;$$

this process dominates for low gas pressures when electrons may have very high energy;

2) two or multistep ionization, which is a stepwise process, as for instance

$$\mathrm{Ne} + \mathrm{e} \rightarrow \mathrm{Ne}^{*}\,(1s_1) + \mathrm{e}, \qquad \mathrm{Ne}^{*}\,(1s_1) + \mathrm{e} \rightarrow \mathrm{Ne}^{+} + 2\mathrm{e};$$

3) associative ionization

$$\mathrm{Ne}_{\mathrm{III}} + \mathrm{Ne}_{\mathrm{III}} \rightarrow \mathrm{Ne}_2^{+} + \mathrm{e}\,.$$

Binding energy of Ne_2 is about 1.3 eV. Therefore, excitation energy of ~ 20.3 eV, being equal to the difference between ionization energy and binding energy of Ne_2^+, is sufficient to create ion-electron pairs. Due to very high probability of such a process, the excitation to one of the group-III levels pratically corresponds to direct ionization.

4) Penning ionization

$$\mathrm{Ne}_{\mathrm{III}} + \mathrm{Ne} \rightarrow \mathrm{Ne}^{+} + \mathrm{Ne} + \mathrm{e}\,.$$

The model proposed in [87] deals with a negative OG effect in the Ne-positive column irradiated by radiation at 594.5 nm corresponding to the $1s_5 \rightarrow 2p_4$ transition.

In order to calculate the absolute magnitude of the OG effect, the positive column dicharge has to be described by a set of rate equations. The model is valid for pressurs of $(1 \div 10)$ Torr, currents of $(1 \div 16)$ mA and radius of the tube of

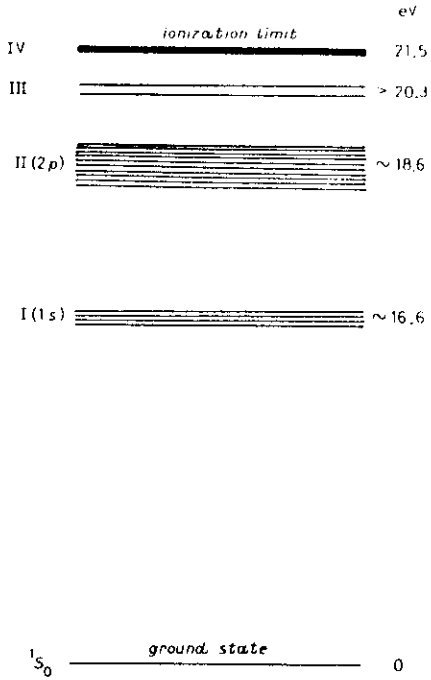

Fig. 14. – Simplified scheme of Ne energy levels involved in a quantitative model of OG effect in a glow discharge.

0.1 cm. In such conditions, ion-electron pairs are produced mainly by multistep processes in which metastable levels play a very important role. Single-step ionization is also possible and included in the model. Recombination process is primarily due to the diffusion to the wall.

The model of the discharge consists of a balance equation for metastable atoms, a balance equation for electrons and a direct-current equation.

A schematic diagram of levels in Ne atom and processes taken into account in the model are shown on fig. 15. For purposes of the model the $1s_5$, $1s_4$ and $1s_3$ levels are lumped together as a single metastable. Actually, the $1s_4$ level is not a pure metastable due to slight triplet-singlet mixing. However, this simplification is justified by the fact that the decay rates of the $1s_3$ and $1s_5$ levels due to diffusion to the wall and the $1s_4$ level due to escape of trapped radiation are substantially smaller than the decay rate of the $1s_2$ level due to escape of trapped radiation. It is then assumed that the $1s_2$ level does not play an important role in multistep ionization and a separate balance equation for this level is not necessary.

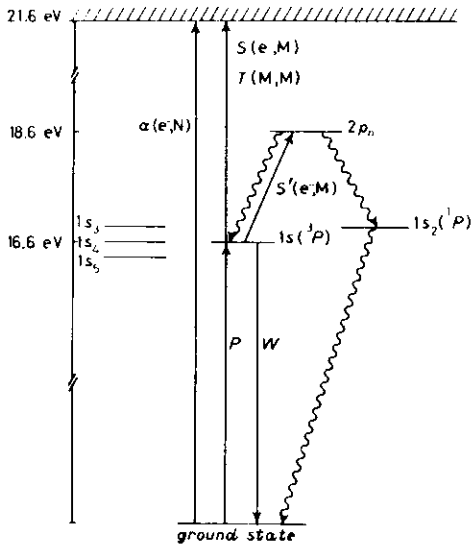

Fig. 15. – Level diagram for Ne. The $1s_3$, $1s_4$ and $1s_5$ levels are lumped together as a single metastable $1s(^3P)$ level. The illustrated processes are discussed in the text. From [87].

The rate of change of the metastable density, dM/dt may be written as follows:

$$\frac{dM}{dt} = PnN - WM - TM^2 - SnM - \frac{S'nM}{4}. \tag{21}$$

In the first term, responsible for the production of metastables, N is the density of ground-state atoms, n the density of electrons and the production rate constant P represents both direct electron-impact excitation of metastable and indirect processes involving electron impact excitation of higher levels followed by radiative decay to metastable level.

Next three terms represent the destruction of metastables due to wall losses at a rate W, collisions between pairs of metastable atoms at a rate T, and electron impact ionization of metastable atoms at a rate S, respectively. The last destructive term represents electron impact excitation from the metastable level to one of the $2p_n$ levels. Since an atom excited to $2p_n$ level has a probability of 3/4 of returning to one of metastable ($1s_3$, $1s_4$, $1s_5$) levels the rate constant $S/4$ represents electron impact destruction with no production of ions.

The second equation of the model describes the rate of change of the electron density dn/dt

$$\frac{dn}{dt} = \alpha v_d n + SnM + \frac{TM^2}{2} - D_a\left(\frac{2.4}{R}\right)^2 n. \tag{22}$$

Production of electrons is due to single-step ionization represented by the product of the first Townsend coefficient α and the electron drift velocity v_d (first term), and due to two-step processes involving metastables mentioned previously (second and third term). The last term corresponds to the loss of electrons due to diffusion to the wall with D_a being the ambipolar diffusion coefficient and R the column radius.

Finally, the third equation necessary to model the discharge is the direct current equation

$$i = env_d\pi R^2. \tag{23}$$

In a steady-state situation when the production of metastables and electrons is balanced by their losses we have

$$\frac{dM}{dt} = 0 \quad \text{and} \quad \frac{dn}{dt} = 0. \tag{24}$$

Both derivatives are functions of the electron density n, metastable density M and the axial electric field in the column E, which can be written as

$$\frac{dM}{dt} = H(n, M, E), \tag{25}$$

$$\frac{dn}{dt} = G(n, M, E). \tag{26}$$

Equations (25) and (26) combined with eq. (23) can, in principle, determine the values of the independent variables n, M and E if the current i is fixed by an external circuit. It is assumed now for the purposes of the model that the OG effect can be observed in the steady state and that it causes, at most, 10% perturbation to i. In such a situation linear-perturbation theory can be applied and three perturbed balance equations can be written

$$\Delta H = \frac{\partial H}{\partial n}\Delta n + \frac{\partial H}{\partial M}\Delta M + \frac{\partial H}{\partial E}\Delta E = \beta Q, \tag{27}$$

$$\Delta G = \frac{\partial G}{\partial n}\Delta n + \frac{\partial G}{\partial M}\Delta M + \frac{\partial G}{\partial E}\Delta E = 0, \tag{28}$$

$$\Delta i = \frac{\partial i}{\partial n}\Delta n + \frac{\partial i}{\partial E}\Delta E. \tag{29}$$

Equation (27) is written for metastables and Q is the number of photons absorbed per unite time and unite volume and β is the branching ratio which represents the probability of destroying a metastable upon absorption of a laser photon. Equation (28) is the perturbed balance equation for charged particles

and eq. (29) is the perturbed current equation. For a voltage source V, the length of the column l and a ballast restistance Z, we have

$$\Delta V = Z\Delta i + l\Delta E = 0 \tag{30}$$

and

$$\Delta i = -\, l\Delta E/z\,. \tag{31}$$

Equations (27)-(29) can be solved for ΔE which subsequenly leads to the following expression for Δi:

$$\Delta i = \beta Q i(Sn + TM)\left(1 + \frac{Z}{l}\,\frac{\mathrm{d}i}{\mathrm{d}E}\right)\left[\left(SnM + \frac{TM^2}{2}\right)W + \left(S - \frac{S'}{4}\right)\frac{nTM^2}{2}\right]^{-1}, \tag{32}$$

representing the optogalvanic effect predicted by the model.

5·1.2. Thermal effects. A limitation of the theory so far described is that it is developed in a two-level scheme which means that other channels of energy transfer (inside the atomic system) have not been taken into account. However, significant features of the OG effect in different types of discharge [88, 89] suggest that modification in the temperature plays an important role. In an experiment on an uranium hollow cathode in which spectrally resolved fluorescence light was investigated, an increase in the discharge temperature was measured under resonant laser illumination [90]. The increase of the discharge temperature shows the importance of an energy transfer of excitation energy into translational energy. This is really important in the case of molecular system as will be discussed later on.

However, the question of heating turned out to play a significant role for an atomic positive column discharge [2, 39]. It was verified in an experiment in which optogalvanic and optoacoustic signals were measured simultaneously. A microphone placed inside the discharge tube detected acoustic disturbance signals produced by the temperature changes in the discharge. The laser absorption modifies the atomic-population distribution and affects the power released into the cell through different channels. The input electrical power P_e is equal to

$$P_e = iEl\,, \tag{33}$$

where l is the positive column length, E is the axial electric field and i is the discharge current.

The total input power is dissipated into the discharge through several channels: ionization, atomic collisional and radiative de-excitation, and heat

conduction of ground-state atoms. In the ionization channel, the energy is ultimately released at the cell walls in the recombination process following the ambipolar diffusion of ions and electrons. In the collisional de-excitation channel the metastable atoms diffuse toward the walls, where they release their internal energy. In the atomic emission the visible light (between the $2p$ and $1s$ states) is transmitted without absorption by the cell walls, while the vacuum ultraviolet resonance radiation (from $1s$ to ground state) is absorbed.

The contributions of the different channels for a positive column Ne discharge are discussed in ref. [87]. They are difficult for the precise determination because of their dependence on various factors as pressure, current and radius of the tube. Anyway, the substantial part of the input electrical power contributes directly or indirectly (through the tube walls) to the gas-discharge temperature. Under absorption of light power Q the input electric power is modified. Most of the absorbed laser power Q is released from the discharge through the spontaneous emission of visible radiation, that is not absorbed by the walls and does not contribute to the discharge temperature. However, the radiation modifies population of metastable levels and electrons, and then the distribution of dissipated power into different channels. In other words, the laser radiation acts as a mechanism modifying indirectly the balance of power of the dicharge.

The optoacoustic signal, being a measure of the change of the discharge temperature, is proportional to the change in the dissipated power ΔP given by

$$\Delta P = f_e \Delta P_e + f_l Q = f_e(lE - Zi)\,\Delta i + f_l Q\,, \tag{34}$$

where f_e and f_l are coefficients representing the fractions of electric (P_e) and light (Q) powers dissipated into the discharge temperature. The last equality results because both i and E are modified under light illumination and due to the constant-voltage power supply we have $l\Delta E = -Z\Delta i$.

The experiment has shown [2] that (according to the eq. (34)) under light illumination a direct compensation between electrical and laser powers may occur. The two terms in eq. (34) can partially cancel each other yielding positive, negative and null contributions to the generated heat. In particular, under appropriate condition a cooling of the laser-irradiated discharge may arise.

The above results show that the understanding of the energy balance of an atomic discharge is far from being complete. A deeper insight into the gas and wall energy deposit and the acoustic-wave production in a weakly ionized plasma is required.

5·1.3. Hollow-cathode discharge. As far as the otpogalvanic effect in a hollow cathode discharge is concerned, it is assumed that two mechanisms can be responsible for the change of the discharge impedance upon irradiation. One of them is called ionization mechanism and is based on the fact that cross-section for

electron-collision–induced ionization increases as the state energy approaches the ionization potential. The second mechanism which was proposed to be dominant in the negative glow region of a hollow-cathode discharge is an increase in the electron temperature of the discharge [89]. The basis for the latter mechanism proposed by Keller *et al.* [91, 92, 89] is that in a hollow-cathode discharge there is an equilibrium established between thermal electrons and the atomic excitation such that, to the first approximation,the electron temperature and the electronic excitation temperature are equal. This equilibrium is a result of many elastic and superelastic collisions between the atoms and electrons. Laser irradiation is a perturbation of those processes. Electron collisions prevent a significant change of the energy-level population and the energy supplied to the atomic system is filtered off to the electrons via superelastic collisions.

A simplified model of the negative glow region of a hollow-cathode discharge based on such a mechanism was presented by Keller *et al.* [89]. From this model contribution to the laser-induced impedance changes becomes clarified and the predominance of the electron temperature mechanism is demonstrated.

5·1.4. Molecular discharges. As far as molecules are concerned, the OG effect was reported for the first time in 1967 [93]. A change of discharge current in a CO_2-laser tube was observed when the laser action was switched off or on. The application of the OG technique to molecular spectroscopy came much later, when several atomic applications were already known.

The mechanism proposed at the beginning to explain the OG effect in atomic discharges was based on the change of ionization probability when an atom is transferred to a higher-energy level. For this reason, it was difficult to forecast the OG effect in molecules where the levels are very close to each other.

However, investigations performed on molecular discharges have shown that optogalvanic effect can be observed for both electronic [94-96] and vibrational [97, 98] transitions. New mechanism were then needed in order to explain the origin of the effect. A very surprising observation was reported by Rettner *et al.* [95], when studying iodine discharge. In fact, OG effect was detected even for laser irradiating the gas sample far from the discharge region. This was of great help in proposing a new model in order to explain I_2 results.

Two mechanism were considered, as responsible for the OG effect. One of them, producing the increase of the discharge current and observed with laser illumination outside the electrode region, was attributed to a travelling pressure wave caused by the degradation of electronic and vibrational energy into translation energy and by molecular dissociation. Time-resolved studies of I_2 discharges [96] demonstrated that strong and very fast positive OG signals generated from irradiation within the discharge may also result from multiphoton ionization of I_2.

Negative OG signal generated only from irradiation of the negative glow is attributed to an increase of dissociative electron attachment to I_2 following electronic and vibrational excitation.

The extension of the OG molecular studies to the infrared region [97, 99] showed many similarities to that observed with a visible laser for I_2. Therefore, Webster and Menzies [97] postulated that a kinetic effect was involved, and like for the optoacoustic effect, absorbed laser energy was degradated to rotational and translation energy. Such a perturbation of the discharge dynamics leads to the positive OG signal. The negative signals which correspond to a decrease of discharge current are believed to result from a large enhancement in the electron attachment rate when the negative glow region is irradiated.

A mechanism proposed to explain infrared OG effect in molecular discharges was recently confirmed by an experiment in which OA and OG effects were simultaneously observed [100]. To provide a complete description of the OG effect, the molecular processes, where the changes in the translational and vibrational temperatures play the dominant role should be determined, but the knowledge of the discharge phenomena is not precise enough. A schematic description of the processes leading to OG and OA effects in molecular discharges is shown in fig. 16.

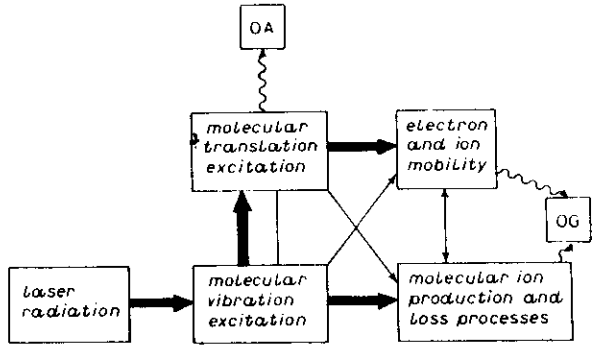

Fig. 16. – Block diagram of the infrared OA and OG effects in molecular discharges. From [100].

We made on overlook on the present status of the theoretical understanding of the optogalvanic effect. Despite the considerable success in several particular cases, the effect is far from being completely understood and no general theory applicable to various situation has been presented. Neverthless, the effect has been widely and succesfully applied to atomic and molecular spectroscopy. Fortunately in almost all spectroscopic applications the knowledge on the microscopic mechanism of the OG effect is not required and the discharge can be

completely ignored or considered as a «black box» with radiation input and electric output.

The reasons for the rapid growing of applications of the OG effect are certainly the simplicity and the versatility of the method.

6. – OG Instrumentation.

Three main types of discharge have been used in optogalvanic spectroscopy: direct current (DC) discharge; hollow-cathode (HC) discharge and radiofrequency (RF) discharge.

Most of the OG experiments have been performed with the DC discharge. In this case the change of the discharge current is measured as a voltage drop across the ballast resistor. In a typical experimental arrangement, schematically shown in fig. 13, a positive column discharge in a glass tube is connected through a ballast resistor R to a voltage-stabilized power supply. The discharge tube, with cathode and anode being offset from the column axis, is longitudinally irradiated with a tunable laser. The beam is mechanically chopped at a frequency of the order of few kHz. A lock-in amplifier monitors the current through the ballast resistor. The capacitor protects the lock-in from the d.c. component of the discharge tube voltage. The OG signal may be also measured with an oscilloscope for some transitions (in some case the voltage change is as large as 3%) but phase-sensitive detection improves substantially the signal-to-noise ratio. Pulsed-laser sources can also be used, which requires some kind of gated detection (for instance, box car integrators).

In order to have a stable discharge with a low-noise level, the tube has to be cleaned by repeatedly running at high current followed by evacuation of the tube. In some case a gentle flow of gas is maintained through the tube. This helps to keep the discharge stable and prevents from its contamination by possible reaction products. Typical operating conditions are: a potential of few hundred volts across the tube, the discharge current of the order of 1 mA and the diameter of the discharge tube of the order of a few mm.

Tunable dye lasers cover all visible range, while CO_2 laser, colour centre lasers or diode lasers are typically used in the infrared. In the mid-infra-red region c.w. tunable diode lasers operating single mode (with linewidths ≈ 10 MHz) produce high-resolution OG spectra. Although laser power is limited to about 1 mW, the diode lasers may be current modulated (and, therefore, frequency modulated), so that harmonic-detection method can be used to give increased sensitivity to the OG technique.

A OG spectrum of a He-Ne glow discharge in the tuning range of Rhodamine 6G was early reported by Johnston [101] and reproduced in many review papers. We report in fig. 17 the OG spectrum corresponding to the same region, but obtained by a hollow-cathode discharge. In addition to the lines originating from

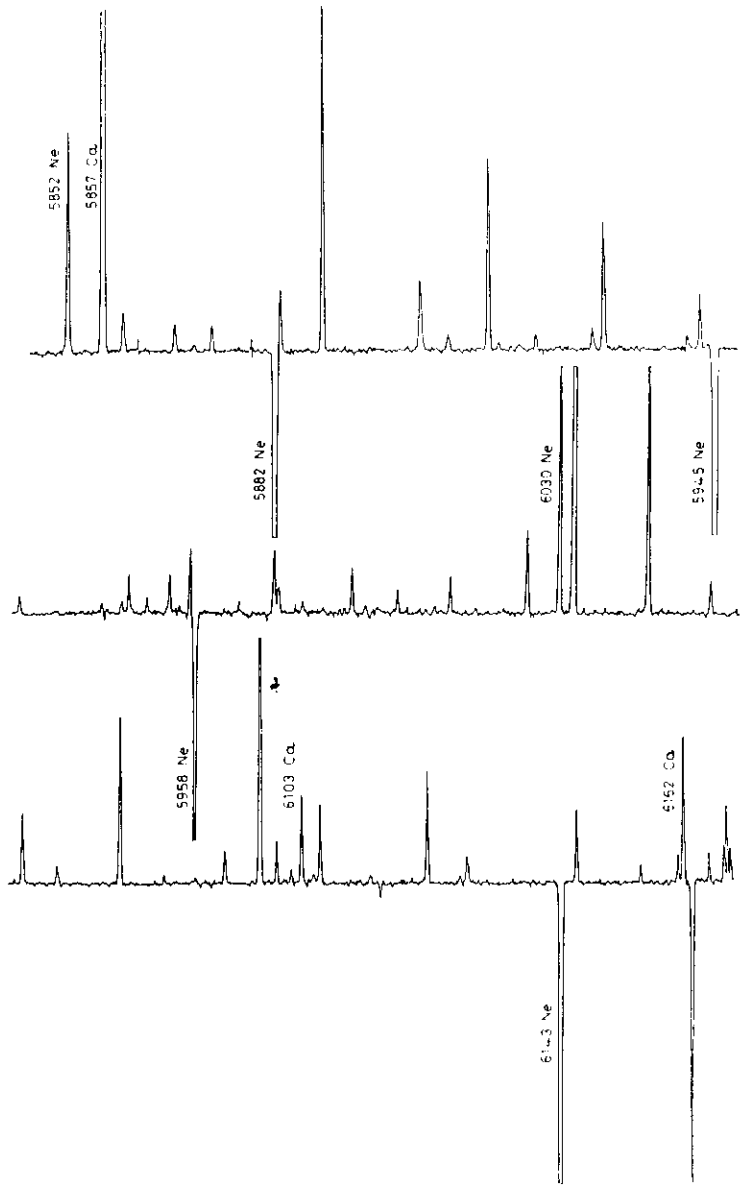

Fig. 17. – OG spectrum recorded by a HC discharge containing sputtered Ca atoms and neon at a pressure of 2 Torr, $I = 65$ mA.

neon used to substain the discharge, OG signals are also recorded from transitions in Ca atoms sputtered from the cathode. The spectrum demonstrates how it is possible to record all the transitions between excited states so rapidly and in such a simple way.

The main advantage of the DC glow discharge consists in its simplicity. HC discharges, instead, turned out to be more suitable for several particular purposes and, in general, provided a better environment for high-resolution spectroscopy. In fact, the width of emission lines from a hollow cathode is usually limited only by Doppler broadening. Furthermore, the investigations are not limited to the gas substaining the discharge but also to refractory elements sputtered from the cathode. The metal concentration obtained by sputtering is far enough sufficient for spectroscopic purposes. For instance, the density of uranium atoms inside the hole of the cathode can easily be of the same order of that obtained in an oven at 2500 °C [102]. The discharge, being a sample under investigation and at the same time a part of the detection system, plays one more important role as a source of the studied species.

An advantage of the HC is that the weak plasma sample to be investigated is more localized than for other discharge configurations. This is of great importance when a uniform external field must be applied on the sample as in the case of Zeeman spectroscopy [103]. HC discharges properly designed for OG spectroscopy have been reported in the literature [92, 102, 104].

The third type of discharge which has been successfully applied to OG spectroscopy is the RF discharge. It presents several advantages. First of all, there are not internal electrodes, hence allowing to work with corrosive gases. Cleaner environment favours higher concentrations of the species of interest. This is, for instance, useful for the study of free radicals produced by the discharge itself. The situation is similar to the production of refractory atoms in a HC discharge. RF discharges can be run at considerably lower pressures than DC discharges, which can be of great importance for high-resolution spectroscopy. RF discharge is spatially uniform and the background noise level is not critically dependent on the gas pressure or type as for a DC discharge.

Sometimes, the RF discharge is the only solution as in the case of Vasudev and Zare who studied the HCO molecule [105]. They were able to maintain a very quiet RF discharge but failed to run a DC discharge because of carbonization of electrodes.

RF field is applied across the discharge tube and a pick-up coil wound around the tube is generally used to detect any laser-induced change in the RF field [106]. In such a scheme, the discharge plays the role of a transmitting antenna and the circuit that of a receiving antenna. The OG effect in the RF discharge has been also detected by either monitoring the reflected RF field in the oscillator power unit [107] or using two electrodes measuring the fluctuations of the current [108].

Because of the specific features and advantages of the different discharge

configurations, OG detection provided a powerful and broadband tool for investigation of an impressively large variety of atoms and molecules. This is illustrated in fig. 18*a*) and *b*). As seen from the diagram, the HC discharge is predominant in applications to atoms. For molecules RF discharges are mostly used.

a)

H	He	Ne	Ar	Kr	Xe			
★	★ ●	★ ● □	★ ●	★	□			
Li	Na	K	Rb	Cs				
●	▲ ●	▲ ●	▲	★ ▲ □				
Be	Mg	Ca	Sr	Ba			Eu	Yb
▲	▲	▲ ●	▲ ★	● ▲ ★			▲ ●	▲ ●
Cu	Mn	Co	Y	Zr	Mo			
●	●	●	●	●	●			
	Ga	In	Hg					
	▲	▲	★					
	La		Sm					
	●		●					
	U							
	●							

b) H_2, He_2, I_2, N_2, CO, NO, CN, H_2O, NO_2, HCO, NH_2, CO_2, HCO_2, H_2CO, HNO_3, $C_2H_2O_2$.

Fig. 18. – Atoms (*a*)) and molecules (*b*)) where OG effect has been observed. Table *a*) is from [109]. □ R.F.; ★ d.c. discharge, ● h.c., ▲ diode. More recently Camus *et al.* (private comm.) have used the OG effect with an ion Fe lamp for standard reference wavelength in the UV.

7. High-resolution OG spectroscopy.

The first experiment of Green *et al.* [83], in which a dye laser was used to irradiate a discharge, demonstrated the simplicity and sensitivity of the method. Since then, the interest for OG spectroscopy has rapidly grown. In fact, the development of the OG technique observed in the late seventies brought new ideas of its possible further applications. In the same period there was an explosion of new nonlinear laser techniques allowing to eliminate the Doppler broadening and then to observe high-resolution spectra. The OG technique using such a «dirty» medium as a discharge was probably underevaluated as good and serious candidate to high-resolution laser spectroscopy.

In 1978 Johnston [101] analysed one of the Ne transitions using a single-mode dye laser and observed the Lamb dip in the OG signal. This result opened new possibilities for optogalvanic detection method. Using intermodulated technique Schawlow and co-workers [110] presented in 1979 experimental measurements of hyperfine splitting in ^{3}He, demonstrating the applicability of OG technique to

quantitative high-resolution spectroscopy. This work showed that the previous avversion to the use of a discharge as a medium for high-resolution spectroscopy was erroneous. Of course, such a result could not be without consequences and soon many papers on high-resolution LOGS were published.

On the other hand, when analysing *a posteriori* the same facts, one can easily notice that many «clean» measurements in discharges had been performed previously. A good example is spectroscopy and transient effects of species which can be produced only in a discharge [111, 112].

At the discharge currents typical for OG spectroscopy, Stark broadening of lines is negligible. Using particular care in the design of the discharge, it is possible to reduce the perturbations to a level such that developing homogeneous linewidth limited spectroscopy makes real sense. In general the linewidths are determined by Doppler broadening. The homogeneous width is caused by pressure broadening, due to atom-atom collisions, while the effect of charged particles can be neglected.

7·1. *Saturation and intermodulated* OG *spectroscopy.* – Typical results obtainable when investigating OG effect with narrow-band tunable lasers are illustrated in fig. 19. The same HC discharge as for the recording shown in fig. 17 has been used. Here the buffer gas is Ar and the pressure is lower. The frequency of a single-mode Dye laser is scanned around the $^3P_0$ - $^3S_1$ transition of Calcium at 6102.7 Å (total scan 5 GHz). In *a*) the Doppler broadened line is

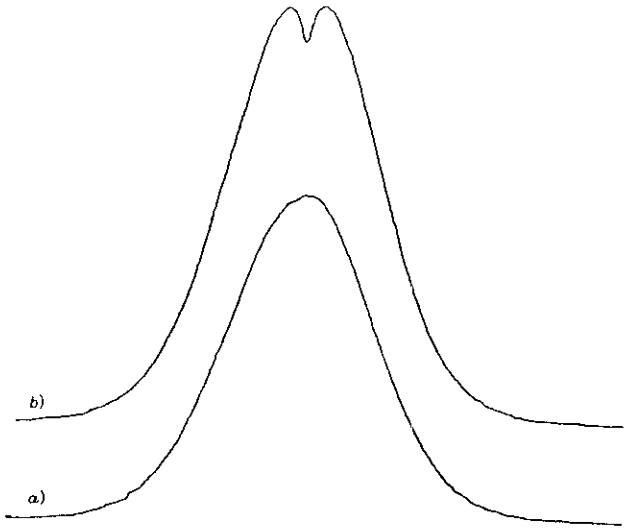

Fig. 19. – OG-detected 610.2 nm transition of calcium obtained by scanning narrow-band tunable laser. Single beam is used in *a*), and two counter-propagating beams in *b*).

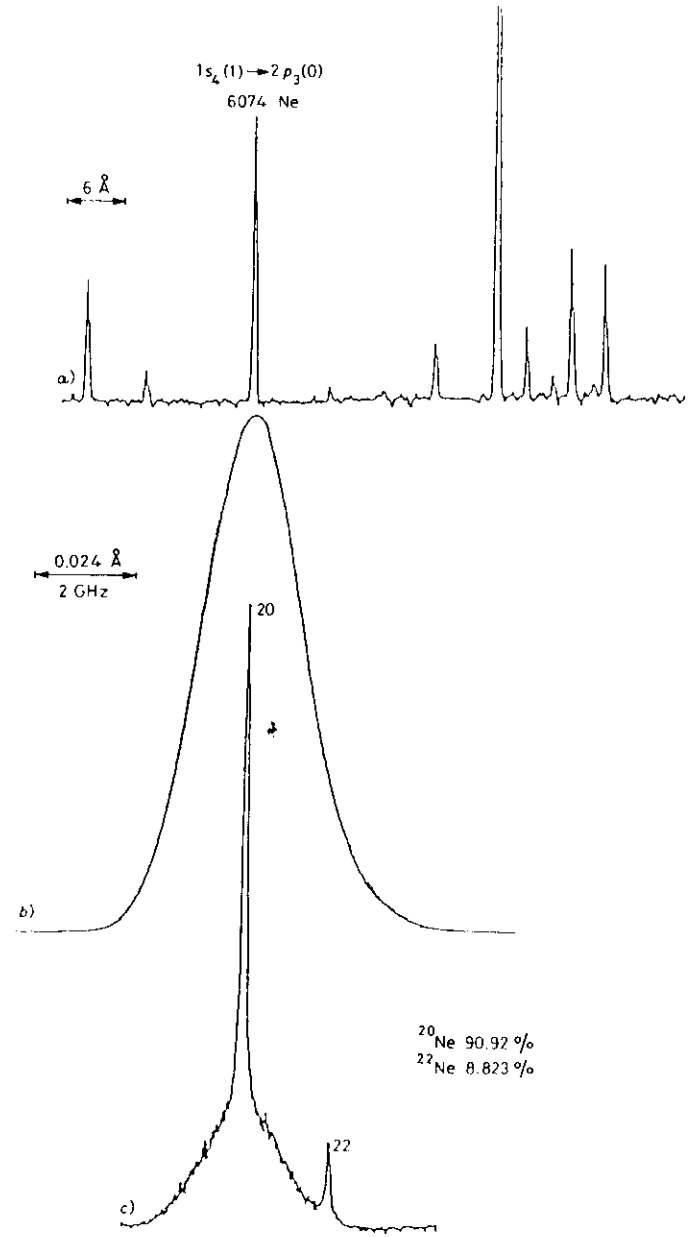

Fig. 20. – OG recordings for Ne discharge: *a*) broad-band scan around 607.4 nm, *b*) narrow-band scan of the Doppler-broadened 607.4 nm transition, *c*) IMOGS recording of the 607.4 nm with isotopic structure fully resolved.

recorded, with good signal-to-noise ratio. The Doppler width is about 1.4 GHz (FWHM), corresponding to a discharge kinetic temperature of about 600 K. Two counter-propagating laser beams are used in *b*) and a saturation dip is easily recorded at the centre of the Doppler profile. Because of the collisions, the homogeneous width of the dip is about seven times larger than the radiative width of the transition.

As already discussed in subsection 4·2, the signal-to-noise ratio for the saturation effect can be substantially improved using the intermodulated scheme. This is shown for the OG detection in fig. 20, where three recordings for a Ne discharge are reported: *a*) a portion of the spectrum obtained with a broadband scan around 607.4 nm; *b*) a narrow-band scan of the Doppler broadened transition; *c*) the intermodulated optogalvanic spectroscopy (IMOGS) recording. Natural abundance Ne had been used. The presence of two isotopic unresolved components causes an asimmetry in the *b*) profile. The isotopic structure is fully resolved in *c*). IMOGS is limited in sensitivity only by shot noise in the direct current substaining the discharge and compares favorably in sensitivity with other Doppler-free methods.

In ref. [110] the authors compare the sensitivity of IMOGS to that of Doppler-free saturated absorption. In IMOGS, the signal is detected as a change in the discharge current rather than a change in probe-beam intensity. Both signal (S) and noise (N) are very different in form from those in saturated absorption spectroscopy. Nevertheless, they tried to estimate the ratio $(S/N)_{IMOGS}/(S/N)_{sat.abs}$ and surprisingly they obtained as much as 100.

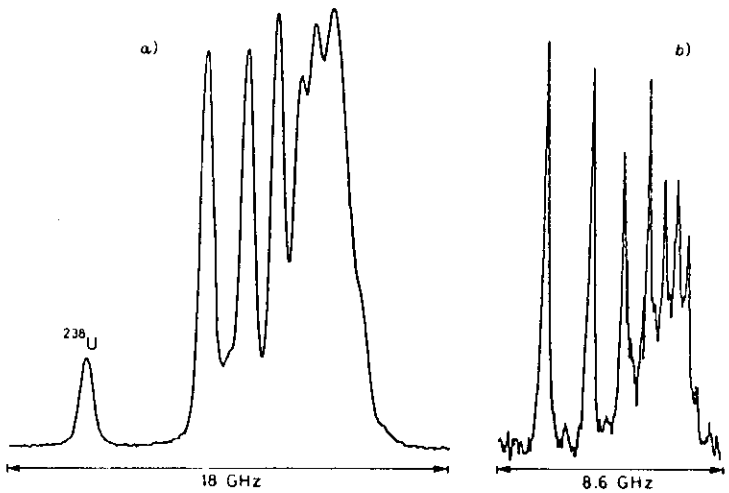

Fig. 21. – OG recording of the U transition at 591.5 nm. The Doppler-limited spectrum is shown in *a*), the Doppler-free intermodulated recording of the ^{235}U hyperfine structure is reported in *b*). From [102].

IMOGS allowed the Doppler-free studies of hyperfine structures and isotope shifts of many elements. Siegel *et al.* [113] measured the isotope shifts for nine transitions of Mo for five even isotopes, achieving linewidths as narrow as 25 MHz. Lorentzen and Niemax [114] reported isotope shift measurements of transitions between excited states of strontium isotopes 88 and 86 using a heat-pipe discharge tube. They were also able to measure optogalvanically both isotopic components of SrII-resonance line at 421.6 nm in a Doppler-free spectrum demonstrating the possibility of using the OG technique to Doppler-free laser spectroscopy of excited ionic levels. Doppler free h.f.s. studies by using IMOGS technique in the spectra of Mn, Co and La have been studied by Behrens [115] showing its applicability to elements with complex spectra. An example of complete resolution of the complex hyperfine structure of the 591.5 nm transition of ^{236}U is shown in fig. 21.

7·2. IMOGS *lineshape*. – In intermodulated spectroscopy, as already mentioned, the homogeneously broadened (Doppler free) lines are normally accompanied by broad Doppler-limited pedestals which result from velocity-changing collisions with rare-gas atoms occurring during the lifetime of the lower level of the transition. The ratios of the height of the homogeneously broadened (Doppler-free) signal to that of the inhomogeneously broadened signal (Doppler-limited background) is dependent on operating pressure and current. Siegel *et al.* [113] noticed a reduction in the relative intensity of the pedestals with increasing discharge current. The effect was interpreted in terms of a shortening of the lifetime of the lower levels through inelastic collisions with electrons in the HC discharge and the corresponding reduction in the number of velocity-changing collisions that can occur during this lifetime. Recently Gough and Hannaford [116] have shown the possibility of suppressing Doppler-limited pedestal by operating the discharge at moderately high current density. The quality of some of the spectra reported, in terms of linewidth and freedom from pedestals, was comparable with that obtained for the same transitions in the much cleaner environment of an atomic beam [117].

At constant operation parameters of the dicharge (pressure, current), the «pedestal» is expected to be higher for transitions originating from metastable or ground states because of the longer lifetime at disposal for the velocity-changing collisions. This is illustrated in fig. 22, where the same HC discharge has been used to investigate the IMOG lineshape for different transitions in Ne. The velocity-changing collisions pedestal is significantly more pronounced for transitions starting from metastable levels (the lower two). Natural abundance neon was used for the measurements and the isotopic shift (IS) between Ne^{20} and Ne^{22} could be evidenced.

Recently Belfrage *et al.* [118] have used IMOG technique in a neon discharge to measure isotopic shifts.

The Doppler-free lineshape is determined by the particular transition under

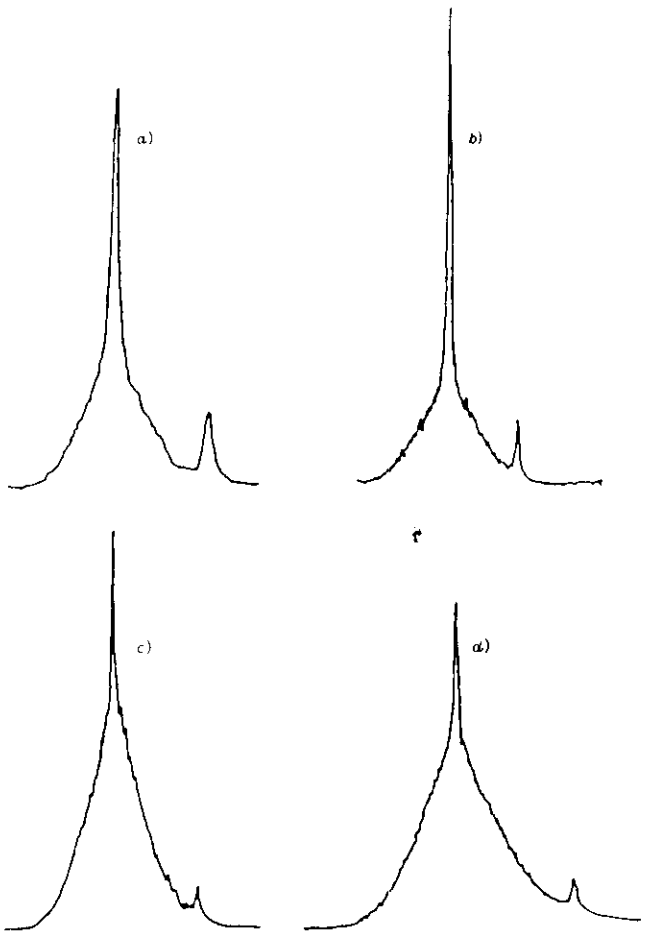

Fig. 22. – Doppler-free intermodulated recordings of natural neon transition involving (lower two) or not (upper two) metastable levels. From [138]. *a*) 5852.5 Å, $1s_2(1)$-$2p_1(0)$, IS: 2.3 GHz; *b*) 6074.3 Å, $1s_4(1) \rightarrow 2p_3(0)$, IS: 1.7 GHz; *c*) 5944.8 Å, $1s_5(2) \rightarrow 2p_4(2)$, IS: 1.6 GHz; *d*) 5881.9 Å, $1s_5(2) \rightarrow 2p_2(1)$, IS: 1.7 GHz.

investigation and by the atoms which are partners in the collisions. The effects produced by collisions on saturated absorption spectroscopy have been the subject of several investigations, both theoretical and experimental. For instance, interesting results can be found in [119-122] and in the recent review by Chebotayev [123].

Recently, Tenenbaum *et al.* [124] reported a systematic study of ^{238}U transitions lineshape of saturated absorption spectroscopy including velocity-

changing collisions. In their case a relatively low density (10^{-5} Torr) of uranium atoms was produced in the presence of helium or xenon buffer gases at a pressure of 0.1 to 10 Torr. Essentially, the uranium atoms were embedded in a bath of perturbers, *i.e.* in an experimental environment similar to that of optogalvanic spectroscopy of elements sputtered into the discharge from the hollow cathode.

The observed lineshapes were interpreted on the basis of a generalized phenomenological model including «strong» and «weak» collisions (Kolchenko *et al.* [125]). «Strong» collisions (heavy-mass atom perturber) tend to reproduce a Gaussian distribution, yielding a signal with a central Lorentzian sitting on a Gaussian background; «weak» collisions (low-mass atom perturber) are, on the contrary, characterized by a small relative velocity change. The effect of a great number of successive weak collisions is described by the Fokker-Plank diffusion model and yields for the lineshape an exponential sitting on a Gaussian.

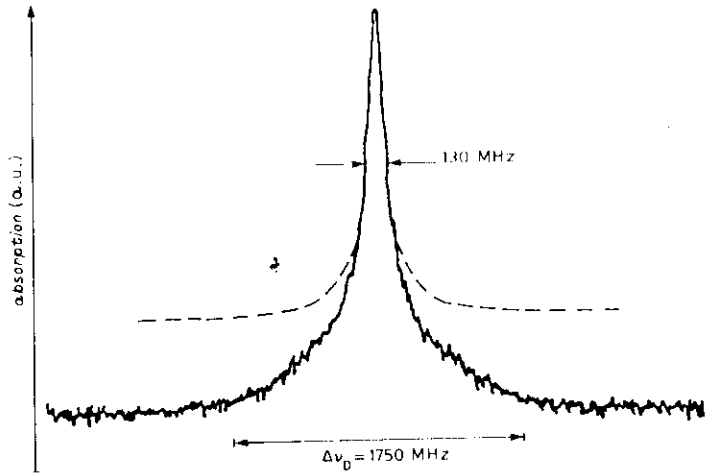

Fig. 23. – Intermodulated OG recording for the Ca transition at 612.2 nm. Doppler-free line shape is fitted to a Lorentzian one (dashed curve).

An example of the first case is shown in fig. 23. The intermodulated optogalvanic spectrum was recorded for a transition of calcium ($m = 40$) in a buffer gas of argon ($m = 40$). The predominant collisions here are «strong» and actually the Doppler-free lineshape can be fitted to a Lorentzian (dashed curve). In ref. [116] the case of weak collisions, yielding an exponential lineshape, was illustrated for uranium transition in the presence of He buffer gas. The optogalvanic intermodulated recording was obtained in [102] using neon as buffer gas. A typical lineshape is reproduced in fig. 24. In the fit of the shape there was no evidence of a predominance of either the exponential weak

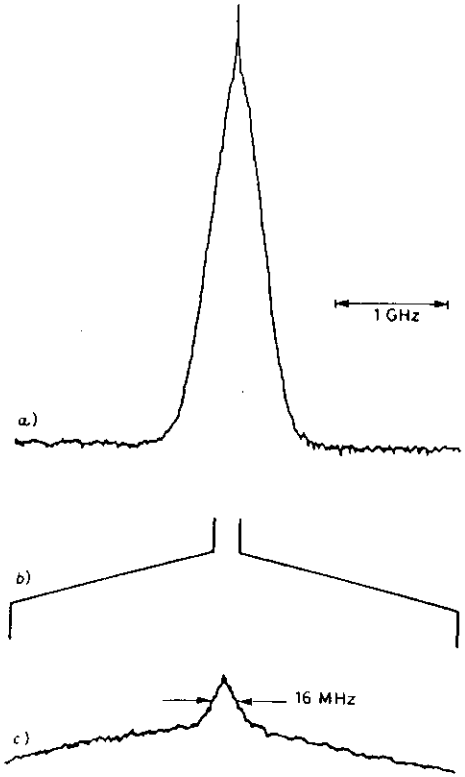

Fig. 24. – IMOGS line shape of the ^{235}U transition at 591.5 nm. From [102]. *a*) 1.1 Torr Ne, 50 mA.

collisions or the Lorentzian strong-collision contribution. This suggested that neon could be considered of «intermediate strength» compared to the external cases observed in [124] (He and Xe).

7·3. POLINEX OG *spectroscopy*. – Polarization intermodulated excitation (POLINEX) was introduced by Hänsch *et al.* [126] and is related to other intermodulated saturation techniques. In the case of POLINEX the chopper is replaced by two polarization modulators, which modulate the polarizations of the two beams at two different frequencies, producing, for instance, alternating left and right-hand circular polarizations, while leaving the intensities unchanged. When the laser is tuned so that both beams are interacting with the same atoms, the total rate of absorption will still be modulated at the sum or difference frequency and because of the combined rate of excitation will, in general, depend on the relative polarization of the two beams. If the two beams have identical

polarization, both lightfields will be preferentially absorbed by atoms of the same orientation. On the contrary, if the two beams have different polarizations, they will tend to interact with atoms of different orientations. The POLINEX signals are due to light-induced atomic alignment or orientation and their magnitude can be predicted with the help of simple rate equations [126].

The Doppler-broadened background caused by velocity-changing collisions in IMOG spectroscopy is absent in POLINEX spectroscopy. This is caused by the fact that the cross-section for disorienting collisions is at least of the same magnitude as the cross-section for velocity-changing collisions. A typical POLINEX optogalvanic recording is shown in fig. 25. In that case, a radiofrequency discharge was used and the POLINEX OG spectrum (top) is compared with the IMOG spectrum (bottom) for the Ne $2p_2$-$1s_5$ transition at 588.2 nm.

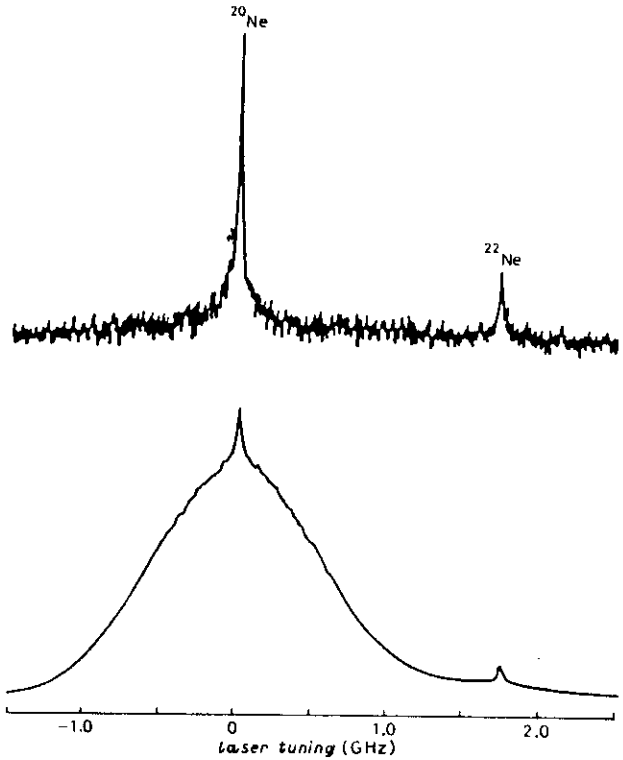

Fig. 25. – Doppler-free spectrum of the Ne $2p_2$-$1s_5$ transition at 588.2 nm recorded by POLINEX RF OG spectroscopy (top) and IMOG detection (bottom). From [127].

7·4. *Doppler-free Zeeman* OG *spectroscopy.* – It is well known that a discharge can be operated in the presence of an external magnetic field. Only, particular care must be put in the configuration of the discharge and on the relative geometry of the magnetic field. These constraints, added to those imposed by the optical geometry for sub-Doppler laser-atom interaction, could seriously affect the feasibility of high-resolution Zeeman optogalvanic spectroscopy. On the contrary, in 1982, Zeeman high-resolution spectroscopy was reported independently in a glow discharge [128], with conventional optical detection, and in a hollow cathode [103], with unconventional OG detection. In [128] the sub-Doppler spectrum of a He transition in a low discharge was recorded on the conventional probe beam transmission from the saturated system. Zeeman components were recorded with a linewidth of the order of few hundred MHz. On the contrary, really optogalvanic detection was used in [103], combined with an intermodulation scheme. The hollow-cathode configuration allowed the resolution of Zeeman components of transitions of both the buffer gas and the atomic element sputtered by the cathode.

In fig. 26 it is shown a Doppler-free Zeeman intermodulated recording of the Ca transition $^3P_0$ - $^3S_1$ at 610.27 nm. In the upper trace a small magnetic field (86 G) is sufficient to resolve the $\Delta M = 1$ and $\Delta M = -1$ components, since neither

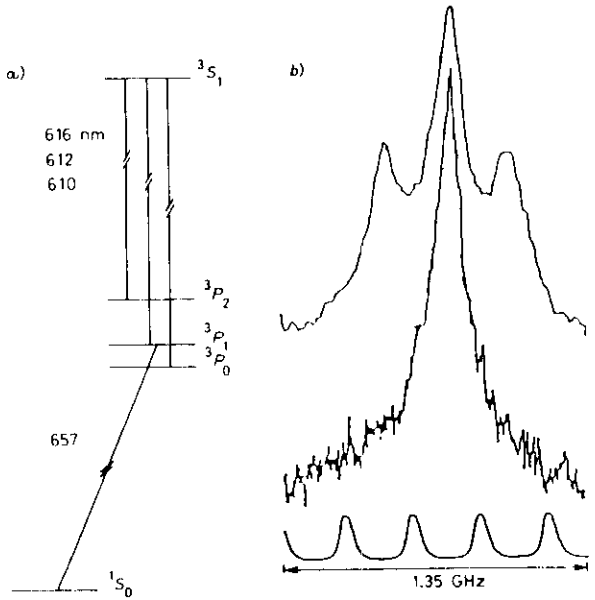

Fig. 26. – Simplified energy scheme of the lower levels of Ca (*a*)) and Doppler-free Zeeman intermodulated OG spectroscopy of the 610.27 nm transition (*b*)). Upper trace corresponds to 86 Gauss and lower trace to 0 Gauss. From [103].

the signal-to-noise ratio nor the sensitivity are affected by the external field. In addition to the two Zeeman components also the central cross-over peak is recorded because the two transitions share a common level ($^3P_0$).

The dependence of the Zeeman splitting on the magnetic field can be easily investigated as shown in fig. 27 for the $1s_4(J = 1) - 2p_3(J = 0)$ Ne transition at 607.4 nm. Also in this case linear laser polarization was orthogonal to the static magnetic field, so that $\Delta M = 1$ and $\Delta M = -1$ Zeeman components were recorded together with the cross-over signal.

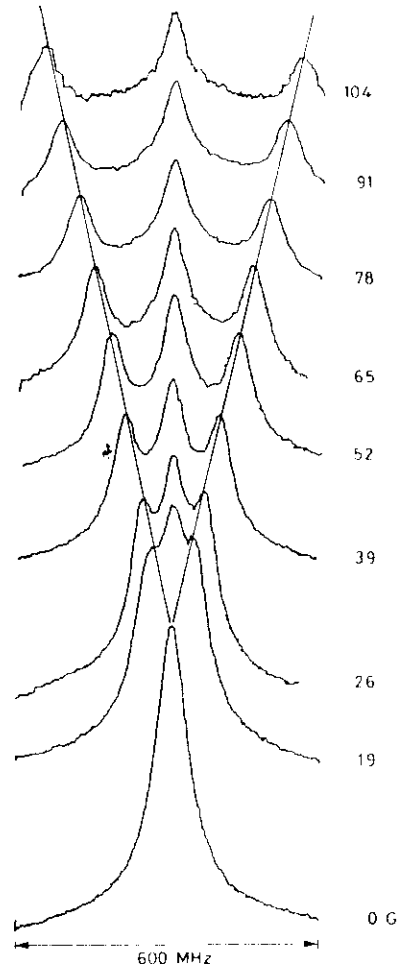

Fig. 27. – Dependence of the Zeeman splitting on the magnetic field for the Ne transition at 607.4 nm.

These results opened the possibility of measuring weak magnetic fields in a discharge. They also could turn out in applications in the study of collisional transfer between magnetic sublevels. For instance, an effect of the velocity-changing collisions on the cross-over signal can be seen in the results of fig. 28.

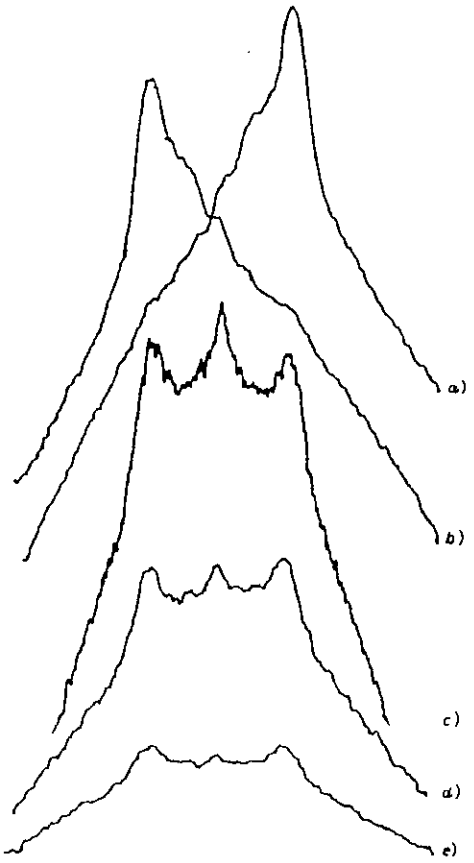

Fig. 28. – Intermodulated Zeeman spectroscopy of the Ne $1s_5$-$2p_2$ transition at 588.2 nm recorded for different polarization of laser beam (*a*) circular right, *b*) circular left, *c*)-*e*) linear orthogonal to the magnetic field).

Here intermodulated Zeeman spectroscopy measurements were performed for a Ne transitions starting from a metastable level, namely the $1s_5(J = 2)$-$2p_2(J = 0)$ transition at 588.2 nm. The magnetic field was the same (65 G) for all the five recordings. In *a*) and *b*) the laser polarization was circular (right and left) so that only the components $\Delta M = +1$ and $\Delta M = -1$ were excited. In *c*)-*e*) the laser

was linearly polarized orthogonal to the magnetic field. The Ne gas pressure was decreased from 900 mTorr in *c*) to 750 mTorr in *e*). It can be observed a dependence on the pressure of the crossover signal intensity relative to the $\Delta M = \pm 1$ signals.

The results so far described demostrated that Doppler-free optogalvanic spectroscopy can be an interesting diagnostic method to measure local magnetic fields under conditions where probe measurements are not possible.

7·5. *Two-photon* OG *spectroscopy.* – In a discharge, essential for the OG spectroscopy, the population is not limited to the ground or close-lying levels, as, on the contrary, is typical for usual gas phase measurements. As a consequence in a discharge the request for two-photon excitation is significantly reduced, which is exclusive in other situations, in order to reach certain high-lying levels. In fact, the richness of the emission spectra is likely to provide accessible one-photon transition to reach a given level.

On the other hand, since the experiment is performed in a discharge environment, the galvanic detection provides advantages with respect to the detection of fluorescence. In fact, the fluorescence induced by the two-photon excitation could be partially masked by the fluorescence induced by the discharge. Optogalvanic detection overcomes this difficulty by detecting the changes in level population caused only by the two-photon excitation.

In the first [129] Doppler-free two-photon optpgalvanic spectroscopy (TOGS) experiment, transitions originating from ^{20}Ne both metastable and nonmetastable levels were recorded in a DC discharge. The signal was enhanced by placing the discharge inside the laser cavity. Incidentally, this was accomplished by quite modest modifications to the outcoupling geometry of a commercial single-frequency dye laser.

In a subsequent work [130] Doppler-free two-photon optogalvanic spectroscopy was reported for a couple of transitions starting from the He metastable ^3S state. In this case, a narrow-band pulsed dye laser was used. Counter-propagating-waves configuration allowed a sub-Doppler recording with partial resolution of the fine structure of the transitions.

7·6. *Optical-optical double resonance.* – Optical-optical double resonance is a well-established method for high-resolution atomic or molecular spectroscopy. The method is applied to a tree-level system (cascade or ladder-type), say level 1-2-3, resonantly interacting with two laser beams of different frequencies w_{12} and w_{23} propagating either in the same direction or in opposite directions [131]. In a typical conventional arrangements the saturation phenomena produced by one laser beam (pump) are monitored on a connected transition through the absorption (or emission) of the other beam (probe).

One of the advantages of this technique is that it is a state selective one. An energy level is, in fact, identified by its being common to two optical transitions

or, also, two nearby levels coupled by collisional energy transfer can act as «commom level». The feature of state selectivity can be a significant advantage in the analysis of extremely dense spectra, like those obtained, for instance, in molecular discharges. For this its extension to optogalvanic detection was suggested [132] as very interesting. The interest is increased by the fact that other state-selective techniques such as laser-induced fluorescence [133] or laser-

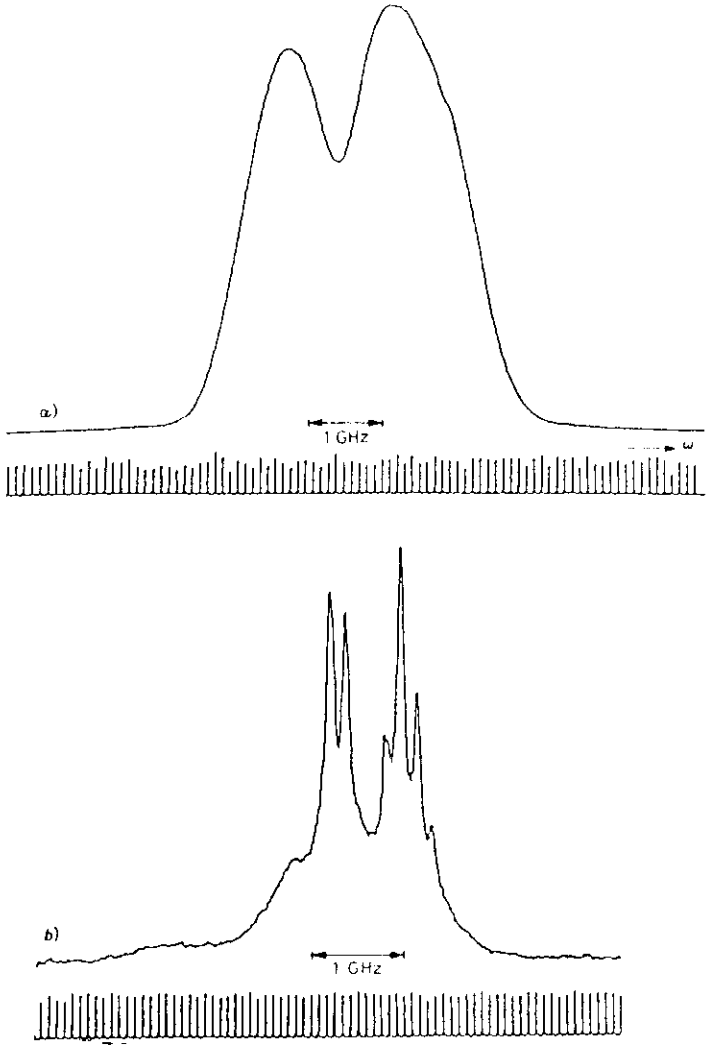

Fig. 29. – Doppler-limited OG recording of gallium transition at 417.2 nm (*a*)) and optical-optical-double resonance recording with two parallel laser beams (*b*)). From [137].

induced polarization spectroscopy [134], can be efficiently applied to radiating plasma discharges.

The first experimental optogalvanic double-resonance spectroscopy measurement was reported in [135]. The elements studied were neon, uranium, and sodium in a commercial hollow-cathode discharge. Two different tunable dye lasers were used, say A and B. The OG signals associated with laser «A» were significantly increased when laser «B» irradiated a transition terminating in a common intermediate level. An important result of this work was that energy transfer, occurring to a nearby level not common to both laser irradiations, was evidenced to cause a conjunctive signal. Energy transfer can be a problem when the technique is used to determine a common intermediate level. But, on the other hand, the effect can give interesting information concerning energy-transfer processes in atoms and molecules.

The efficiency of the optical-optical double-resonance technique in recording simplified complex molecular spectra was demonstrated in [136]. It is worth noting that both in [135] and [136] Doppler-broadened signals were reported. On the contrary, the sub-Doppler lineshape in this case is an important feature to be investigated, particularly for studies of energy transfer mechanisms.

For instance, an opened question is whether energy transfers are caused by simple atom-atom collisions or if there is an important intermediate role of the electrons in the discharge. The two effects could be discriminated since the first can produce Doppler-free lineshapes. Also, in this case the velocity changing cross-section could be compared with that for energy transfer collisions.

Doppler-free optical-optical double-resonance spectroscopy was reported simultaneously by [137] and [138]. Sharp Doppler-free signals on a broad pedestal allowed [137] to resolve the hyperfine structure and isotopic shifts in indium and gallium atoms introduced by sputtering in a hollow-cathode plasma.

A typical experimental result is summarized in fig. 29. The Doppler-limited OG recording of the transition at 417.206 nm is shown in *a*). To obtain Doppler-free signals, a second collinear laser beam at 641.4 nm, amplitude modulated, was sent into the discharge. The frequency of modulation was sent as reference to a lock-in amplifier. When the first laser was scanned now the sub-Doppler spectrum was obtained *b*).

A study of the lineshape is shown in fig. 30. In this case the two laser beams were counterpropagating. Both the beams were amplitude modulated at frequencies, respectively, f_1 and f_2. The reference at the sum $f_1 + f_2$ was sent to the lock-in amplifier. The wavelength of one of the lasers was fixed and the signal at $f_1 + f_2$ was recorded by scanning the wavelength of the other. The homogeneously broadened signals is well evident over the large background caused by velocity changing collisions (note that the common level shared by two transitions is metastable, as also shown in fig. 22). Different atomic velocity groups could be selected by changing the wavelength of the fixed laser within the Doppler profile.

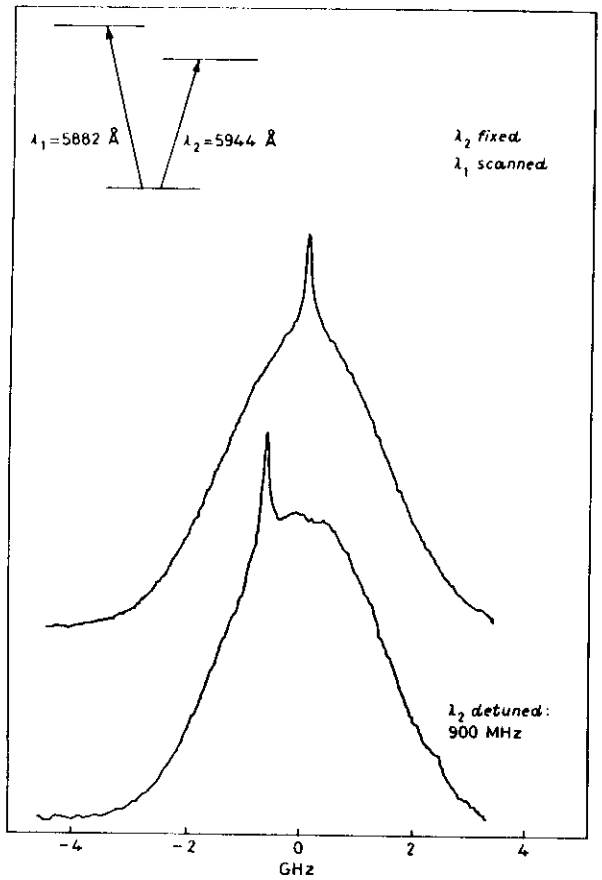

Fig. 30. – Optical-optical double-resonance Doppler-free OG spectroscopy in Ne. The two laser beams intensity was about 100 mW and the gas pressure 1 Torr. From [138].

7·7. *Optical pumping.* – As is well known, optical pumping consists in the creation of nonscalar (*i.e.* noninvariant in rotations) observables induced in an atomic or molecular gas by light absorption. For instance, the optical pumping can result in the orientation or alignment of a given level. As it was early recognized [139] the orientation of metastable atoms in a discharge by optical pumping modifies the number of produced electrons, hence affects the discharge impedance.

There are various mechanisms which may relate nonscalar observables created by optical pumping to the discharge impedance. For instance, the discharge impedance can be directly related to the atomic alignment when an anisotropy, for instance arising from the electronic motion [140], exists in the

discharge. However, the change of impedance can be obtained after optical pumping or alignment, also in case of isotropic discharge [141-143].

Pinard and Julien [143, 144] have carefully used the OG method to detect the optical pumping in metastable states of Ne. They performed experiments using both a single pumping beam and two pumping beams from the same laser counterpropagating in the cell. The signal arises from two interactions of a given atom with the pumping beams and it is Doppler free as shown in fig. 31. For these atoms, with no longitudinal velocity, the depletion due to crossed pumping effects is different according as the two beams have the same circular polarization or not. The background which appears under the Doppler-free signal may have two origins. In addition to velocity, changing collisions, already discussed for intermodulated and POLINEX spectroscopy, then could also be a contribution of ionizing collisions between two oriented metastable atoms.

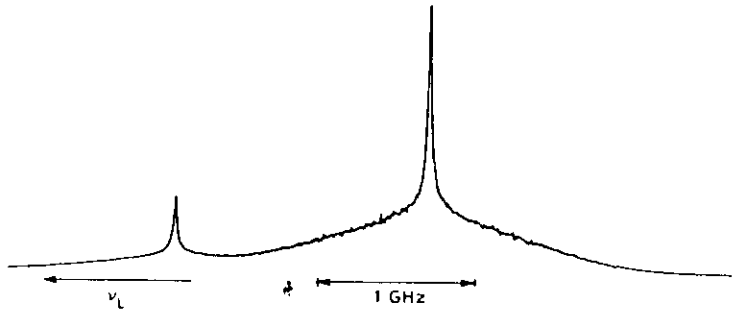

Fig. 31. – OG signal due to electronic orientation in the $^3P_2$ state obtained with two counterpropagating pumping beams frequency swept through atomic resonance at 614.3 nm. From [143].

7·8. *Hanle effect and level crossing.* – As we have been discussing so far, mostly all the high-resolution laser techniques, yielding homogeneous linewidths, have been applied to OG detection. However, it is worth noting that also the limit of homogeneous linewidth could be overcome. This was accomplished by means of nonlinear Hanle effect (NLHE).

The effect was already discussed in the section devoted to OA detection. The main difference is that the investigations with OG detection are performed on atoms instead of on molecules. A variety of atomic transitions, involving various quantum numbers and selection rules could be investigated and the results could be quantitatively compared with a theoretical model [60].

The effect manifests itself as an increase in the OG signal when a static uniform magnetic field, orthogonal to the laser polarization, is applied to the discharge and removes the zero-field degeneracy. It could be observed for several atomic elements from Ne to Ca, Zr, Yb [60, 142, 145].

The effect was also extended to level crossings at finite fields by Hannaford and Series [146]. A practical result was the measurement of gyromagnetic factors and hyperfine structures in ground and excited ^{89}Y atomic levels.

But let us come back to the subhomogeneous linewidth recordings by means of optogalvanic NLHE. This possibility originates from the fact that one can separate the contribution to the signal linewidth of the degeneracy removal in the upper and lower state of the optical transition. In ref. [147] this was

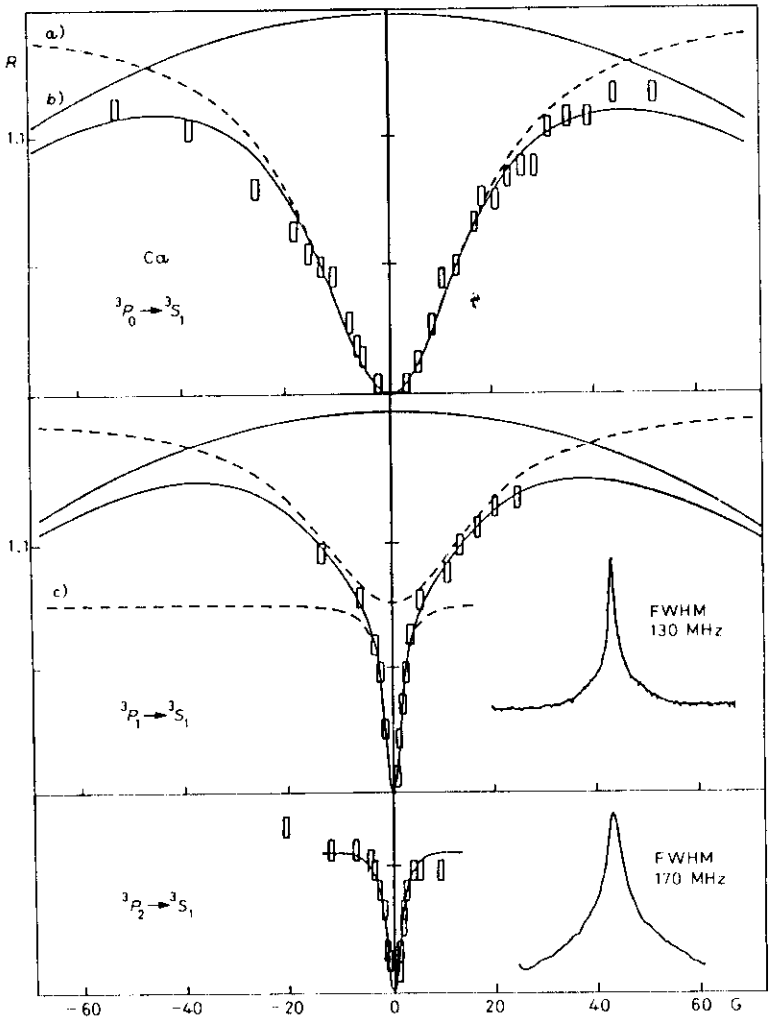

Fig. 32. – Experimental demonstration of sub-homogeneous linewidth OG spectroscopy by means of NLHE. Details are discussed in the text. From [147].

evidenced using the fine-structure Ca triplet starting from the metastable ^3P levels to the $^3S_1$ level. A hollow-cathode discharge was used to produce metastable atoms. A first experiment was performed on the $^3P_0$-$^3S_1$ transition at 610.2 nm. In this case the Zeeman degeneracy to be removed by the magnetic field is only in the upper level of the transition and the lower $^3P_0$ level does not contribute to the effect. As a consequence the experimental results of the enhancement of the OG signal as a function of the magnetic field can be fitted using the Lorentzian corresponding to the Zeeman tuning in the $^3S_1$ level. This is shown in fig. 32*a*). Note that the real fit is performed subtracting from the Lorentzian lineshape (dashed curve) a Gaussian curve to take into account also the Zeeman tuning out of resonance of the Doppler-broadened absorption.

The second measurement was performed on the $^3P_1$-$^3S_1$ transition at 612.2 nm. In this case, there are two independent NLHE, in the upper and in the lower state. As a consequence the lineshape is the sum of two Lorentzians of the same height and different widths, corresponding to different g factors and broadenings of upper and lower levels. In the fit shown in fig. 32*b*) the parameters of one Lorentzian were fixed to those obtained in the previous case, while from the second Lorentzian it was obtained for the $^3P_1$ level a FWHM corresponding to 8 MHz. Note that this width is much smaller than the homogeneous linewidth of the transition as obtained from the intermodulated spectroscopy recording shown in the inset.

The case of the $^3P_2$-$^3S_1$ transition at 616.2 nm is more complicated to be analysed [60, 147] but, again, a resonance width much narrower than that for the optical transition was obtained as shown in fig. 32*c*).

It is worth noting that these results demonstrating the possibility of subhomogeneous linewidth also evidence the limitation of OG detection for very high-resolution spectroscopy. In fact, the ^3P triplet in Ca is metastable, hence the radiative widths are of the order of few hundred Hz. The observed resonances are broadened because of collisions in the discharge. Recently, the same experiment has been performed [148] on an atomic beam and widths three orders of magnitude smaller than those for the OG detection were observed.

8. – OG Spectroscopy of Rydberg atoms.

There has been in the last years a strong interest in the spectroscopy of Rydberg states. Due to tunable and narrow-band laser sources high-lying single Rydberg levels could be selectively excited and investigated by means of various detection techniques. The OG method was applied to detect transitions involving Rydberg states in 1979 by Katayama *et al.* [149] who observed atomic helium transitions from the metastable $2s^1S$ state to high ($n = 14$ to 36) Rydberg states, and by Camus *et al.* [150] who investigated highly excited levels of barium atoms. Since then other atoms have been also investigated.

Interesting results were obtained by studying Rydberg states in Xe atoms. Labastie *et al.* [151] determined the first ionization limit and quantum defects. OG detection method was then applied to study collisions between a Rydberg atom and a rare-gas atom in the ground state allowing to determine the shifts and broadenings of the optical lines connecting the $6p^5 6p$ configuration to various states [152]. Lemoigne *et al.* [153] have demonstrated that the system constituted by a Xe atom in a strong magnetic field allowed to study the diamagnetic behaviour of highly excited Rydberg states.

Although the OG effect turned out to be very sensitive and it was successfully used for transitions in the visible, the technique did not seem to be applicable in the infrared. There were essentially two reasons for that. First of all, highly excited states tend to be very closely spaced, and upper and lower levels might have comparable probabilities for collisional ionization. On the other

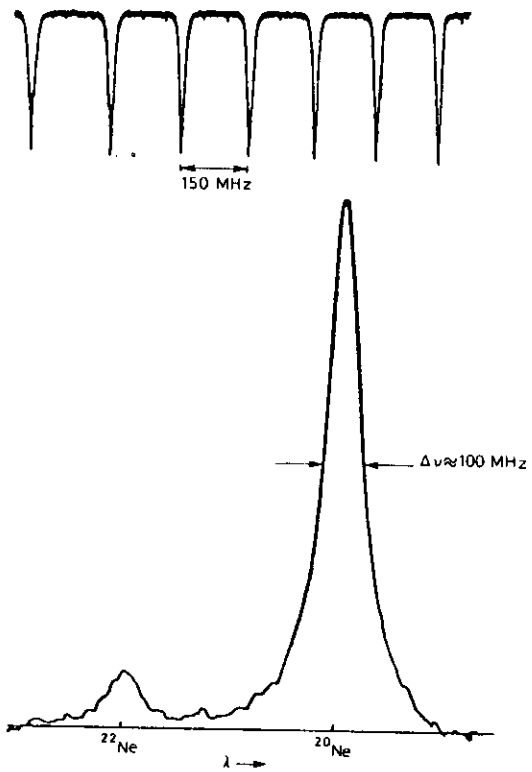

Fig. 33. – Doppler-free scan of Ne $3s_5$-$5p_{10}$ transition at 2.55 μm. The relative strengths of the lines from the two different isotopes are proportional to the natural abundances. The upper trace displays frequency markers. From [156].

hand, for levels very close to the ionization limit, the probability of collisional ionization might be higher than that of population of this high lying states. Observation of Jackson *et al.* [154] indicated, however, that the OG technique could become a sensitive detection tool also for spectroscopy in the infrared. Using a colour centre laser operating near 2.6 μm, they detected OG spectra in H and He atoms for transitions from $n = 4$ to $n = 6$ states. It is worth noting that very low concentrations of excited atoms ($6 \cdot 10^5$ cm^{-3}) could be detected at these long wavelengths which seems to be promising for systematic atomic and molecular spectroscopy in the infrared.

Infrared OG measurements using colour centre laser were further extended [155] to Rydberg states of Ne and Ar as well as to Li and Ba atoms sputtered from the cathode in a HC discharge.

Finally, the Doppler-free measurement by intermodulated OG spectroscopy have also been performed [156]. By studying highly excited states in He and Ne atoms in a HC discharge, tube lines as narrow as 60 MHz were observed. Doppler-free scan of the $3s_5$-$5p_{10}$ transition is shown in fig. 33.

As far as molecules are concerned, the OG technique was applied to a study of the Rydberg states of N_2 [157] excited in a RF discharge. Two visible bands were investigated, first with a Doppler-limited resolution of 0.05 cm^{-1}. Then a Doppler-free method was also applied to resolve overlapped lines. Precise wave numbers were determined for the rotational transitions of the two Rydberg bands.

9. – Calibration spectroscopy.

As we have been describing so far, OG detection is a simple tool for recording atomic or ionic spectra of both gaseous and refractory elements. The spectral lines, being essentially Doppler broadened can be useful for quick calibration of the wavelengths of tunable laser sources. This possibility was early recognized by King *et al.* [158] who used commercial HC lamps to calibrate dye laser wavelenghts in the visible. They demonstrated that the bandwidths could be determined down to 0.01 nm and laser wavelengths for single-frequency excitation experiments to 10^{-4} nm. More recently [159] an automated pulsed dye laser calibration was reported using OG detection combined with microprocessor control.

The electric signal derived from the discharge irradiated by a c.w. dye laser can be used to lock the laser to characteristic transition frequencies of species in the discharge, as early demonstrated by Green *et al.* [160]. Again, the advantage of the technique was that the same apparatus could be used for locking the laser to various atomic and molecular transitions.

Keller *et al.* [161] introduced an atlas for OG wavelength calibration based on uranium transitions. They compared the atlas with an optical one. Uranium is an

excellent wavelength standard because it is heavy, essentially monoisotopic, vith no hyperfine structure and with a dense spectrum from the UV to IR region. Some of the uranium transitions were measured to high accuracy combining OG detection with wavemeter determination of dye laser frequencies [162]. Wave numbers for several reference transitions could be given with 0.0006 cm^{-1} uncertainty. The uranium OG atlas was actually used for wave length calibration of pulsed lasers [163].

Stoicheff and co-workers used OG calibration for their experiments on vacuum UV laser spectroscopy. The VUV radiation was generated by four-wave frequency mixing (4-WFM) in Mg and Zn [164, 165]. Two dye lasers were used. One was tuned to a two-photon ($2\nu_2$) allowed transition in the nonlinear medium, while the other freely variable. VUV radiation was generated at the sum frequency $2\nu_1 + \nu_2$. The wavelength was determined by exciting the OG spectrum of a uranium neon commercial HC lamp with a small portion of the tunable dye laser radiation (ν_2). The OG signal was averaged in a channel of the box-car averager and displayed simultaneously with the VUV spectrum. A typical scan is shown in fig. 34. The unknown frequencies in the VUV region could be determined with a final absolute accuracy of about 4 parts in 10^6.

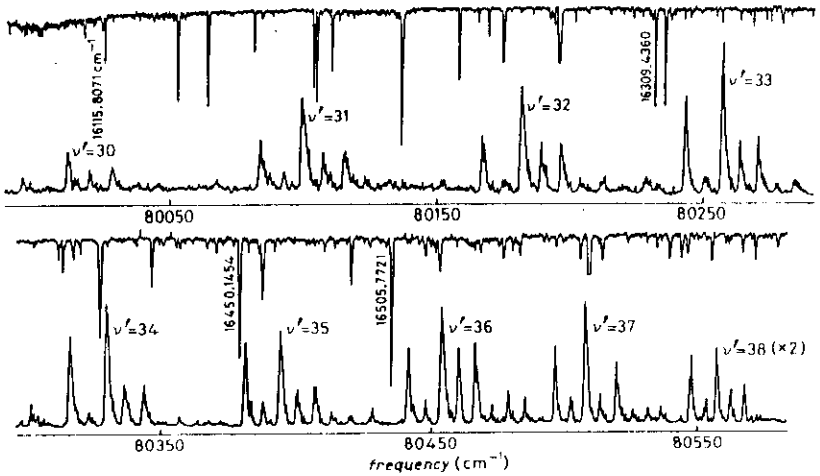

Fig. 34. – Fluorescence excitation spectrum of Kr_2 near 124 nm showing different vibronic bands with structure due to isotopic molecules. The upper traces are OG spectra of U used for wavelength calibration. From [165].

OG detection was also used as a secondary-frequency standard in the measurement of fundamental atomic transition [166]. Here the 1^3S_1-2^3S_1 two-photon transition of positronium was observed and measured. The frequency of the laser at 486 nm was obtained by simultaneously measuring a Doppler-free

Te_2 molecular line via saturation spectroscopy. As a secondary-frequency standard the $n=2\rightarrow 4$ lines of deuterium, recorded by Doppler-free OG spectroscopy in a Wood discharge tube, were used.

Further developments can be forecast in the application of OG detection to spectral calibration. For instance, Webster [167] suggested the use of OG calibration for laser-based techniques in monitoring of atmospheric species. The spectral complexity of the atmosphere makes secondary wavelength standards often unacceptable. The proposal was, when searching for a given stable or free radical or ionic species in radiation from the atmosphere, to use discharges to produce in laboratory the same species, possibly unstable, and simultaneously recording the laboratory spectrum with OG detection.

10. – Conclusions.

Each of the techniques, conventional or nonconventional, developed for spectroscopic applications presents its advantages and disadvantages, and, of course, none meets the needs of all possible experiments. As we have discussed in the present review, much work has been reported for OG detection systems. Good sensitivities and spectral resolution have been demonstrated in an impressively broad variety of cases. In several situations, the discharge is in any way necessary for the production of the species under investigation, and the OG detection does not introduce additional dirtiness in the system.

Of course, really high-resolution spectroscopy will be seriously limited in comparison with other existing, cleaner techniques. We have discussed this aspect in subsect. 8·8 comparing linewidths obtained in a discharge with those recorded on an atomic beam. By using an optical heterodyne absorption method, Hall and co-workers [168] demonstrated an enhancement in signal-to-noise ratio of more than 1000 compared to results from OG experiment.

Nevertheless, the OG technique though not achieving a fundamental noise limit has a real advantage in its inherent simplicity.

We think that it will continue to be developed in several laboratories both for spectroscopic applications and to extract information useful in the diagnostic of discharges.

Note added in proof.

During the time interval between this review paper was submitted for pubblication and the proofs received, several new works have been performed using unconventional techniques. This gives evidence of the still growing interest in this field.

Completely new possibilities were opened thanks to the use of optogalvanic detection in cases where no alternative methods are accessible. For istance CO laser could be, for

the first time, frequency stabilized and now is available for high-resolution specroscopy (M. Solmeeder, A. Hinz, A. Groh, K.M. Evenson, W. Urban, *Appl. Phys. B*, to be published).

Also, radiofrequency OG detection made possible the development of the firts c.w. sub-Doppler optical spectroscopy of atomic oxigen (M. Inguscio, P. Minutolo, A. Sasso, G. Tino, *Phys. Rev. A*, to be published).

REFERENCES

[1] M. CIOCCA, A. SASSO and E. ARIMONDO: to be published.
[2] E. ARIMONDO, M. G. DI VITO, K. ERNST and M. INGUSCIO: *Opt. Lett.*, **9**, 530 (1984).
[3] G. ALZETTA, E. ARIMONDO, C. ASCOLI and A. GOZZINI: *Nuovo Cimento B*, **52**, 379 (1967).
[4] A. G. BELL: *Philos. Mag.*, **11**, 510 (1881).
[5] W. C. RONTGEN: *Philos. Mag.*, **11**, 308 (1881).
[6] J. TYNDALL: *Proc. Roy. Soc. London*, **31**, 307 (1881).
[7] C. F. DEWEY: in *Optoacoustic Spectroscopy and Detection*, edited by Y. H. PAO (Academic Press, New York, N. Y., 1977).
[8] A. ROSENCWAIG: *Photoacoustics and Photoacoustic Spectroscopy*, (Wiley, New York, N. Y. 1980).
[9] V. S. LETOKHOV and V. P. ZAROV: *Laser Optoacoustic Spectroscopy*, (Springer, Berlin, 1986).
[10] M. J. COLLES, N. R. GEDDER and E. MEHDIZADEH: *Contemp. Phys.*, **20**, 11 (1979).
[11] C. K. N. PATEL and A. C. TAM: *Rev. Mod. Phys.*, **53**, 517 (1981).
[12] A. I. FERGUSON: *Philos. Trans. R. Soc. London, Ser. A*, **307**, 645 (1982).
[13] G. A. WEST, J. J. BARRET, D. R. SIEBERT and K. V. REDDY: *Rev. Sci Instrum.*, **54**, 797 (1983).
[14] A. C. TAM: in *Ultrasensitive Laser Spectroscopy*, edited By D. S. KLIGER (Academic Press, New York, N. Y., 1983) p. 1.
[15] A. C. TAM: *Rev. Mod. Phys.*, **58**, 381 (1986).
[16] *Technical Digest to the Topical Meeting Of Photoacoustic Spectroscopy, August 1979, Ames, Iowa.*
[17] *II International Meeting on Photoacoustic Spectroscopy*, in *Appl. Opt.*, **21**, 19 (1882).
[18] *III International Topical Meeting on Photoacoustic and Photothermal Spectroscopy*, in *J. Phys. (Paris)*, C6, **44**, (1983).
[19] A. C. TAM and H. COUFAL, *J. Phys. (Paris), Colloq.*, C6, **44**, 9 (1983).
[20] S. L. CHIN, D. K. EVANS, R. D. MCALPINE and W. N. SELANDER: *Appl. Opt.*, **21**, 65 (1982).
[21] J. M. HERITIER and A. E. SIEGMAN: *IEEE J. Quantum Electron.*, QE-**19**, 1551 (1983).
[22] K. V. REDDY: *J. Mol. Spectr.*, **82**, 127 (1980).
[23] R.G. BRAY and M. J. BERRY: *J. Chem. Phys.*, **71**, 4909 (1979).
[24] K. V. REDDY, D. F. HELLER and M.J. BERRY: *J. Chem. Phys.*, **76**, 2814 (1982).
[25] G. STELLA, J. GELFAND and W. H. SMITH: *Chem. Phys. Lett.*, **39**, 146 (1976)
[26] S. A. JOHNSON: *Analytical Proc.*, **23**, 1 (1986).
[27] L.B. KREUZER and C. K. N. PATEL: *Science*, **173**, 45 (1971).
[28] C. F. DEWEY: in *Optoacoustic Spectroscopy and Detection*, edited by Y. H. PAO (Academic Press, New York, N. Y., 1977) p. 47.

[29] M. TONELLI, P. MINGUZZI and A. DI LIETO: *J. Phys. (Paris)*, 44, 553 (1983).
[30] S. SHTRIKMAN and M. SLATKINE: *Appl. Phys. Lett.*, **31**, 830 (1977).
[31] R. GERLACH and N. M. AMER: *Appl. Phys.*, **23**, 319 (1980).
[32] D. R. SIEBERT, G. A. WEST and J. J. BARRET: *Appl. Opt.*, **19**, 53 (1980).
[33] N. IOLI, P. VIOLINO and M. MEUCCI: *J. Phys. E*, **12**, 168 (1979).
[34] C. K. PATEL and R. J. KERL: *Appl. Phys. Lett.*, **30**, 578 (1977).
[35] L. B. KREUZER, N. D. KENYON and C. K. PATEL: *Science*, **177**, 347 (1972).
[36] C. K. PATEL, *Science*, **202**, 157 (1978).
[37] K. P. KOCH and W. LAHMANN: *Appl. Phys. Lett.*, **32**, 289 (1979).
[38] C. K. PATEL: in *Laser Spectroscopy II*, edited by S. HAROCHE, J.C. PEBAY-PEYROULA, T. W. HANSCH AND S. E. HARRIS (Springer-Verlag, Berlin, 1975).
[39] E. ARIMONDO, M. G. DI VITO, K. ERNST and M. INGUSCIO: *J. Phys. (Paris)*, C7, **44**, 267 (1983).
[40] C. K. PATEL: *Phys. Rev. Lett.*, **40**, 535 (1978).
[41] M. INGUSCIO, A. MORETTI and F. STRUMIA: *Opt. Commun.*, **30**, 355 (1979).
[42] M. INGUSCIO: in *Advances in Laser Spectroscopy*, edited by F. T. ARECCHI, F. STRUMIA and H. WALTHER (Plenum Press, New York, N.Y., 1983) p. 297.
[43] M. S. SOREM and A. L. SCHAWLOW: *Opt. Commun.*, **5**, 148 (1972).
[44] K. SHIMODA: *Appl. Phys.*, **1**, 77 (1973).
[45] E. E. MARINERO and M. STUKE *Opt. Commun.*, **30**, 349 (1979).
[46] A. DI LIETO, P. MINGUZZI and M. TONELLI: *Opt. Commun.*, **31**, 25 (1979).
[47] J. N. DAHIYA, K. IQBAL, H. G. GRAFT, W. C. EUC and J. W. BEVAN: *Infr. Phys.*, **22**, 77 (1982).
[48] P. MINGUZZI, M. TONELLI and A. CARROZZI: *J. Mol. Spectr.*, **96**, 294 (1982).
[49] P. MINGUZZI, S. PROFETI and M. TONELLI: *J. Opt. Soc. Am.*, in press.
[50] A. QUATTROPANI and R. GIRLANDA, *Riv. Nuovo Cimento*, **6**, 1-37 (1983).
[51] E. GIACOBINO and B. CAGNAC: in *Progress in Optics*, edited by E. WOLF (North-Holland, Amsterdam 1980).
[52] P. MINGUZZI, S. PROFETI, M. TONELLI and A. DI LIETO: *Opt Commun.*, **42**, 237 (1982).
[53] M. INGUSCIO, A. MORETTI and F. STRUMIA: *IEEE J. Quantum Electron.*, QE-16, 955 (1980).
[54] M. INGUSCIO, S. MARCHETTI, A. MORETTI and F. STRUMIA: *Int. J. IR mm waves*, **3**, 97 (1982).
[55] A. DI LIETO, P. MINGUZZI and M. TONELLI: *Appl. Phys. B*, **27**, 1 (1982).
[56] W. HANLE: *Naturwiss.*, **11**, 691 1923.
[57] A. L. LUNTZ, R. G. BREWER, K. L. FOSTER and J. D. SWALEN: *Phys. Rev. Lett.*, 23, 951 (1969).
[58] M. S. FELD, A. SANCHEZ, A. JAVAN and B. J. FELDMAN: *Coll. Int. du CNRS, Publ. n. 217* (Paris 1974) pp. 87-104.
[59] M. INGUSCIO, A. MORETTI and F. STRUMIA: *Appl. Phys. B*, **28**, 88 (1982).
[60] N. BEVERINI, K. ERNST, M. INGUSCIO and F. STRUMIA: *Appl. Phys. B*, **37**, 17 (1985).
[61] F. STRUMIA and M. INGUSCIO: in *Infrared and Millimeter Waves*, edited by K. J. BUTTON Vol. 5, (Academic Press, New York, N. Y., 1975), p. 169.
[62] F. STRUMIA: *J. Phys. (Paris)*, C7, **44**, 117 (1983).
[63] J. J. BARRET and D. F. HELLER: *J. Opt. Soc. Am.*, **71**, 1299 (1981).
[64] J. J. BARRETT and M. J. BERRY: *Appl. Phys. Lett.*, **34**, 144 (1979).
[65] G. A. WEST, D. R. SIEBERT and J. J. BARRETT: *J. Appl. Phys.*, **51**, 2823 (1980).
[66] D. M. COX: *Opt. Commun.*, **24**, 336 (1978).
[67] T. FUKUMI; *Opt. Commun.*, **30**, 351 (1979).

[68] F. BOGANI, K. ERNST and R. QUERZOLI: *II ECAMP, Amsterdam 1985*, Book of Abstracts, p. 141.
[69] V. N. BAGRATASHVILI, I. N. KNYAZEV, V. S. LETOKHOV and V. V. LOBKO: *Opt. Commun.*, **18**, 525 (1976).
[70] N. BLOEMBERGEN and E. YABLONOVITCH: *Physics Today*, May (1978) p. 23.
[71] N. J. SMITH, C. C. DAVIS and I. W. SMITH: *J. Chem. Phys.*, **80**, 6122 (1984).
[72] D. FOURNIER, A. C. BOCCARA, N. M. AMER and R. GERLACH; *Appl. Phys. Lett.*, **37**, 519 (1980).
[73] N. M. AMER: *J. Phys. (Paris)*, C6, **44**, 185 (1983).
[74] A. C. BOCCARA, D. FOURNIER and J. BADOZ: *Appl. Phys. Lett.*, **36**, 130 (1980).
[75] A. C. TAM, H. SONTAG and P. HESS: *Chem. Phys. Lett.*, **120**, 280 (1985).
[76] J. P. GORDON, R. C. LEITE, R. S. MOORE, S. P. PORTO and J. R. WHINNERY: *J. Appl. Phys.*, **36**, 3 (1965).
[77] F. R. GRABINER, D. R. SIEBERT and G. W. FLYNN: *Chem. Phys. Lett.*, **17**, 189 (1972).
[78] G. C. NIEMAN and S. D. COLSON: *J. Chem. Phys.*, **68**, 2994 (1978).
[79] V. VAIDA, R. E. TURNER, J. L. CASEY and S. D. COLSON: *Chem. Phys. Lett.*, **54**, 25 (1978).
[80] H. L. FANG and R. L. SWOFFORD: in *Ultrasensitive Laser Spectroscopy*, edited by D. S. KLIGER (Academic Press, New York, N.Y., 1983), p. 176.
[81] CH. J. BORDE: *J. Phys. (Paris)*, C6, 44, 593 (1983).
[82] F. PENNING: *Physica*, **8**, 137 (1928).
[83] R. B. GREEN, R. A. KELLER, G. C. LUTHER, P. K. SCHENCK and J. C. TRAVIS: *Appl. Phys. Lett.*, **29**, 727 (1976).
[84] J. E. M. GOLDSMITH and J. E. LAWLER: *Contemp. Phys.*, **22**, 235 (1981).
[85] *Int. Coll. on Optogalvanic Spectroscopy and its applications: J. Phys. (Paris)*, C7, **44**, (1983).
[86] D. H. PARKER: *Laser Ionization Spectroscopy and Mass Spectroscopy: Ultrasensitive Laser Spectroscopy*, Chapt. 4, edited by D. S. KLIGER (Academic Press, New York, N.Y., 1983), p. 223.
[87] D. K. DAUGHTY and J. E. LAWLER: *Phys. Rev. A*, **28**, 773 (1983).
[88] C. R. WEBSTER and R. T. MENZIES: *J. Chem. Phys.*, 78, 2121 (1983).
[89] R. A. KELLER, B. E. WARNER, E. F. ZALEWSKI, P. DYER, R. JR. ENGLEMAN and B. A. PALMER: *J. Phys. (Paris)*, C7, **44**, 23 (1983).
[90] C. DREZE, J. DEMERS and J. M. GAGNÉ: *J. Opt. Soc. Am.*, **72**, 912 (1982).
[91] R. A. KELLER and E. F. ZALEWSKI: *Appl. Opt.*, **19**, 3301 (1980).
[92] R. A. KELLER and E. F. ZALEWSKI: *App. Opt.*, **21**, 3992 (1982).
[93] A. I. CARSWELL and I. I. WOOD: *J. Appl. Phys.*, 38, 3028 (1967).
[94] D. FELDMANN: *Opt. Commun.*, **29**, 67 (1979).
[95] C. T. RETTNER, C. R. WEBSTER and R. N. ZARE: *J. Phys. Chem.*, 85, 1105 (1981).
[96] D. A. HANER, C. R. WEBSTER, P. H. FLAMANT and I. S. MCDERMID: *Chem. Phys. Lett.*, **96**, 302 (1983).
[97] C. R. WEBSTER and R. T. MENZIES: *J. Chem. Phys.*, 78, 2121 (1983).
[98] G. HAMEAU, J. WASCAT, D. DANGOISSE and P. GLORIEUX: *Opt. Commun.*, **49**, 423 (1984).
[99] C. WEBSTER and C. RETTNER: *Laser Focus, February*, (1983) p. 41.
[100] C. HAMEAU, E. ARIMONDO, J. WASCAT and P. GLORIEUX: *Opt. Commun.*, 53, 375 (1985).
[101] T. F. JOHNSTON jr.: *Laser Focus, March* (1978), p. 58.
[102] B. BARBIERI, N. BEVERINI, M. GALLI, M. INGUSCIO and F. STRUMIA: *Nuovo Cimento D*, **4**, 172 (1984).

[103] N. BEVERINI, M. GALLI, M. INGUSCIO, F. STRUMIA and G. BIONDUCCI: *Opt. Commun.*, **43**, 261 (1982).
[104] J. E. LAWLER, A. SIEGEL, B. COUILLAUD and T. W. HANSCH: *J. Appl. Phys.*, 52, 4375 (1981).
[105] R. VASUDEV and R. N. ZARE: *J. Chem. Phys.*, **76**, 5267 (1982).
[106] T. SUZUKI: *Opt. Commun.*, **38**, 364 (1981).
[107] C. STANCINLESCU, R. C. BODULESCU, A. SURMEIAN, D. POPESCU, I. I. POPESCU and C. B. COLLINS: *Appl. Phys. Lett.*, **37**, 888 (1980).
[108] P. LABASTIE, F. BIRABEN and E. GIACOBINO: *J. Phys. B*, **15**, 2595 (1982).
[109] P. CAMUS: *J. Phys. (Paris)*, C7, **44**, 87 (1983).
[110] J. E. LAWLER, A. I. FERGUSON, J. E. M. GOLDSMITH, D. J. JACKSON and A. L. SCHAWLOW: *Phys. Rev. Lett.*, **42**, 2605 (1979).
[111] M. INGUSCIO, K. LEOPOLD, J. S. MURRAY and K. M. EVENSON: *J. Opt. Soc. Am. B*, **2**, 1566 (1985).
[112] E. HIROTA: *High Resolution Spectroscopy of Transient Molecules*, Springer Series in Chemical Physics, Vol. **40** (Springer-Verlag, Berlin, 1985).
[113] A. SIEGEL, J. E. LAWLER, B. COUILLAUD and T. W. HÄSCH: *Phys. Rev. A*, **23**, 2457 (1981).
[114] C. J. LORENZEN and K. NIEMAX: *Opt. Commun.*, 43, 26 (1982).
[115] H. O. BEHRENS and G. H. GUTHÖRLEIN: *J. Phys. (Paris), Colloq.*, C7, **44**, 149 (1983).
[116] D. S. GOUGH and P. HANNAFORD: *Opt. Commun.*, **55**, 91 (1981).
[117] D. W. DUQUETTE, D. K. DOUGHTY and J. E. LAWLER: *Phys. Lett. A*, **99**, 307 (1983).
[118] CH. BELFRAGE, P. GRAFSTROM, S. KROLL and S. SVANBERG: *Phys. Scrip.*, **27**, 367 (1983).
[119] P. R. BERMAN: *Adv. At. Mol. Phys.*, **13**, 57 (1978).
[120] C. BRECHIGNAC, R. VETTER and P. R. BERMAN: *Phys. Rev. A*, **17**, 1609 (1978).
[121] S. N. JABR and W. R. BENNET: *Phys. Rev. A*, **21**, 1518 (1980).
[122] P. F. LIAO, J. E. BJORKHOLM and P. R. BERMAN: *Phys. Rev. A*, **21**, 1927 (1980).
[123] V. P. CHEBOTAYEV and L. S. VASILENKO: *Progr. Quantum Electron.*, QE-8, 79 (1983).
[124] J. TENENBAUM, E. MIRON, S. LAVI, J. LIRAN, M. STRAUSS, J. OREG and G. EREZ: *J. Phys. B*, **16**, 4543 (1983).
[125] A. P. KOLCHENKO, A. A. PUKNOW, S. G. RAUTIAN and A. M. SHALAGIN: *Sov. Phys. JEPT*, **36**, 619 (1973).
[126] T. W. HÄSCH, D. R. LYONS, A. L. SCHAWLOW, A. SIEGEL, Z. Y. WANG and G. Y. YAN: *Opt. Commun.*, 37, 87 (1981), Erratum: *Opt. Commun.*, 38, 47 (1981).
[127] D. R. LYONS, A. L. SCHAWLOW and G. Y. YAN: *Opt. Commun.*, 38, 35 (1981).
[128] H. ODENTAL, R. RAMBAN, E. K. SOUN and J. UHLENBUSCH: *Physica C*, 113, 203 (1982).
[129] J. E. GOLDSMITH, A. I. FERGUSON, J. E. LAWLER and A. L. SCHAWLOW: *Opt. Lett.*, **4**, 230 (1979).
[130] J. E. GOLDSMITH and A. V. SMITH: *Opt. Commun.*, 32, 403 (1980).
[131] A recent review of laser spectroscopy in Doppler-broadened three-level system can be found in: E. ARIMONDO: *Acta Phys. Pol. A*, **66**, 423 (1984).
[132] C. R. VIDAL: *Opt. Lett.*, **5**, 158 (1980).
[133] W. DEMTRÖDER: *Phys. Rep. C*, 7, 223 (1973).
[134] C. WIEMAN and T. W. HÄNSCH: *Phys. Rev. Lett.*, 36, 1170 (1976).
[135] R. ENGLEMAN jr. and R. A. KELLER: *Opt Lett.*, **5**, 465 (1980).
[136] K. MIYAZAKI, H. SCHEINGRABER and C. R. VIDAL: *Phys. Rev. Lett.*, **50**, 1046 (1983).

[137] H. O. BEHRENS, G. H. GUTHÖHRLEIN and A. KASPER: *J. Phys. (Paris), Colloq.*, C7, 44, 239 (1983).
[138] M. INGUSCIO: *J. Phys. (Paris), Colloq.*, C7, **44**, 217 (1983).
[139] L. D. SCHEARER and L. A. RISEBERG: *Phys. Lett. A*, **33**, 325 (1970).
[140] G. W. SERIES: *Comm. At. Mol. Phys.*, **10**, 199 (1981).
[141] N. BEVERINI and M. INGUSCIO: *Lett. Nuovo Cimento*, **29**, 10 (1980).
[142] P. HANNAFORD and G. W. SERIES: *J. Phys. B*, **14**, L661 (1981).
[143] M. PINARD and L. JULIEN: *J. Phys. (Paris), Colloq.*, C7 **44**, 129 (1983).
[144] L. JULIEN and M. PINARD: *J. Phys. B*, **15**, 2881 (1982).
[145] P. HANNAFORD and G. W. SERIES: *Opt. Commun.*, **41**, 427 (1982).
[146] P. HANNAFORD and G. W. SERIES: *Phys. Rev. Lett.*, **48**, 1326 (1982).
[147] B. BARBIERI, N. BEVERINI, G. BIONDUCCI, M. GALLI, M. INGUSCIO and F. STRUMIA in *Laser Spectroscopy IV*, edited by H. P. WEBER and W. LUTHY (Springer-Verlag, Berlin, 1983), p. 133.
[148] G. BERTUCELLI, N. BEVERINI, M. GALLI, M. INGUSCIO, F. STRUMIA and G. GIUSFREDI: *Opt. Lett.*, **10**, 6 (1985).
[149] D. H. KATAYAMA, J. M. COOK, V. E. BONDYBEY and T. A. MILLER: *Chem. Phys. Lett.*, **62**, 542 (1979).
[150] P. CAMUS, M. DIEULIN and C. MORILLON: *J. Phys. Lett.*, **40**, L513 (1979).
[151] P. LABASTIE, F. BIRABEN and E. GIACOBINO: *J. Phys. B*, **15**, 2595 (1982).
[152] P. LABASTIE, E. GIACOBINO and F. BIRABEN: *J. Phys. B*, **15**, 2605 (1982).
[153] J. P. LEMOIGNE, J. P. GRANDIN, X. HUSSON and H. KUCAL: *J. Phys. (Paris)*, **45**, 249 (1984).
[154] D. J. JACKSON, E. ARIMONDO, J. E. LAWLER and T. W. HÄSCH: *Opt. Commun.*, **33**, 51 (1980).
[155] H. BEGEMAN and J. SAYKALLY: *Opt Commun.*, **40**, 277 (1982).
[156] D. J. JACKSON, H. GERHARDT and T. W. HÄSCH: *Opt. Commun.*, **37**, 23 (1981).
[157] T. SUZUKI and M. KAKIMOTO: *J. Mol. Spectr.*, **93**, 423 (1982).
[158] D. S. KING, P. K. SCHENCK, K. C. SMYTH and J. C. TRAVIS: *Appl. Opt.*, **16**, 2617 (1977).
[159] J. R. NESTOR: *J. Phys. (Paris), Colloq.*, C7, **44**, 387 (1983).
[160] R. B. GREEN, R. A. KELLER, G. G. LUTHER, P. K. SCHENCK and J. C. TRAVIS: *IEEE J. Quantum Electron.*, QE-13, 63 (1977).
[161] R. A. KELLER, R. ENGELMAR Jr. and B. A. PALMER: *Appl. Opt.*, **19**, 837 (1980).
[162] B. A. PALMER, R. A. KELLER, F. V. KOWALSKI and J. L. HALL: *J. Opt. Soc. Am.*, **71**, 948 (1981).
[163] N. J. DOVICHI, D. S. MOORE and R. A. KELLER: *Appl. Opt.*, **21**, 1468 (1982).
[164] R. H. LIPSON, P. E. LA ROCQUE and B. P. STOICHEFF: *J. Chem. Phys.*, **82**, 4470 (1985).
[165] B. STOICHEFF, P. R. HERMAN, P. R. LA ROCQUE and R. H. LIPSON: in *Laser Spectroscopy VII*, edited by T. W. HANSCH and Y. R. SHEN (Springer-Verlag, Berlin 1985), p. 174.
[166] S. CHU, A. P. MILLS Jr. and J. L. HALL: in *Laser Spectroscopy VI*, edited by H. P. WEBER and W. LUTHY (Springer-Verlag, Berlin, 1983), p. 28.
[167] C. R. WEBSTER: *Appl. Opt.*, **21**, 2298 (1982).
[168] L. HOLLBERG, MA LONG SHENG, M. HOHENSTATT and J. L. HALL: in *Laser Based Ultrasensitive Spectroscopy and Detection*, edited by R. A. KELLER: *Proceedings of SPIE, - S. Diego (1983)*, Vol, **426**, p. 91.

Direttore responsabile: RENATO ANGELO RICCI

Questo periodico è iscritto all'Unione Stampa Periodica Italiana

Questo fascicolo è stato realizzato in fotocomposizione dalla Monograf, Bologna e stampato dalla tipografia Compositori, Bologna nel mese di Giugno 1988

LAST PUBLISHED PAPERS

E. GATTI and P. F. MANFREDI – Processing the signals from solid-state detectors in elementary-particle physics.
G. BARBIELLINI and C. SANTONI – Experimental status of weak interactions.
G. COSTA and F. ZWIRNER – Baryon and lepton number nonconservation.
C. LEONARDI, F. PERSICO and G. VETRI – Dicke model and the theory of driven and spontaneous emission.
S. A. BONOMETTO and A. MASIERO – Phase transitions in the early Universe.
E. RECAMI – Classical tachyons.
H. GRUPPELAAR, P. NAGEL and P. E. HODGSON – Pre-equilibrium processes in nuclear-reaction theory: the state of the art and beyond.
G. L. FOGLI – Neutrino-induced deep inelastic scattering and the structure of the neutral current. A review and an updated analysis.
V. R. MANFREDI – Old and new results in statistical nuclear spectroscopy.
I. A. BATALIN and E. S. FRADKIN – Operator quantization and Abelization of dynamical systems subject to first-class constraints.
V. BORTOLANI and A. C. LEVI – Atom-surface scattering theory.
C. CASO and M. C. TOUBOUL – Measurements of heavy-flavour lifetimes.
A. LOINGER – On some basic concepts of quantum mechanics.
S. NARISON – Chiral-symmetry breaking and the light-meson systems.
M. DOBROWOLNY – The TSS project: electrodynamics of long metallic tethers in the ionosphere.
S. CESARE and C. DEL DUCA – Tensor algebra for the icosahedral group.
U. BIZZARRI, F. CIOCCI, G. DATTOLI, A. DE ANGELIS, E. FIORENTINO, G. P. GALLERANO, T. LETARDI, A. MARINO, G. MESSINA, A. RENIERI, E. SABIA and A. VIGNATI – The free-electron laser: status and perspectives.
L. PELITI and L. PIETRONERO – Random walks with memory.
M. TRAINI, G. ORLANDINI and R. LEONARDI – A study of the Thomas-Reiche-Kuhn sum rule in finite nuclei.
V. FLAMINIO and B. SAITTA – Neutrino oscillation experiments.
J. VERVIER – Boson-fermion symmetries and supersymmetries in nuclear physics.
F. MARTINELLI and E. SCOPPOLA – Introduction to the mathematical theory of Anderson localization.
R. CASSINIS and A. RANZONI – Advancements in seismological science (1979-1985).
L. L. JENKOVSZKY – High-energy elastic hadron scattering.

FORTHCOMING PAPERS (in alphabetical order)

R. BADII – Conservation laws and thermodynamic formalism for dissipative dynamical systems.
R. BARBIERI – Looking beyond the standard model: the supersymmetric option.
M. BATTEZZATI – The Legendre transformation and complementary relations for second-order Hylleraas-type homogeneous functionals.
S. BELLUCCI – Higher-order corrections to electroweak processes.
N. N. BOGOLUBOV jr. and V. N. PLECHKO – Approximation methods in the polaron theory.
R. BRUZZESE, A. SASSO and S. SOLIMENO – Multiphoton excitation and ionization of atoms and molecules.
M. BUCCIOLINI and L. CIRAOLO – Tomography by nuclear magnetic resonance.
D. CANARUTTO – An introduction to the geometry of singularities in general relativity.
G. DATTOLI, J. C. GALLARDO and A. TORRE – An algebraic view to the operational ordering and its applications to optics.
M. GRECO – Radiative corrections to e^+e^- reactions at LEP/SLC energies.
N. KIM, G. C. LA ROCCA, S. RODRIGUEZ and E. BASSANI – Inversion asymmetry and magneto-optics in zincblende semiconductors.
B. H. LAVENDA and C. SCHERER – Statistical inference in equilibrium and nonequilibrium thermodynamics.
A. LOINGER – On Weyl's *Raumproblem*.
G. STRINATI – Application of the Green's function method to the study of the optical properties of semiconductors.
I. R. YUKHNOVS'KII – Solution of the three-dimensional Ising model for the description of the second-order phase transition.

LA RIVISTA DEL NUOVO CIMENTO della società italiana di fisica

Quote di abbonamento alla *Rivista del Nuovo Cimento* per l'anno 1988:

Per i Soci in Italia	L. 200.000
Per i non Soci in Italia	L. 250.000

Abbonamento cumulativo al *Nuovo Cimento*, Sezioni A, B, C e D, *Rivista del Nuovo Cimento*:

Per i Soci in Italia	L. 1.475.000
Per i non Soci in Italia	L. 1.850.000

La *Rivista del Nuovo Cimento* è in vendita anche in fascicoli separati al prezzo di lire 30.000 ciascuno; per ordini cumulativi di almeno 10 copie sarà concesso uno sconto del 10% sul prezzo complessivo.
Le somme per l'abbonamento vanno versate (direttamente o per mezzo di un libraio) a **Editrice Compositori, via Stalingrado, 97/2 - 40128 Bologna**, alla quale occorre rivolgersi anche per l'acquisto di volumi arretrati o numeri isolati.
Trascorsi 3 mesi dalla data di pubblicazione, non saranno più accettati reclami per i fascicoli non pervenuti.

Subscriptions to *Rivista del Nuovo Cimento* for the year 1988:

To members abroad	US $ 190.00
To nonmembers abroad	US $ 240.00

Combined subscription to *Il Nuovo Cimento*, Sections A, B, C and D, *Rivista del Nuovo Cimento*:

To members abroad	US $ 1400.00
To nonmembers abroad	US $ 1755.00

Subscribers who wish to receive their issues by air mail will be charged extra postage. The airmail postage for 1988 amounts to US $ 35.00.
Single issues of *Rivista del Nuovo Cimento* may be purchased at the price of US $ 23.00 each; 10% discount on this price will be allowed for bulk orders of 10 copies or more.
Subscriptions should be sent, either directly or through a bookseller, to **Editrice Compositori, via Stalingrado, 97/2 - I 40128 Bologna (Italy)**. Requests for back numbers or single copies should be directed to the same address.
3 months after publication we will not consider complaints for issues not received.

Per qualsiasi ordinazione rivolgersi a
For any order please write to

EDITRICE COMPOSITORI **Via Stalingrado, 97/2** **I 40128 Bologna (Italy)**

Autorizzazione del Tribunale di Bologna n. 3382 del 21 dicembre 1968

OPTOGALVANIC SPECTROSCOPY

A) BASIC PRINCIPLES AND DETECTION SCHEME

- STEADY [illegible] REGIME
- [illegible] VOLATILE GASES
- ATOMIC REGIME
- HOLLOW CATHODE
- RADIO FREQUENCY DISCHARGES
- MICROWAVE DISCHARGES

B) SPECTROSCOPICAL METHODS

- DOPPLER - LIMITED SPECTROSCOPY
- DOPPLER - FREE SPECTROSCOPY
  - INTERMODULATED SPECTROSCOPY
  - POLINEX
  - TWO - PHOTON SPECTROSCOPY
  - OPTICAL - OPTICAL DOUBLE RESONANCE

:) APPLICATIONS

- ISOTOPE SHIFT
- ZEEMAN EFFECT
- HYPERFINE STRUCTURE
- LASER FREQ. STABILIZ.
- WAVELENGTH CALIBRATION

CONVENTIONAL SPECTROSCOPY:

INTERACTION RADIATION - MATTER IS USUALLY STUDIED OBSERVING RADIATION

Ex.: Fluorescence
Absorption

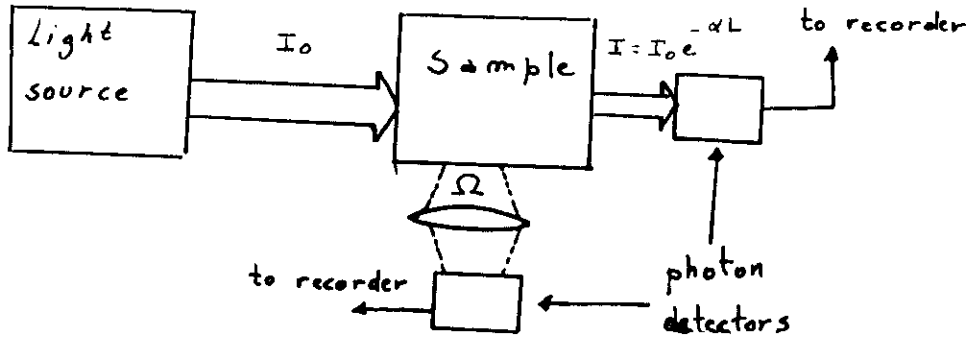

Limits

- quantum efficiency of detectors $\eta < 1$
- geometrical efficiency (collection optics) $\Omega < 4\pi$ rad.
- large backgrounds

⇓

RECENT DEVELOPMENT OF "UNCONVENTIONAL" SPECTROSCOPIC [illegible]

CHARGE BASED TECHNIQUE : K

I

S

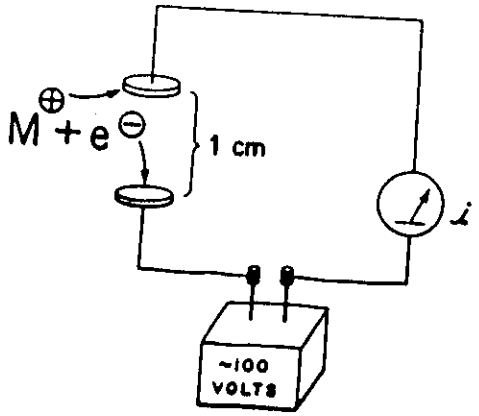

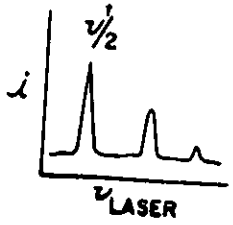

RIS SCHEMES

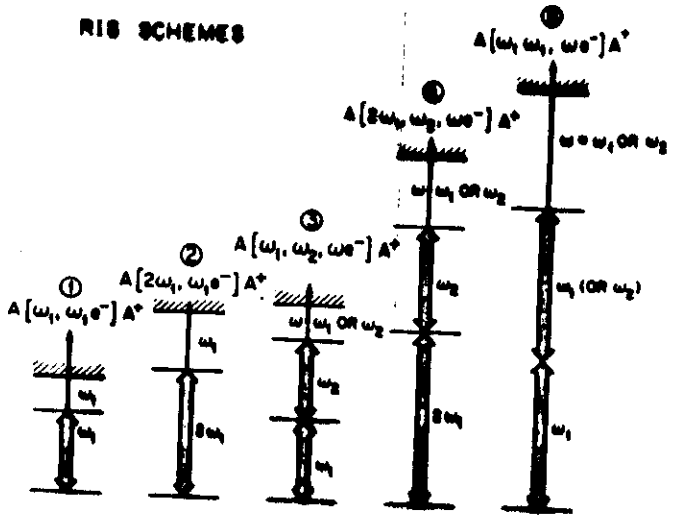

Advantages :

HIGH SELECTIVITY (RESONANT ABSORPTION)

HIGH SENSITIVITY (HIGH EFFICIENCY FOR CHARGES COLLECTION $\ell = 1$)

Single Atom Detection

S.S. Hurst, M.G. Payne, S.D. Kramer, T.P. Young :
Rev. Mod. Phys. 51, 767-819 (1979)

OPTOGALVANIC EFFECT :

VARIATIONS PRODUCED BY RADIATION IN DISCHARGES.

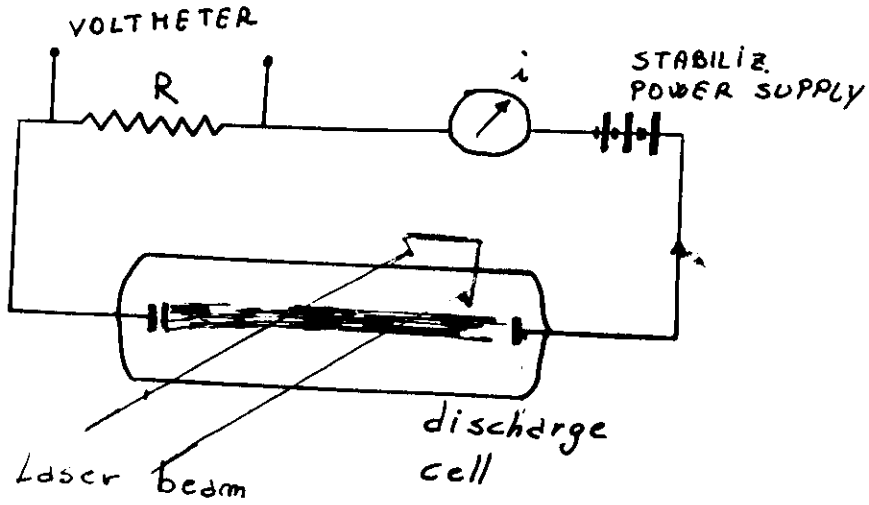

"MICROSCOPIC" PROCESSES AS ATOM-PHOTON INTERACTION ARE DETECTED BY MEANS OF "MACROSCOPIC" CHANGES IN THE REACTION OF THE SYSTEM (electrical current).

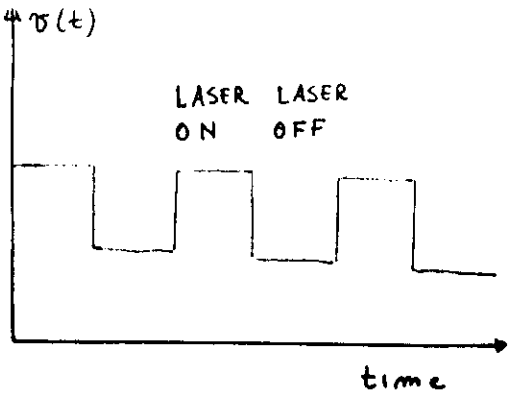

SOMETIMES LARGE OG SIGNALS ARE EASLY OBSERVABLE BY A SCOPE ; MORE SENSITIVITY IS OBTAINED WITH A PHASE-SENSITIVE DETECTION SCHEME (LOCK-IN Amplifier).

OPTOGALVANIC "SPECTROMETER"

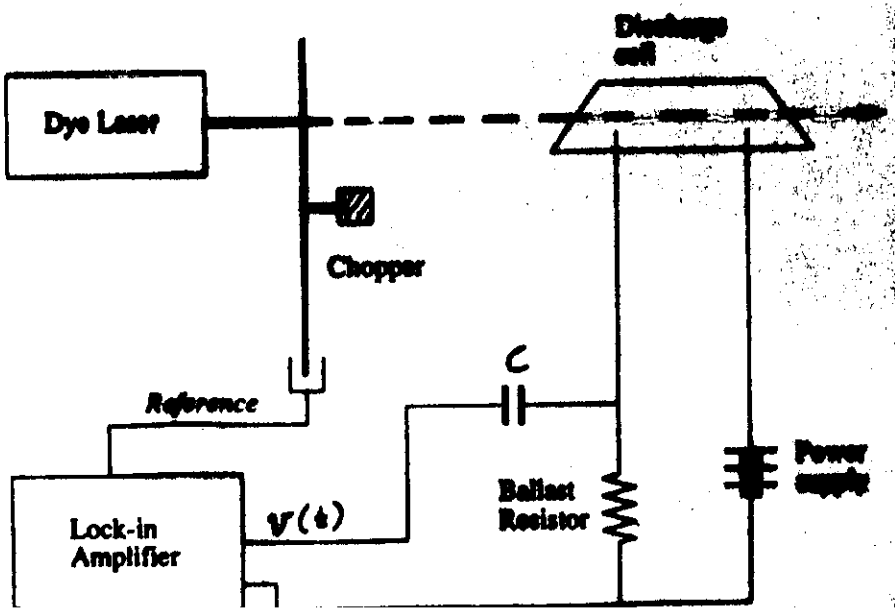

OPTOGALVANIC EFFECT : HISTORY

FIRST DISCOVERY of EFFECT in 1928

F. Penning : Physica 8, 137-140 (1928)

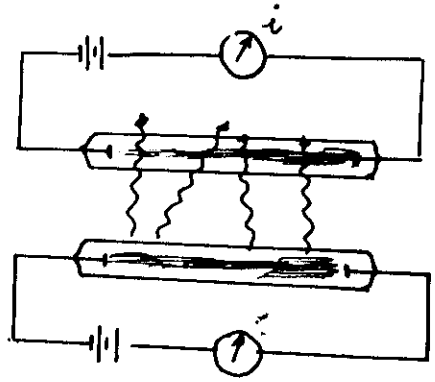

the discharge current circulating in a discharge tube was altered when irradiated by a similar discharge tube.

NEW WIDE INTEREST AS SPECTROSCOPIC TECHNIQUE WITH THE DEVELOPMENT OF TUNABLE LASER:

Green et. al. 1976 : Appl. Phys. Lett. 29, 727-729

REVIEW PAPERS :

- A. FERGUSON : Phyl. Trans. R. Soc. Lond. A 307, 645-657 (1982)
- Conference on Opt. Spect. Aussois, France 1983 : in J. Phys. (Paris) C 7-1983
- V.N. Ochkin et al. Sov. Phys. Usp. 29, 260-280 (1987)
- K. ERNST, M. INGUSCIO, La Rivista del Nuovo Cimento vol. 11 1988
- [illegible] & BARBIERI : Rev. Mod. Phys, in press.

OPTOGALVANIC MODELING

[illegible] DISCHARGE [illegible] BE CONSIDERED AS A "BLACK-BOX"

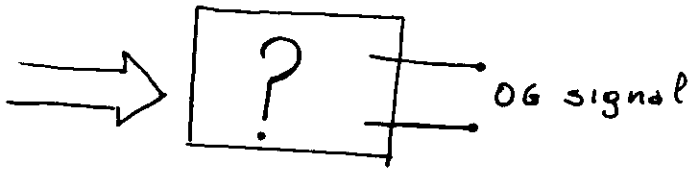

THE MECHANISMS GOVERNING OG SIGNAL PRODUCTION ARE DIFFICULT BECAUSE DISCHARGE PLASMA ARE COMPLEX MEDIUM (electrons, ions, atomic and molecular excited species, etc).

A QUANTITATIVE UNDERSTANDING OF OGE IS POSSIBLE IF A "REASONABLE" MODEL OF THE INVESTIGATED DISCHARGE EXISTS.

UNFORTUNATELY, ONLY FOR FEW CASES THIS IS POSSIBLE

$$\Delta i = f(\text{discharge and atomic peremeters})$$

f is a complex function.

glow discharge

$V \simeq 500 \div 1000$

$I = 1 \div 50$ mA

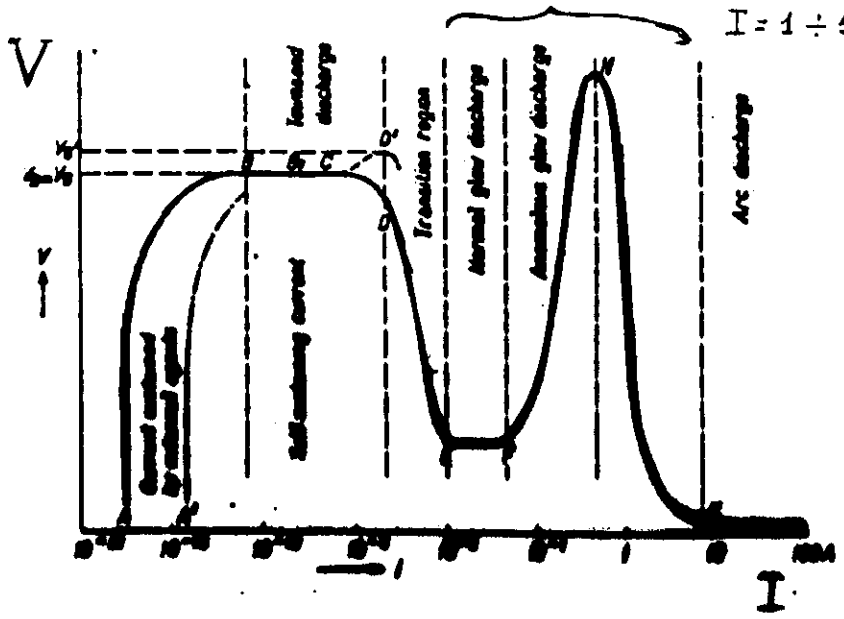

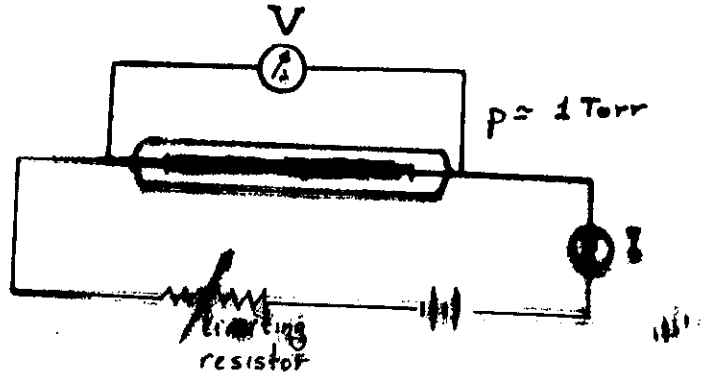

For a more complete description of the discharge see:

M.J. DRUYVESTEYN AND F.M. PENNING: Rev. Mod. Phys. 12, 87-174 (1940).

VON ENGEL A.: "Ionized Gases", 2nd ed. Clarendon Press, Oxford 1965.

SPATIAL DISTRIBUTION OF DARK AND LUMINOUS

ONES IN A GLOW DISCHARGE

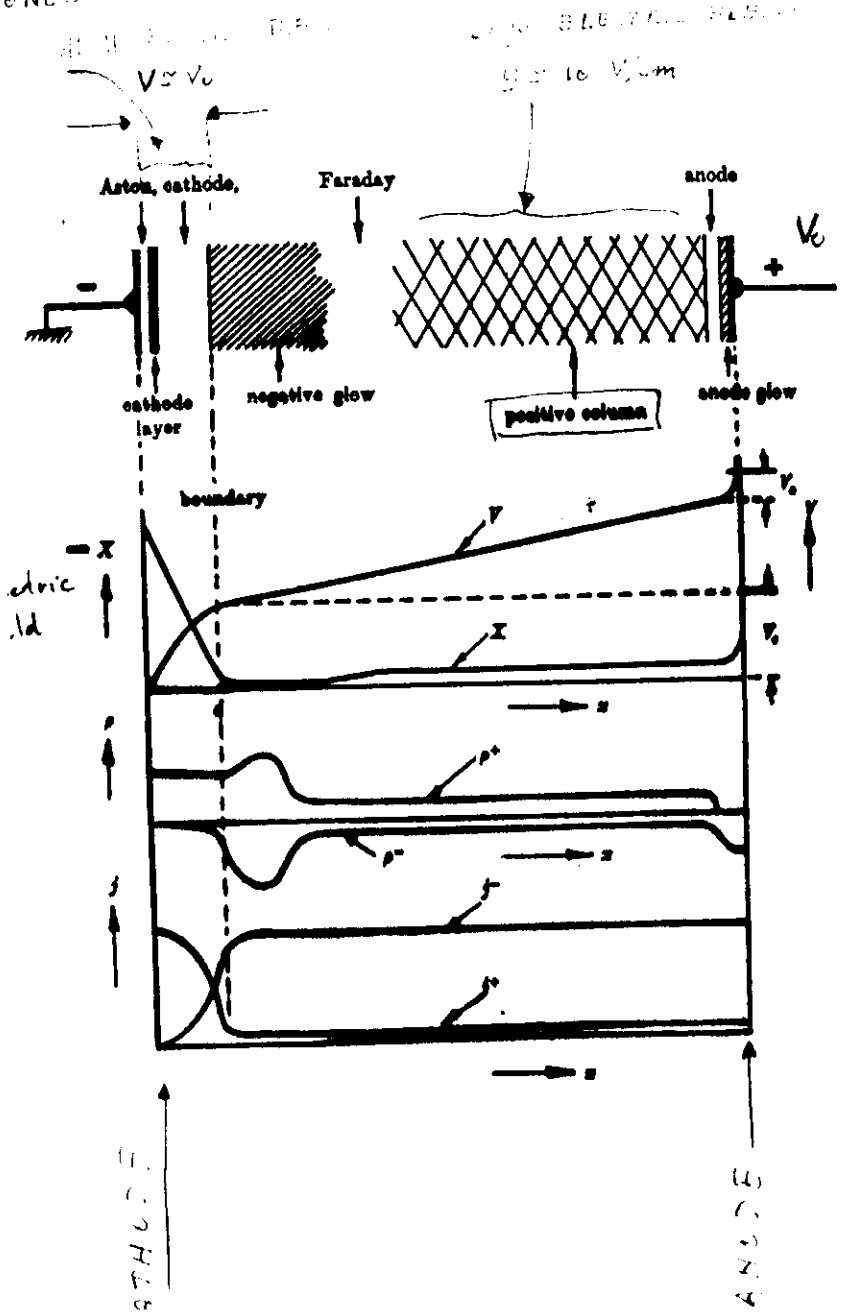

EXCITATION AND IONIZATION MECHANISMS

IN A GLOW DISCHARGE

typical electron temperature $\approx 10^4 K \equiv 4\ eV$

$A + e^-_{fast} \rightarrow A^* + e^-_{slow}$ electron impact excitation

$A + e^- \rightarrow A^+ + 2e^-$ single-step ionization

$A + e^- \rightarrow A^* + e^-$

$A^* + e^- \rightarrow A^+ + 2e^-$ two-step (or multi-step)

$A + B^* \rightarrow A^* + B + \Delta E$ excitation transfer

$A + B^* \rightarrow A^+ + B$ Penning ionization

$A^* + A \rightarrow A_2^+ + e^-$ Associative ionization

Neon

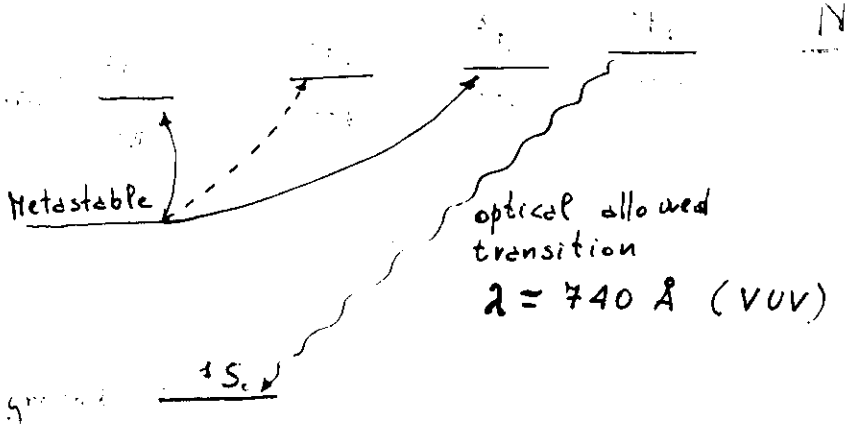

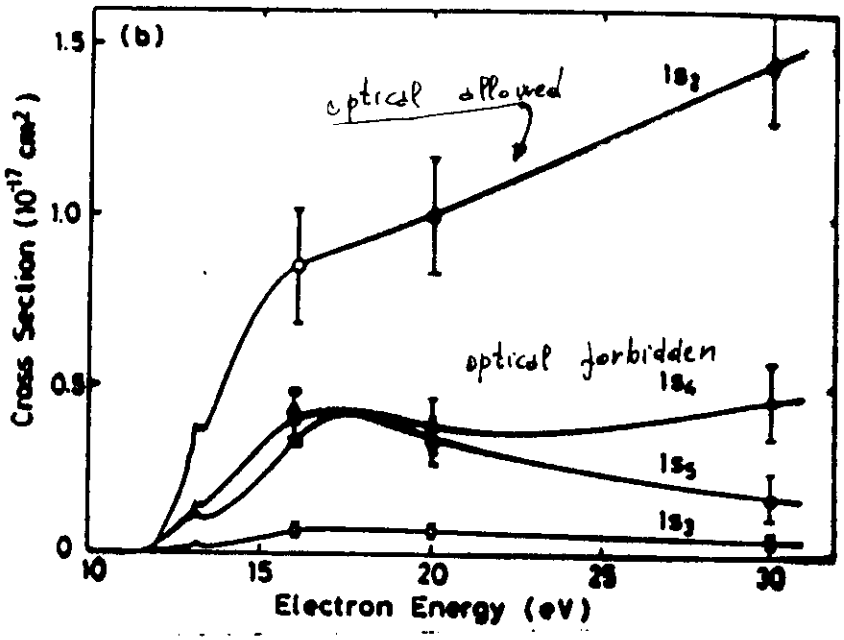

OTHERS MECHANISMS : LOSSES

- neutrals
  - DIFFUSION
  - DEEXCITATION (WALLS, ATOMS, ELECTRONS)

$$A^* + e^- \rightarrow A + e^-_{fast}$$ super-elastic collision

- charges
  - AMBIPOLAR DIFFUSION
  - RECOMBINATION
  - ATTACHMENT

SIMPLE (PHENOMENOLOGICAL) CG MECHANISM

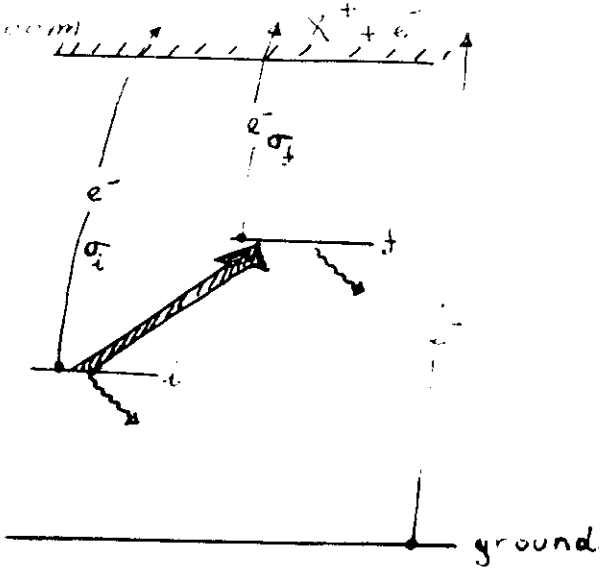

ABSORPTION OF PHOTONS CHANGES THE POPULATION OF TWO (OR MORE) LEVELS; USUALLY WITH DIFFERENT IONIZATION CROSS-SECTION. AS A CONSEQUENCE, A VARIATION OF THE ELECTRON-ION PAIRS PRODUCTION IS INDUCED.

DOUGHTY AND LAWLER MODEL:

"NEON POSITIVE COLUMN"

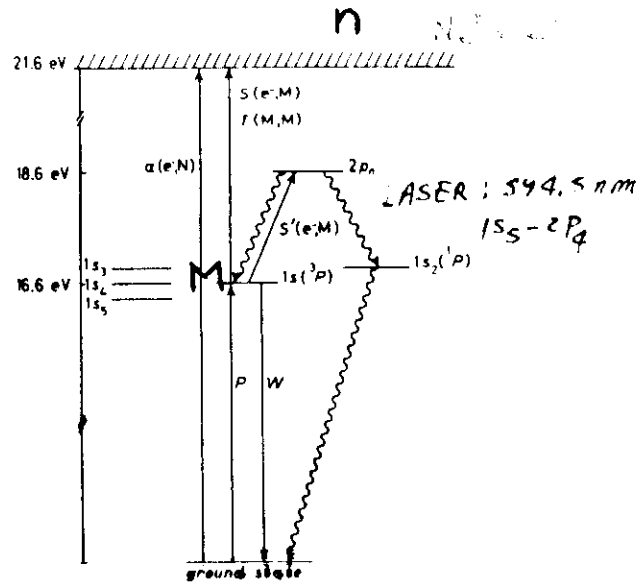

$$\begin{cases} \dfrac{dM}{dt} = PnN - WM - TM^2 - SnM - \dfrac{S'nM}{4}. & \text{Metastable density } M \\ \dfrac{dn}{dt} = \alpha v_d n + SnM + \dfrac{TM^2}{2} - D_a\left(\dfrac{2.4}{R}\right)^2 n. & \text{electron density } n \\ i = e n v_d \pi R^2. \end{cases}$$

$[n_{electr} = n_{ions}$ in positive column$]$

$$\frac{dM}{dt} = 0 \quad \text{and} \quad \frac{dn}{dt} = 0.$$

Doughty and Lawler : Phys. Rev. A 28, 773-780 (1983)

PERTURBED BALANCE EQUATIONS

$$\Delta H = \frac{\partial H}{\partial n}\Delta n + \frac{\partial H}{\partial M}\Delta M + \frac{\partial H}{\partial E}\Delta E = \beta Q,$$

$$\Delta G = \frac{\partial G}{\partial n}\Delta n + \frac{\partial G}{\partial M}\Delta M + \frac{\partial G}{\partial E}\Delta E = 0,$$

$$\Delta i = \frac{\partial i}{\partial n}\Delta n + \frac{\partial i}{\partial E}\Delta E.$$

Q = number of photons absorbed per unit time and volume

$$\frac{dM}{dt} = H(n, M, E),$$

$$\frac{dn}{dt} = G(n, M, E).$$

$$V = Z \cdot i + l\,E$$

Working on a voltage-stabilized

$$\begin{cases} \Delta V = Z\Delta i + l\Delta E = 0 \end{cases}$$

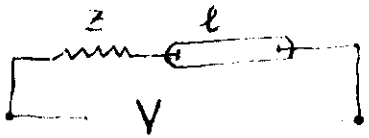

$$\Delta i = -\,l\Delta E/.$$

$$\Delta i = \beta Q\, i\, (S n + T M) \frac{1}{\left(1 + \frac{Z}{R_d}\right)\cdot\left[\left(S n M + \frac{T}{2}M^2\right)W + \left(S - \frac{S'}{2}\right)\frac{nTM^2}{2}\right]}$$

R_d = differential resistance

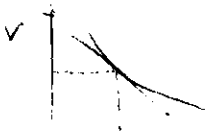

COMPARISON BETWEEN EXPERIMENT AND D.&L. THEORY: GOOD BUT IN A "NARROW" EXPERIM. RANGE

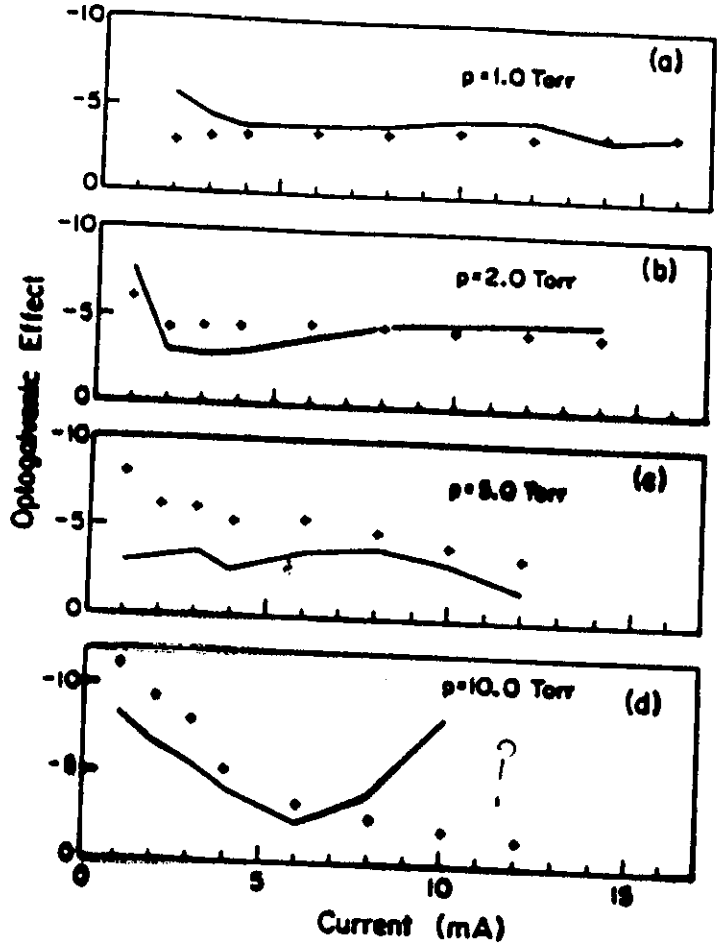

ONLY ONE LINE IS CONSIDERED

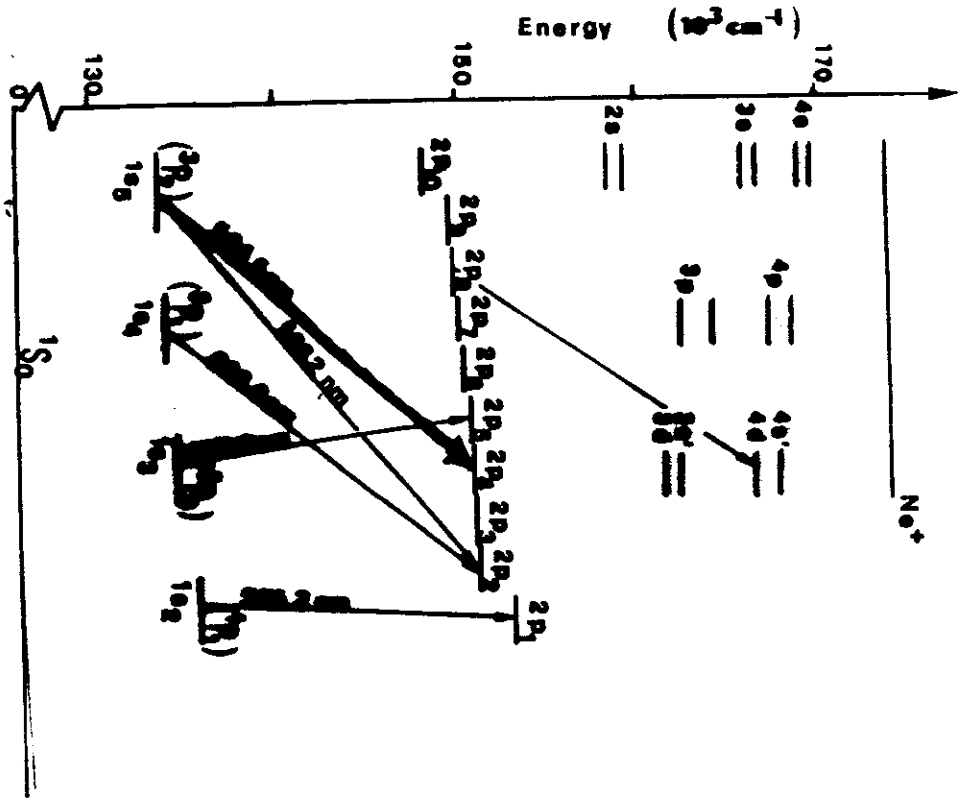

Optogalvanic spectra of Ne - positive column

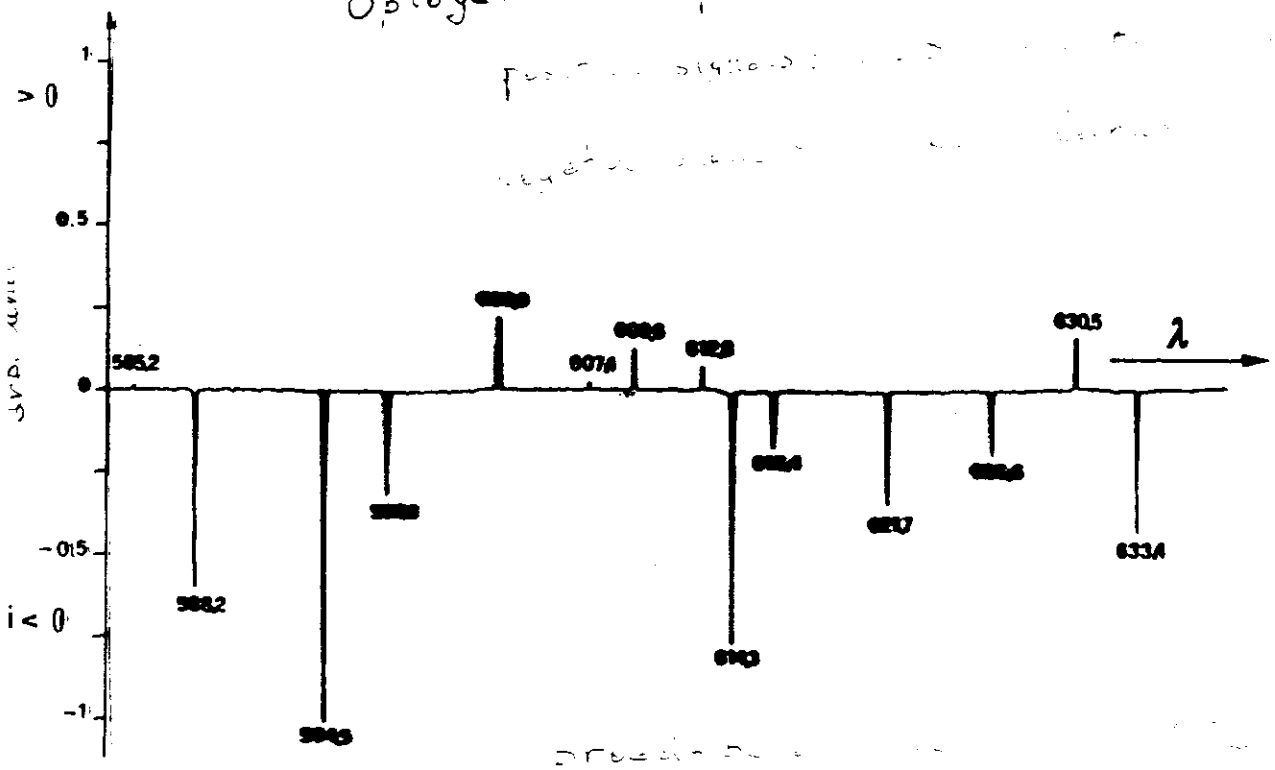

$P_{Ne} \simeq 1$ Torr

$i = 1$ mA

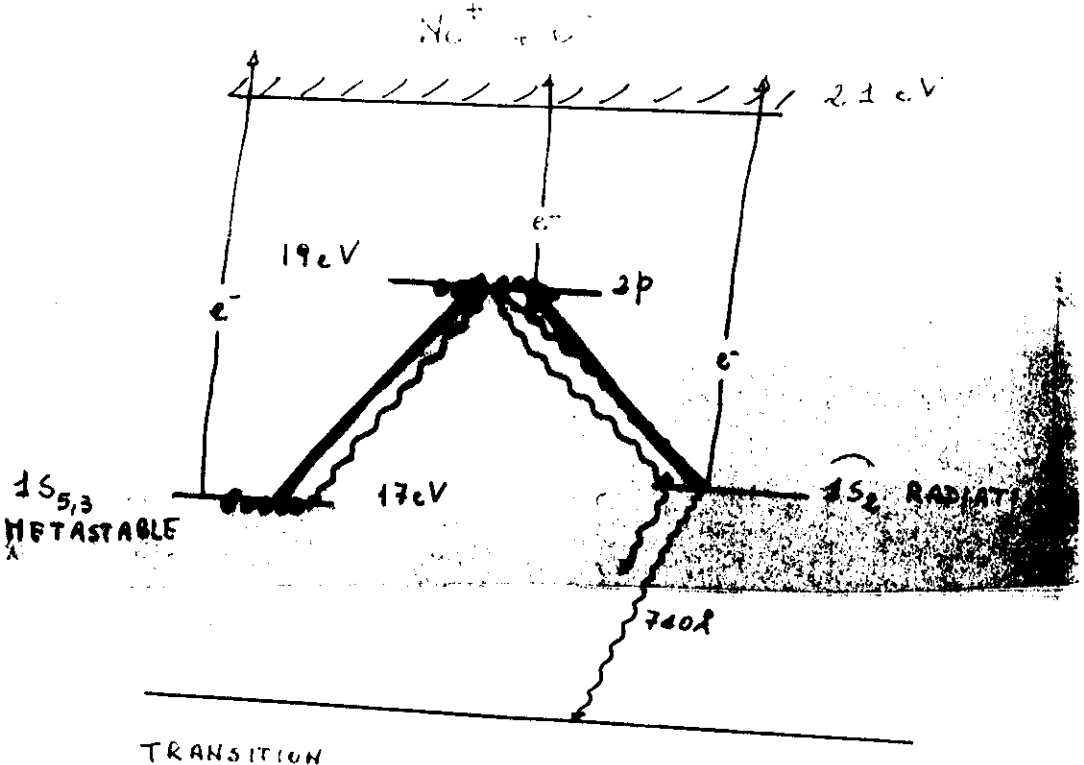

OG - SIGN

$1S_{5,3} - 2p$ { + increase 2p population
— decrease metastable pop

$1S_2 - 2p$ { + increase 2p
increase metastable

GENERALIZED DOUGHTY & CAWLER MODEL

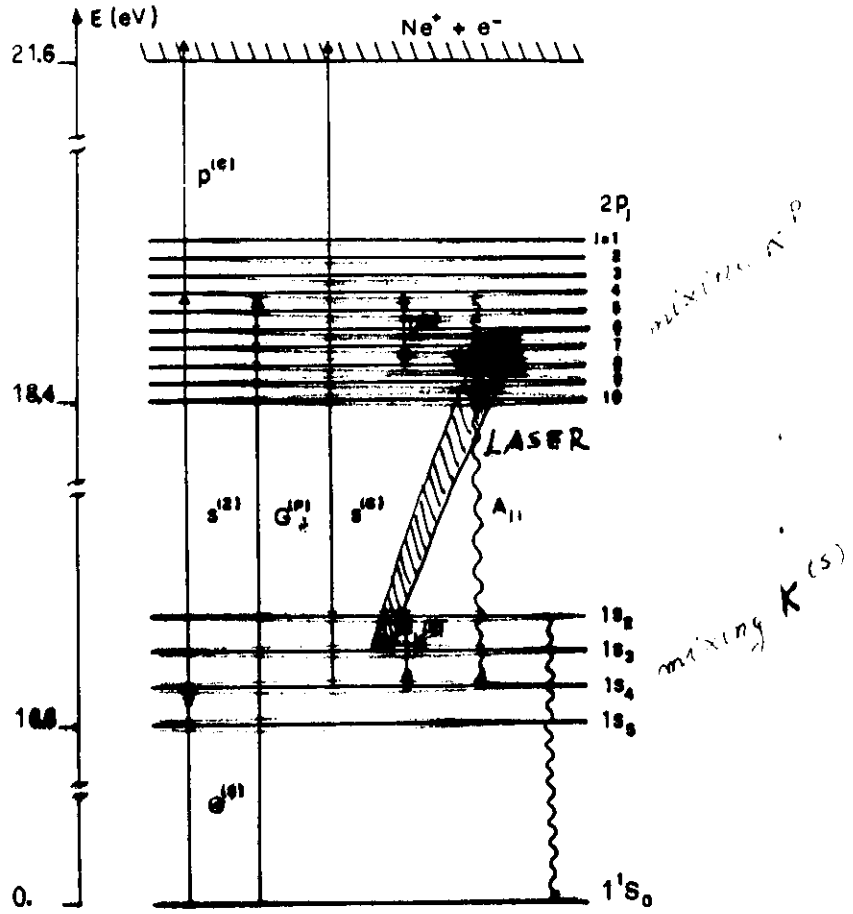

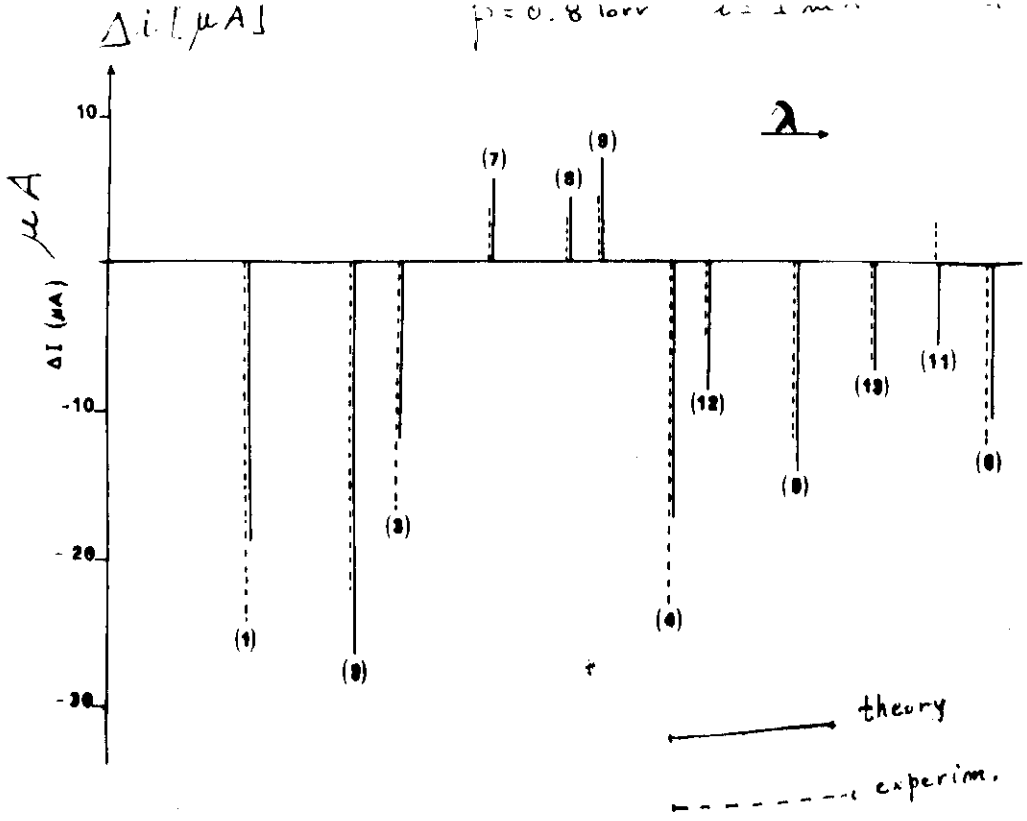

Table Wavelengths of the Observed Lines and Their Spectroscopic Assignment (Paschen Notation)

Designation	Neon Transition (Paschen)	Wavelength (nm)
(1)	[illegible]	[illegible]
[illegible]	[illegible]	[illegible]
[illegible]	[illegible]	[illegible]
[illegible]	[illegible]	[illegible]
[illegible]	[illegible]	[illegible]
[illegible]	[illegible]	[illegible]
[illegible]	[illegible]	[illegible]
[illegible]	[illegible]	[illegible]
[illegible]	[illegible]	[illegible]
[illegible]	[illegible]	[illegible]
[illegible]	[illegible]	[illegible]
[illegible]	[illegible]	[illegible]
[illegible]	[illegible]	[illegible]
[illegible]	[illegible]	[illegible]
[illegible]	[illegible]	[illegible]
[illegible]	[illegible]	[illegible]

[illegible] HASSO, [illegible] HAIMOND : J. Opt. Soc. Am. B 5, [illegible] (1988)

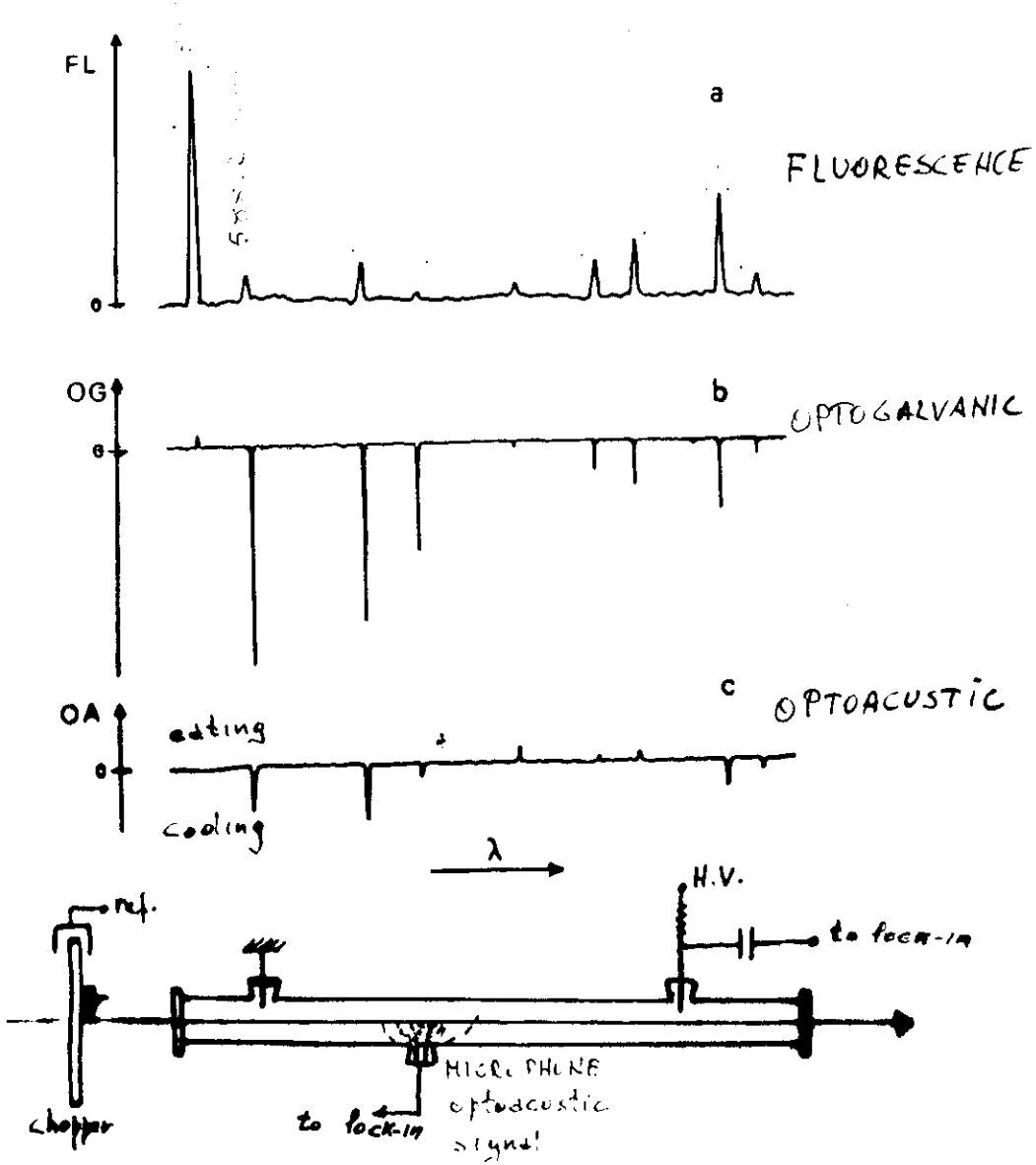

ACUSTIC SIGNALS MONITOR EATING OR COOLING OF THE ELECTRON TEMPERATURE

OG EFFECT IN THE CATHODIC REGION

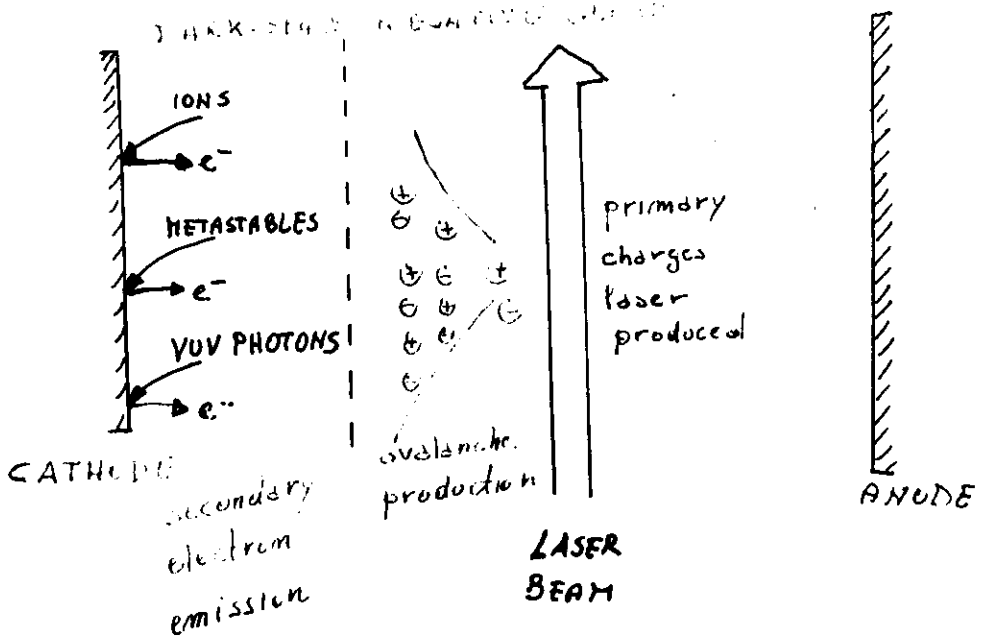

WHEN THE LASER BEAM CROSSES THE CATHODIC REGION IS CHANGED

1) GAS IONIZATION (avalanche production)

2) SECONDARY ELECTRON EMITTED FROM THE CATHODE SURFACE

USUALLY OG SIGNAL ARE STRONGER THAN IN POSITIVE COLUMN.

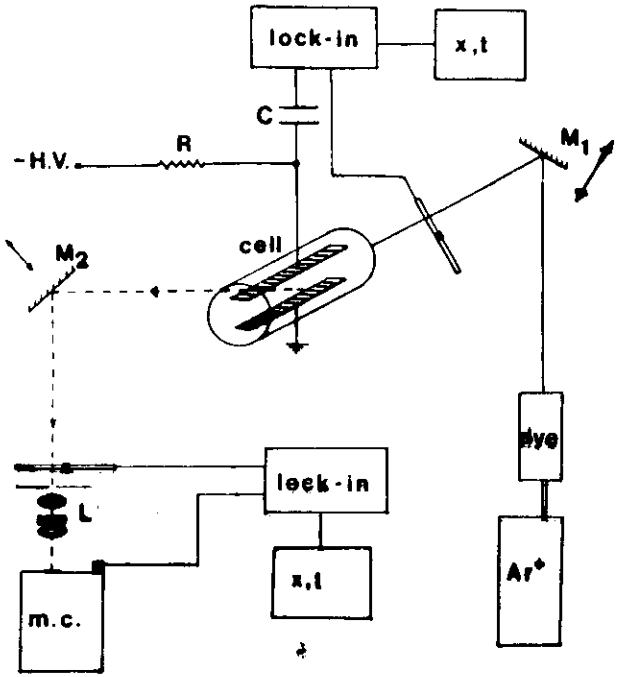

FIG. 2. Experimental setup: M1 and M2, translatable mirrors; m.c., monochromator; L, lens system; R, ballast resistor; C, coupling capacitor; x,t, chart recorder.

EXPERIMENTAL APPARATUS TO INVESTIGATE THE SPATIAL BEHAVIOURS OF OG and FL AS A FUNCTION OF THE CATHODE SURFACE.

OPTOGALVANIC SPECTROSCOPY

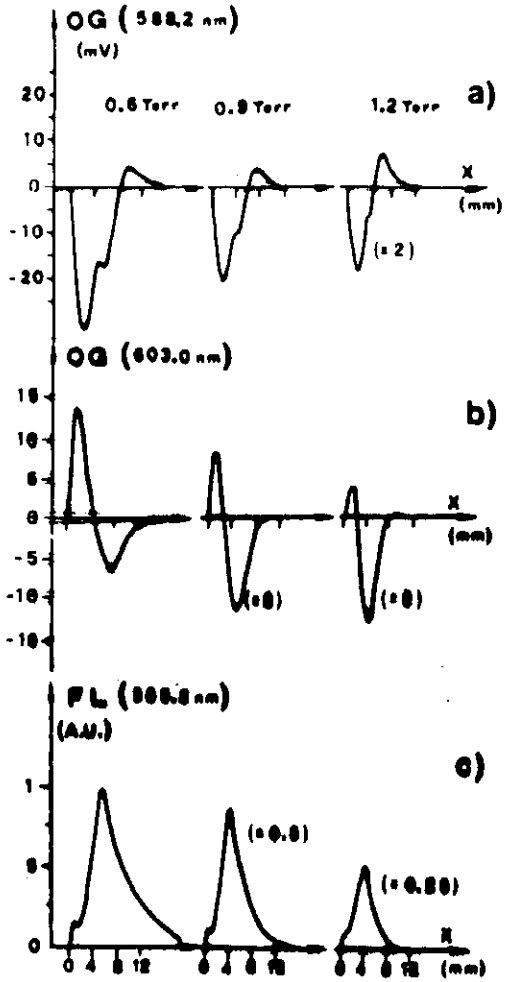

a) OG METASTABLE $1S_5 - 2P_2$

b) OG RADIATIVE $1S_4 - 2P_2$

c) FL

ADVANTAGES

[THE BASIC PRINCIPLE IS THE SAME AS THE OPTOACOUSTIC AND OPTOTHERMAL EFFECT]

1) ECONOMICAL AND EASY TECHNIQUE [NO VACUUM]

2) HIGH SENSITIVITY [DETECTION OF CURRENT]

3) WIDE SPECTRAL RANGE : IR → UV [FLAT RESPONSE]

4) VERSATILE : ATOMS, MOLECULES, IONS, RADICALS...

5) TYPE OF LASERS : C.W., PULSED, DIODE ...

6) SEVERAL DISCHARGES CONFIGURATIONS [Hollow cathode
Positive column
R.F., Microwave]

7) STUDY OF EXCITED LEVELS [OTHERWISE OF DIFFICULT OPTICAL EXCITATION]

8) STUDY OF ATOMS PRODUCED BY DISSOCIATION (OXYGEN)

9) HIGH RESOLUTION SPECTROSCOPY

[INTERMODULATED OPTOGALVANIC SPECTROSCOPY
POLINEX, Time - Photon].

DISADVANTAGES

OG SPECTRA IN Ca - HOLLOW CATHODE

POSITIVE COLUMN

p = 1 ÷ 10

i = 1 ÷ 20 mA

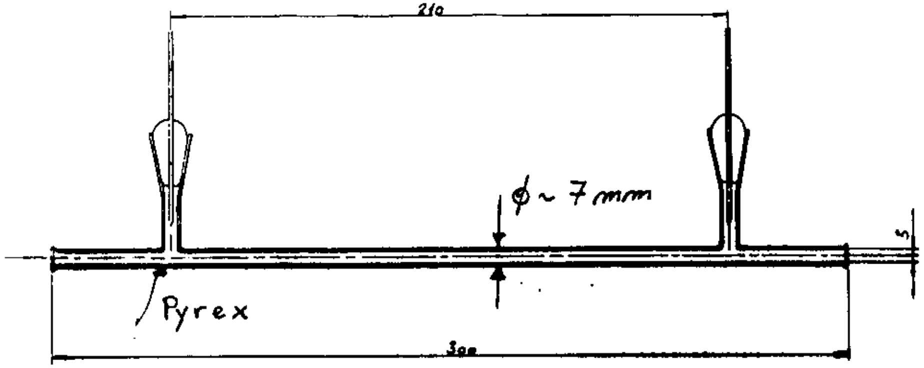

HOLLOW CATHODE

- HIGH DENSITY CURRENT
- SPUTTERING : REFRACTORY ELEM.

$i \leq 200$ mA

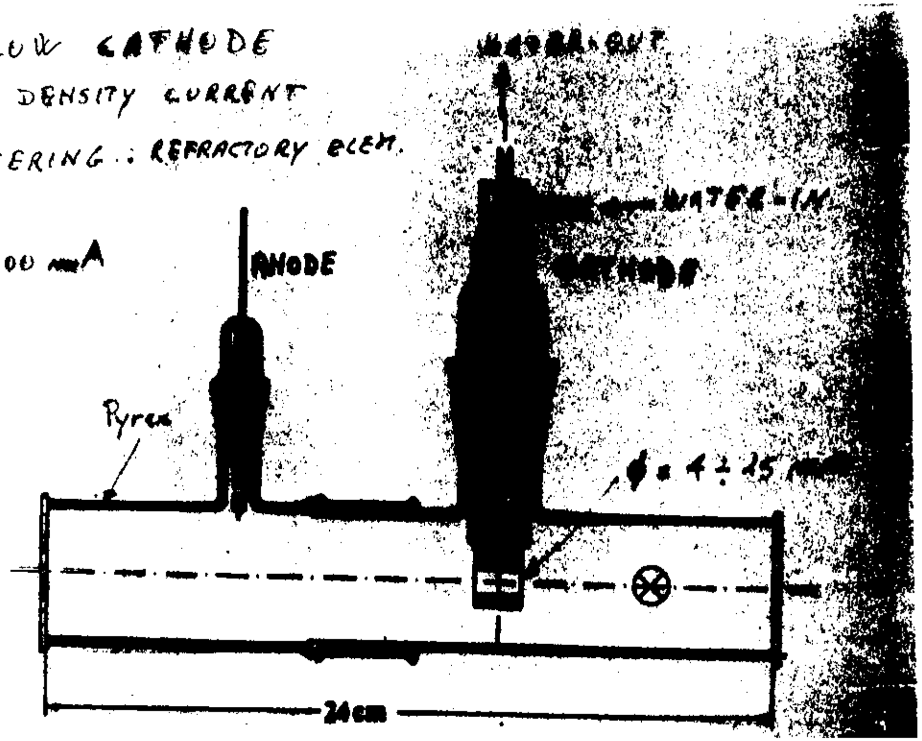

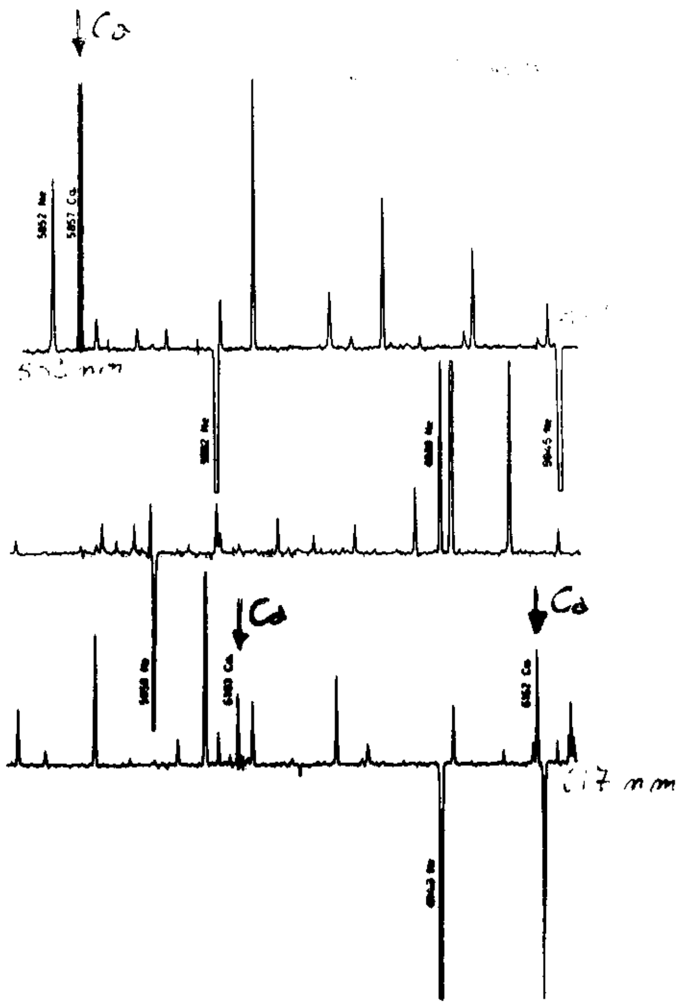

Fig. 17. – OG spectrum recorded by a HC discharge containing sputtered Ca atoms and neon at a pressure of 3 Torr, I = 60mA.

RADIO FREQUENCY DISCHARGE

a)

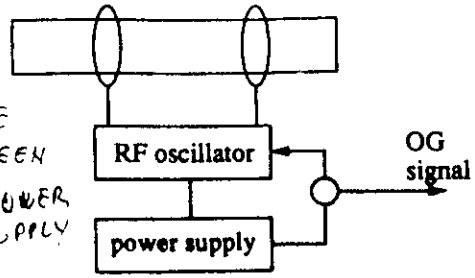

REGENERATIVE SIGNAL BETWEEN OSCILLATOR – POWER SUPPLY

b)

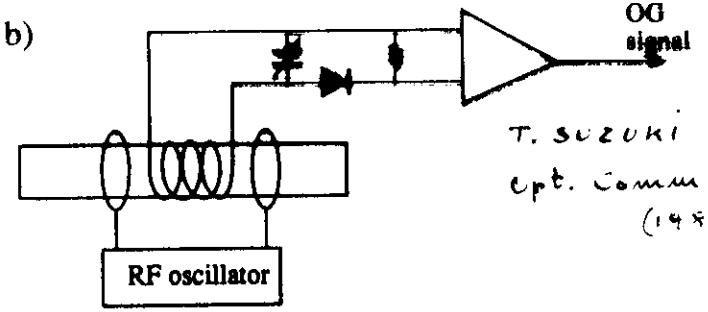

pick-up coil

T. SUZUKI
Opt. Comm. 35, 364 (1980)

c)

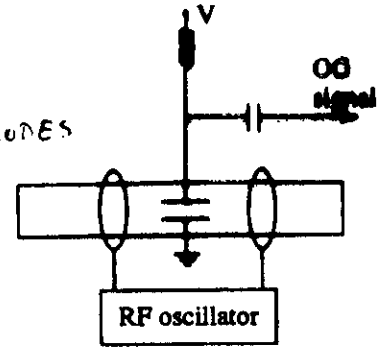

ACTIVE ELECTRODES

JABASTIE ET AL.
J. Phys. E 15, 1345 (1982)

NEW APPROACH TO IMPEDANCE SPECTROSCOPY

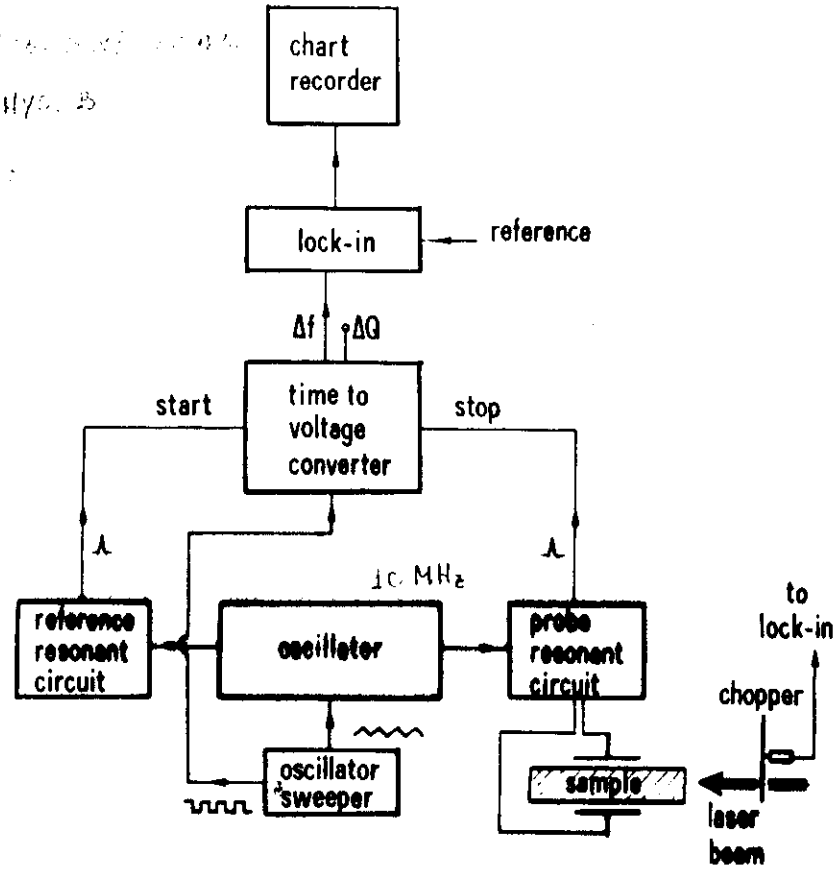

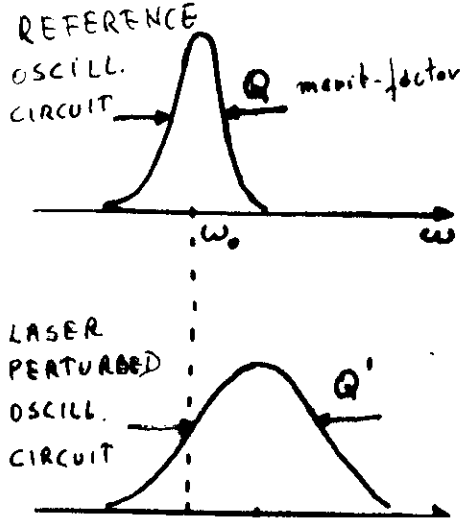

$$\Delta\varepsilon = -\frac{4\pi e^2}{m\omega(\omega - i\beta)}\Delta n_e$$

$$\Delta\varepsilon\big|_{real} \Rightarrow \Delta\omega = \omega_0' - \omega_0$$

$$\Delta\varepsilon\big|_{Im} \Rightarrow \Delta Q = Q' - Q$$

TEST !!

607.4 mm

Ne transition

DOPPLER LIMITED

ΔQ (×2)

Δf

10

06 (×10)

DOPPLER-FREE

^{20}Ne

^{22}Ne

ΔQ Δf

C = 3pF

DISCHARGE CELL

LASER

OSCILL PERTURB.

OSCILL. REF

06

C

R_b

H.V.

"IMPEDANCE" SPECTROSCOPY

Neon spectra

626.6

621.7

616.4

614.3

612.8

607.4

597.6

594.5

588.2

585.2

ΔQ

MPEDANCE SPECTROSCOPY : Na DISCHARGE

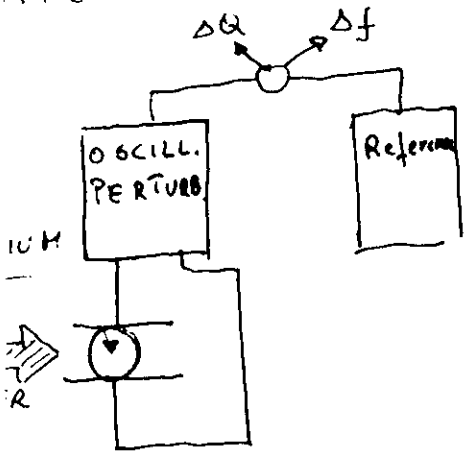

SODIUM VAPOUR

$$\Delta\varepsilon = -\frac{4\pi e^2}{m\omega(\omega - i\beta)}\Delta n_e$$

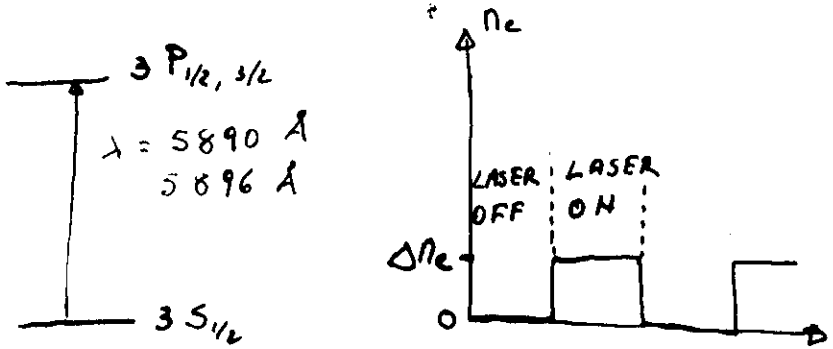

$$Na(3P) + Na(3P) \rightarrow Na_2^+ + e^-$$

Associative ionization

MICROWAVE OG SPECTROSCOPY

T. Sugai
Jpn. Phys. B 39
247 (1986)

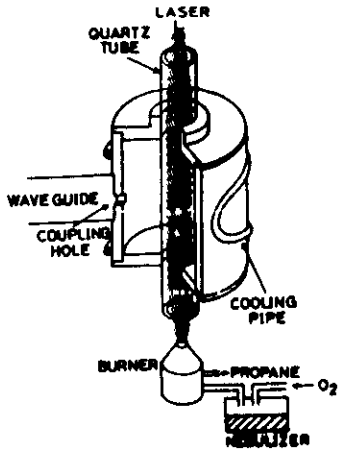

Fig. 1. Schematic representation of a microwave cavity and flame configuration

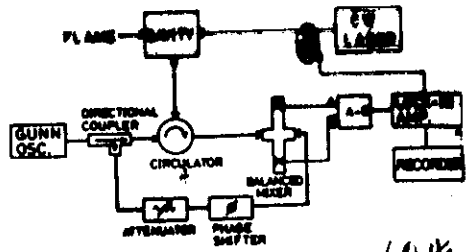

APPLICATION TO FLAMES DIAGNOSTIC

LOW CONCENTRATION SODIUM DETECTION

0.4 μg/ml

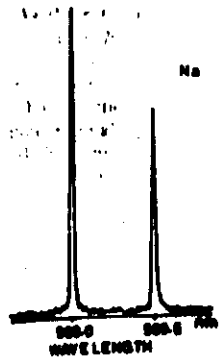

ATOMS AND MOLECULES WHERE OG EFFECT HAS BEEN OBSERVED

a)

H	He	Ne	Ar	Kr	Xe	C	
★	★●	★●□	★●	★	□	□	
Li	Na	K	Rb	Cs			
●	▲●	▲●	▲	★▲□			
Be	Mg	Ca	Sr	Ba		Eu	Yb
▲	▲	▲●	▲★	●▲★		▲●	▲●
Cu	Mn	Co	Y	Zr	Mo		
●	●	●	●	●	●		
	Ga	In	Hg				
	▲	▲	★				
	La		Sm				
	●		●				
	U						
	●						

□ [illegible]
★ D C
● H C
▲ DIC D S

b) H_2, He_2, I_2, N_2, CO, NO, CN, H_2O, NO_2, HCO, NH_2, CO_2, HCO_2, H_2CO, HNO_2, $C_2H_2O_2$.

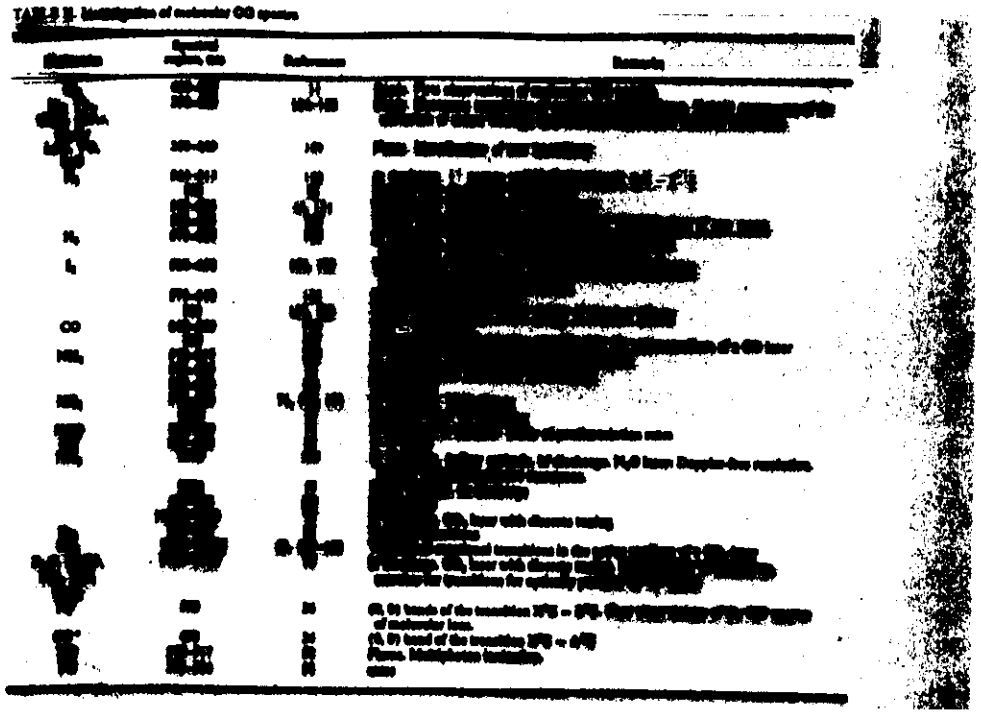

from Beverini, Desso, Darbieri
Rev. Mod. Phys, in press

Authors	element	kind of discharge	laser source	experimental results
Begemann and Saykally, 1982	Ar, Ne	d.c.	col.centre	ir spectrum (3600-4100) cm^{-1} in R6G dye region
Su et al., 1986	Ar	h.c.	cw dye	wavelength calibration
Suzuki et al., 1983	Ar	m.w.	cw dye	first OG spectroscopy in microwave discharge
Murnick et al., 1986	Ar	r.f.	cw dye	isotope shift in optical transitions for $^{36,38,40}Ar$ (IMOGS)
Moscatelli et al., 1986	Ar	r.f.	cw dye	isotope shift (IMOGS)
Camus et al., 1982	Ba	h.p	cw dye	Two-step excitation of Rydberg states
Rinneberger and Neukammer, 1983	Ba	h.p.	cw dye	Rydberg states spectroscopy of the states $6snp^{1,3}P$ and $6snf^{1,3}F$ by two-step excitation
Beigang et al., 1983	Be,Mg	h.p.	pulsed dye	Rydberf series of mono and mand configurations (n=10-70)
Inguscio, 1983	Ca, Ne, U	h.c.	cw dye	Doppler-free spectroscopy, isotope shifts, h.f. structures (IMOGS)
Bobulesco et al., 1980	Cs	r.f.		
Aymar et al, 1986	Cd	r.f.	pulsed dye	autoionising profiles of resonances $5s6p^3P_J - 5p^23P$
Gerstenberger et al., 1979	Cu	h.c.	cw dye	hyperfine structure, isotope shifts (IMOGS)
Beverini et al., 1982	Cu	h.c.	cw dye	hyperfine structure, isotope shifts (IMOGS)
Lawler et al., 1981	Cu, Mo	h.c.	cw dye	Doppler-free spectroscopy
Babin et al., 1987	Fe	h.c.	pulsed dye	wavelength calibration
Hansch et al., 1981	He, Ne	d.c.	cw dye	hyperfine structure of $^3He\,3^3P - 3^3D$ transitio
Katayama et al., 1981	He	d.c.	pulsed dye	Rydberg levels investigation np^1S (n=14-60)
Goldsmith and Smith, 1969	He	d.c	pulsed	demonstration of two-photon OG spectroscopy in $^4He\,2^3S - 3^3S$ transitions and $2^3S - 3^3D$
Jackson et al., 1981	He, Ne	h.c.	col.centre	IR Rydberg series
Ganguly and Garscadden, 1985	He	d.c.	cw dye	Allowed and forbidden Rydberg series $2s^1S - ns^1S, np^1P, nd^1D(n < 46)$
Lawler et al., 1979	He	d.c.	cw dye	first demonstration of IMOGS of $^3He\,2^3P - 3^3D$ transition at 587.5 nm
Hansch et al., 1981	He	d.c.	cw dye	first demonstration of POLINEX with OG detection of $^3He\,2^3P - 3^3D$ transition
Van De Weijer, 1986	Ne	d.c.	pulsed dye	two-step photoionization
Wada et al., 1986, 1987	Kr	h.c.	cw dye	autoionising visible transitions: $6p'-6d'$, $6p'-6s'$
Delsart et al., 1981	Kr	d.c.	pulsed dye	Rydberg states $nd[3/2]_2$ ($n = 15 \div$ [illegible])
Behrens et al., 1986b	I,Ge	h.c.	cw dye	hyperfine constants of $5p^2P$ and $6p^2P$ isotope shifts
Bagloman et al., 1966	Lu	h.c.	cw dye	Hyperfine structure of the $^2D^o_{3/2} - ^2D_{5/2}$ transition and isotope shifts in $^{175,176}Lu$
Behrens and Guthohrlein, 1986a	Mn,Cu,La	h.c.	cw dye	Doppler limited and Doppler-free spectroscopy (IMOGS)
Beigang and Timmermann, 1983	Yb,Eu,Bull Mg, Ca Sr, Ca	h.p.	cw dye	hyperfine structure and isotope shifts of Rydberg series by Doppler-free two-photon spectroscopy
Siegel et al., 1981	Mo	h.c.	cw dye	isotope shifts
Wakata et al., 1981	Na	h.c.	pulsed dye	two-step and two-photon excitation

Beverini et al., 1985	Ne	h.c.	cw dye	Optogalvanic nonlinear Hanle effect
Goldsmith et al. 1979	Ne	d.c.	cw dye	demonstration of Doppler-free two-photon OG spectroscopy
Nestor, 1982	Ne,Ar	d.c.	pulsed dye	two-photon OG spectroscopy
Belfrage et al., 1983	Ne,Mo	h.c.	cw dye	comparison of Doppler-free techniques (IMOGS, POLINEX, Polarisation)
Lyons et al., 1981	Ne	r.f.	cw dye	Doppler-free spectra of $1s^2 - 2p_1$ transition at 585.2 nm
Julien and Pinard, 1982	Ne	r.f.	cw dye	optical pumping
Miyazaky et al., 1983	Ne	h.c.	cw dye	double resonance
Bickel et al., 1985	Ne	h.c.	pulsed dye	two-photon and two-color OG investigations
Caesar and Heully, 1983	Ne	h.c.	pulsed dye	Rydberg series (3p'-ns,nd) and autoionising series (3p'-ns',nd')
Keaton and Noger, 1987	O	d.c.	pulsed dye	hygly-excited atoms detection
Inguscio et al., 1988	O	r.f.	cw dye	fine structure of $4d^5D_{4-0}$ levels (IMOGS)
Ernst et al., 1989	O	r.f.	cw dye	isotope shift in 16,18O optical transitions
Reddy and Rao, 1987	PrI, PrII	h.c.	cw dye	Doppler-limited hyperfine structure of optical transitions
Lorensen and Niemax, 1982	SrI, SrI	h.p.		isotope shifts measurements
Naveedullah and Naqui, 1985	Th	h.p.	pulsed dye	pressure broadening and isotope shifts of $6^3F_{1/2} - 6^3F_{1/2,3/2}$ transitions
Langlois and Gagne', 1987	U	h.c.	cw dye	og detection of hfs/iso patterns (IMOGS)
Broglia et al., 1983a	U	h.p.	pulsed dye	highly excited spectrum for isotope separation study
Palmer et al., 1981	U	h.c.	cw dye	wavelength measurements of spectral lines
Piyakis and Gagne', 1988	UIII	h.c.	cw dye	identification of doubly-ionized uranium transitions in noble gase discharge
Pianarosa et al., 1984	U	h.c.	cw dye	Doppler-limited isotope shifts ($^{234,235,236}U$) measurements
Dovichi et al., 1982	U	h.c.	pulsed dye	wavelength calibration
Kroll and Persson, 1985	^{51}V	h.c.	cw dye	hyperfine structure of the $3d^44s^6D - 3d^44p^6F$ transition
Grandin and Husson, 1981	Xe	r.f	cw dye	Rydberg states $np[1/2]_1 (n = 15 - 19)$; $nf[3/2]_1 (n = 11 - 43)$ autoionizing states $6p^57p'[5p^5nf'(n = 4 - 7)$
Labastie et al., 1982a	Xe	r.f.	cw dye	Rydberg series: $np[3/2]_2 - ns[3/2]_1$, $ns[3/2]_2$ $np[3/2]_1 - ns[3/2]_1$ (n=12-27) $np[3/2]_1 - nd[3/2]_1 (n = 12 - 27)$
Labastie et al., 1982b	Xe	r.f.	cw dye	[illegible] and broadening [illegible] levels
Lemoigne et al., 1983,1984	Xe,Kr	r.f.	cw dye	[illegible] in magnetic field
Hannaford et al, 1983a, 1983b	Kr, Y	d.c.	cw dye	demonstration of level crossing
Chevalier et al., 1986	Kr	h.c.	cw dye	hyperfine constants for the levels $^3P_2^\circ, ^3P_1^\circ, ^3P_1^\circ, ^3D_1^\circ$, $^3P_2^\circ, ^3D_2^\circ, ^3D_3^\circ$ (POLINEX, IMOGS)
Chevalier et al., 1987	Kr	h.c.	cw dye	isotope shifts measurements of optical transitions for $^{80,81}Kr$ (POLINEX,IMOGS)
Bourne et al., 1985	Zr	h.c.	cw dye	hyperfine structure and isotope shifts for $a^3F_3 - z^3D_3^\circ$ transitions (IMOGS)

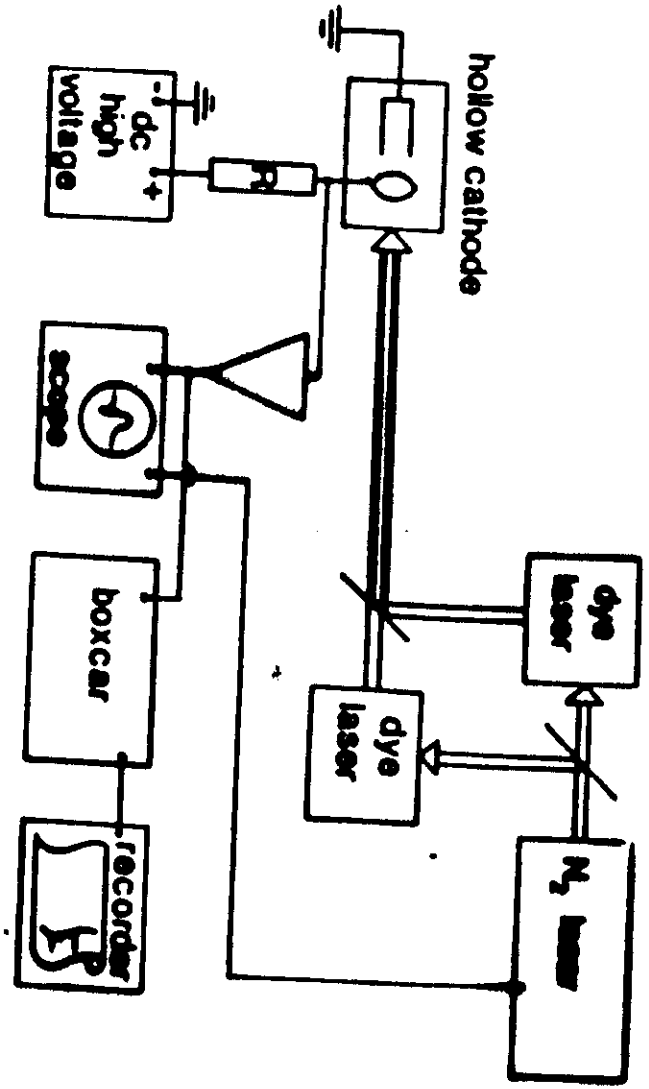

WIDTH OF SPECTRAL LINES

HOMOGENEOUS BROADENING : COLLISIONS
LIFETIMES
TIME OF FLIGHT
SATURATION

DOPPLER BROADENING : MOTION OF ATOMS

VISIBLE : $\nu \sim 5 \cdot 10^{14}$ Hz

DOPPLER WIDTH $\Delta\nu_D \sim 10^9$ Hz = 1 GHz

HOMOG. - WIDTH $\Delta\nu_H \sim 10^7$ Hz = 10 MHz

TO PERFORM SUB-DOPPLER SPECTROSCOPY NEED LASERS WHOSE BANDWIDTH IS LESS THAN $\Delta\nu_H$ ($\Delta\nu_{LASER} \leq 1$ MHz) AND TECHNIQUES TO REMOVE DOPPLER SHIFT :

- ATOMIC BEAM SPECTROSCOPY
- SATURATION SPECTROSCOPY } "OPTOGALVANIC VERSION"
- TWO-PHOTONS SPECTROSCOPY }
- TRAPPED PARTICLES SPECTROSCOPY

SATURATION SPECTROSCOPY

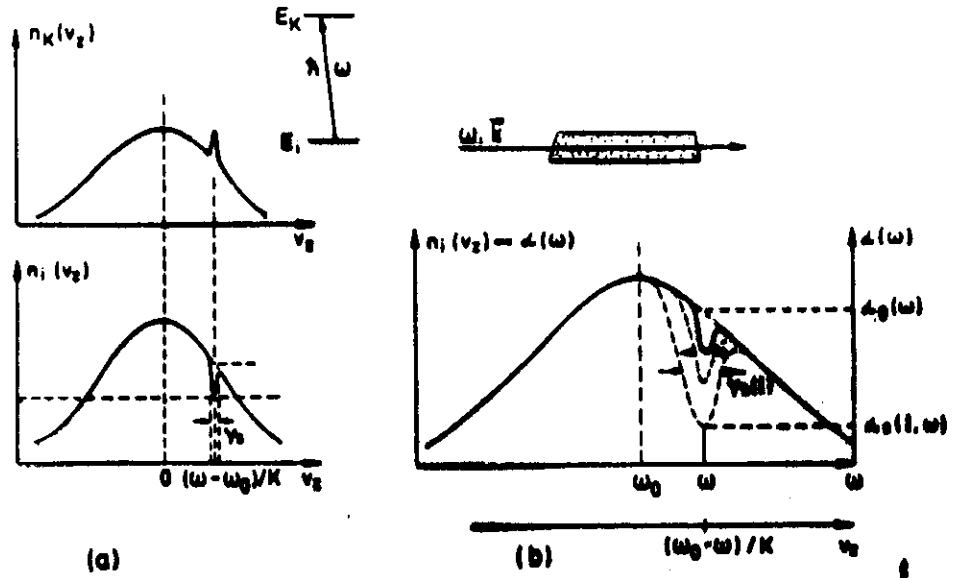

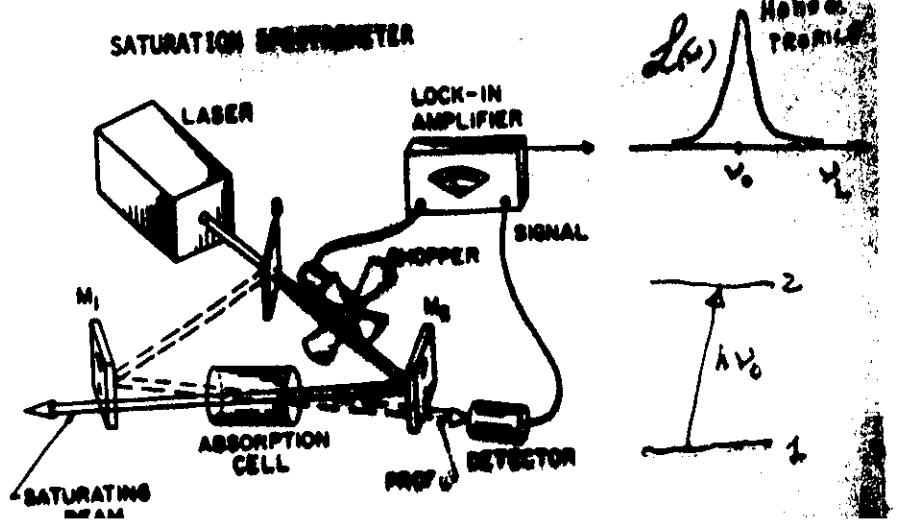

SOMETIME THE SENSITIVITY OF SATURATION SPECTROSCOPY IS NOT ENOUGH (DIP CONTRAST)

NEW TECHNIQUES

- ⊙ INTERMODULATED SPECTROSCOPY
- ⊙ POLINES
- ⊙ POLARIZATION SPECTROSCOPY

AND ISOTOPE SHIFT OF ATOMIC OXYGEN

[illegible] SATURATION SPECTROSCOPY

[illegible] : Neon transition

FROM METASTABLE $1s_4 \rightarrow 2p_3$

$\lambda = 6074$ Å

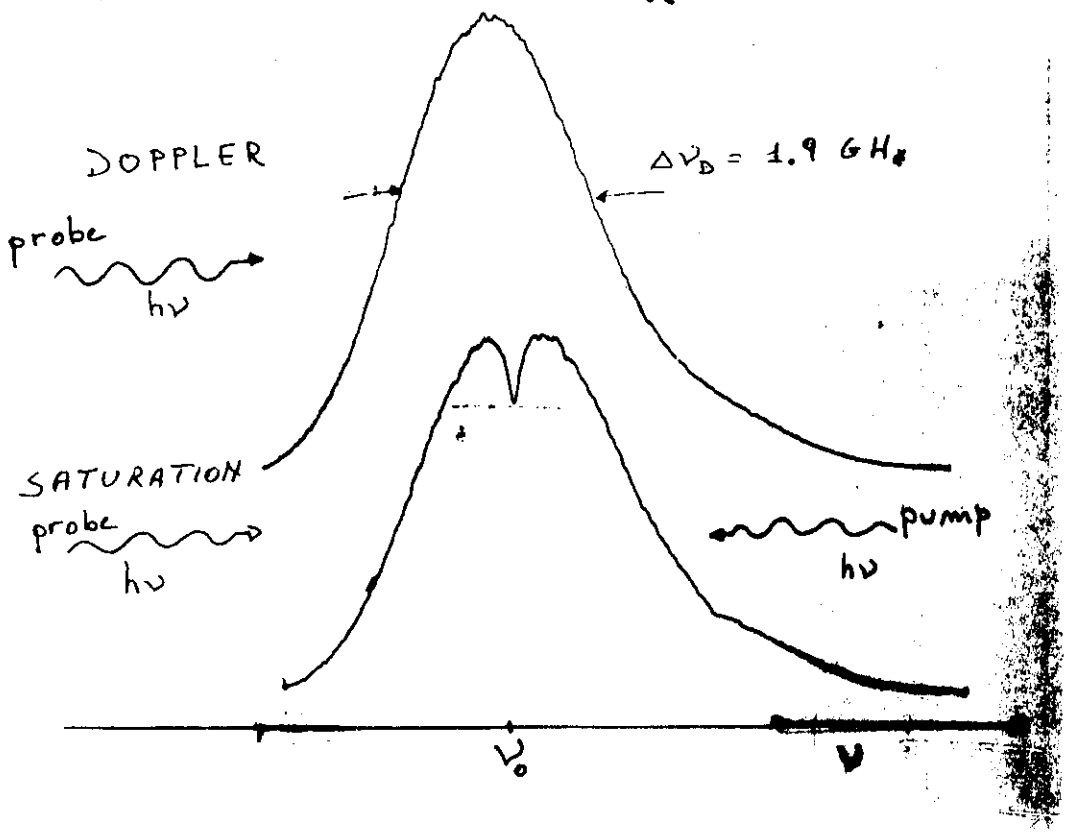

HOW REMOVE THE DOPPLER BACKGROUND?

INTERMODULATED OPTOGALVANIC SPECTR.

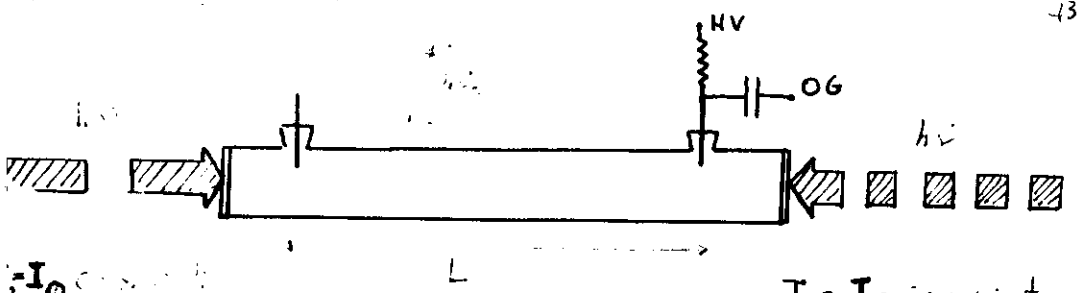

THE OG SIGNAL INDUCED BY TWO COUNTERPROP. BEAMS, MODULATED AT FREQUENCIES

$\omega_1 = 2\pi f_1$; $\omega_2 = 2\pi f_2$

$I = I_1 + I_2$

is given by

$$S_{OG} = K I \left[1 - e^{-\alpha(\omega) L} \right] \qquad K = \text{const.}$$

where

$$\alpha(\omega) = \alpha_0(\omega) \left[1 - \frac{S_0}{2} \frac{(\gamma_s/2)^2}{(\omega - \omega_0)^2 + (\gamma_s/2)^2} \right]$$

If $\alpha L \ll 1$ ("optically" thin sample)

$$S_{OG} = K L \alpha_0(\omega) \left[I - \frac{I^2}{2 I_{SAT}} \frac{(\gamma_s/2)^2}{(\omega - \omega_0)^2 + (\gamma_s/2)^2} \right]$$

Being:

$$I = I_1 + I_2 = I_0 \sin\omega_1 t + I_0 \sin\omega_2 t$$

$$= I_0 \left(\sin\omega_1 t + \sin\omega_2 t \right)$$

$$S_{OG} = K L \alpha_0(\omega) \Big|_{\omega_1} + \quad \Leftarrow \text{DOPPLER}$$

$$K L \alpha_0(\omega) \Big|_{\omega_2} + \quad \Leftarrow \text{DOPPLER}$$

$$K L \alpha_0(\omega) \Big|_{(\omega_1+\omega_2)\ \text{or}\ (\omega_2-\omega_1)} \cdot \frac{(\gamma_s/2)^2}{(\omega - \omega_0)^2 + (\gamma_s/2)^2} \Leftarrow \text{SUB-DOPPLER}$$

FINALLY

$$S_{OG}^{(\omega_1+\omega_2)} = K \cdot e^{-\left[\frac{(\omega-\omega_0)}{\Delta\omega_D}\right]^2} \cdot \frac{(\gamma_s/2)^2}{(\omega - \omega_0)^2 + (\gamma_s/2)^2}$$

If $\gamma_s \ll \Delta\omega_D$

$$S_{OG}^{(\omega_1+\omega_2)} = K \frac{(\gamma_s/2)^2}{(\omega - \omega_0)^2 + (\gamma_s/2)^2}$$ HOMOGENEOUS LINESHAPE

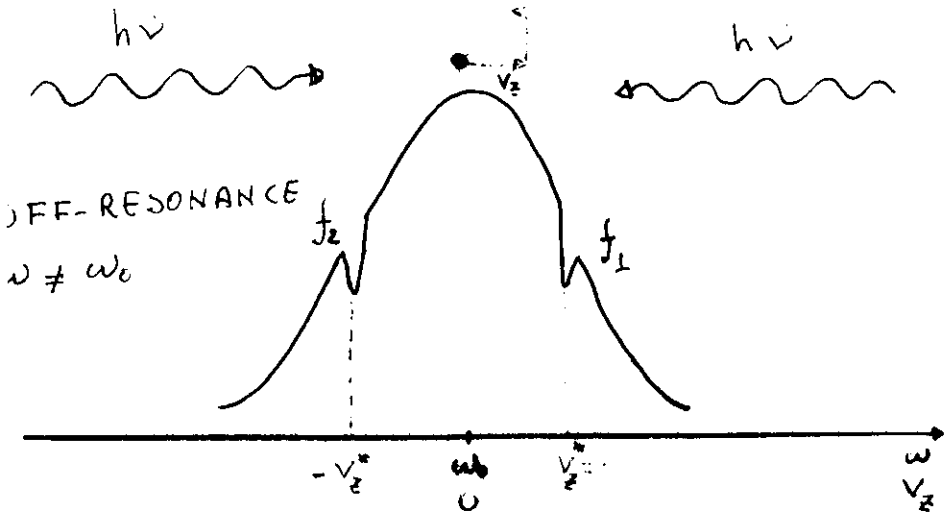

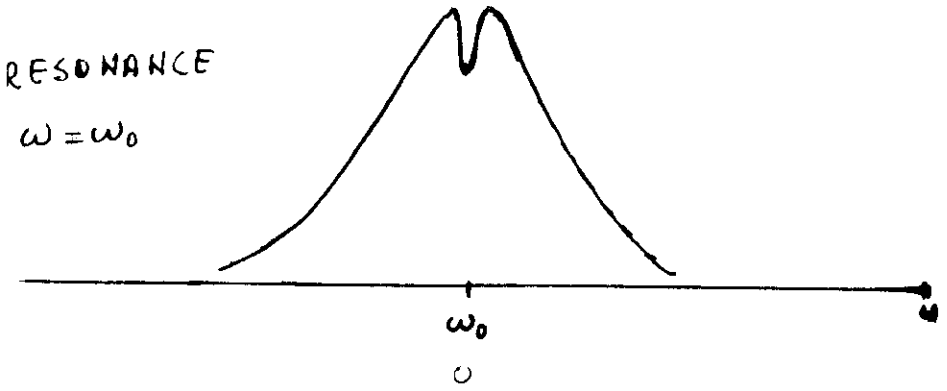

IN RESONANCE THE TWO LASER BEAMS INTERACT WITH ATOMS WHOSE VELOCITY

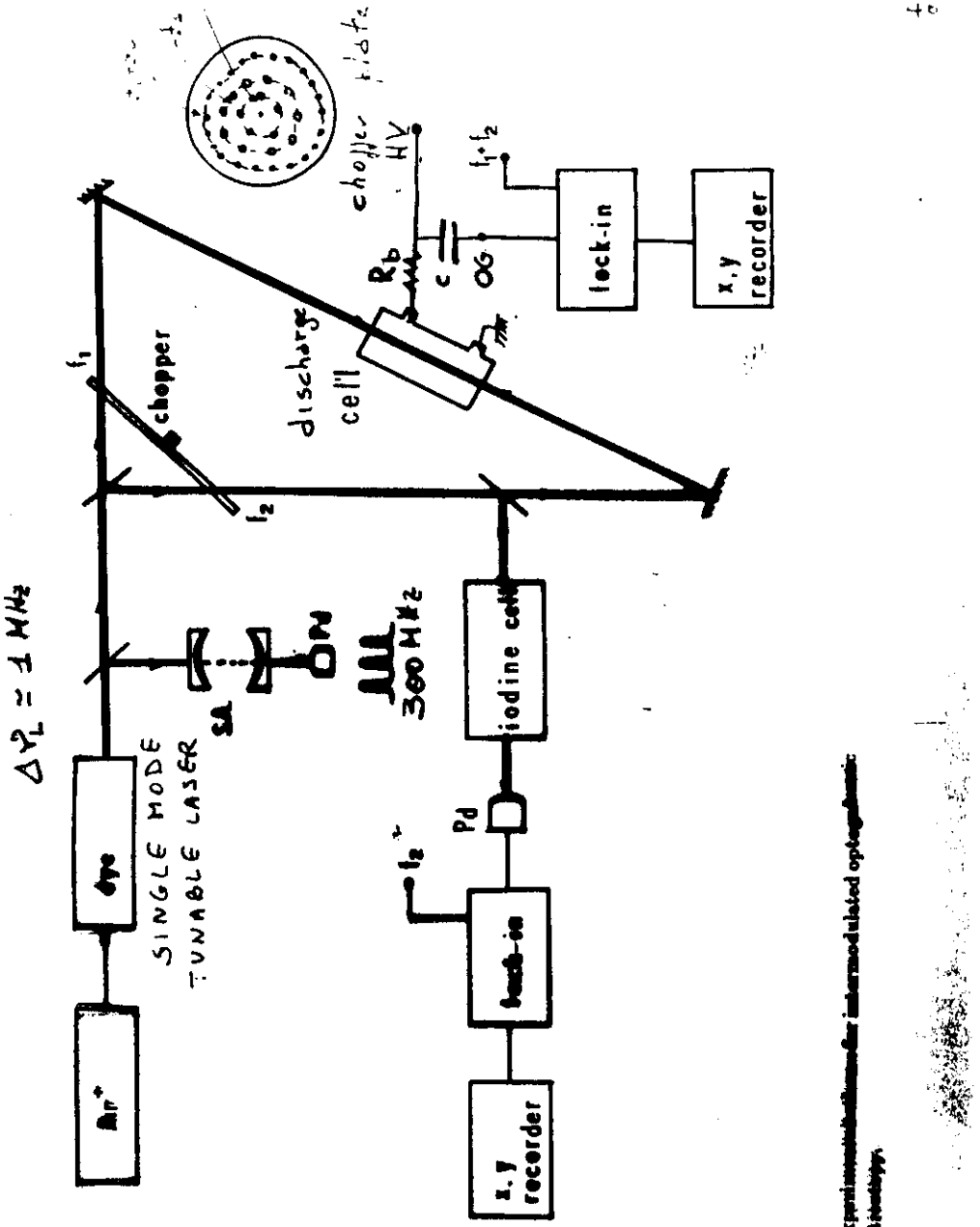

Experimental set-up for intermodulated optogalvanic spectroscopy.

$1s_4(J=2) - 2p_3(J=1)$

6074 Ne

6 Å

Laser multimode

.024 Å / 2 GHz

DOPPLER

20

Laser monomode

~ 2 GHz

$f_1 + f_2$

~ 90 MHz

INTERM.

^{20}Ne 90.92%

^{22}Ne 8.82 3%

22

f_1

$f_1 + f_2$

$\Delta\nu_H$ = 0.09 GHz

($\Delta\nu_{mod.}$ = 2.6 GHz (I.S.)

VELOCITY CHANGING COLLISIONS

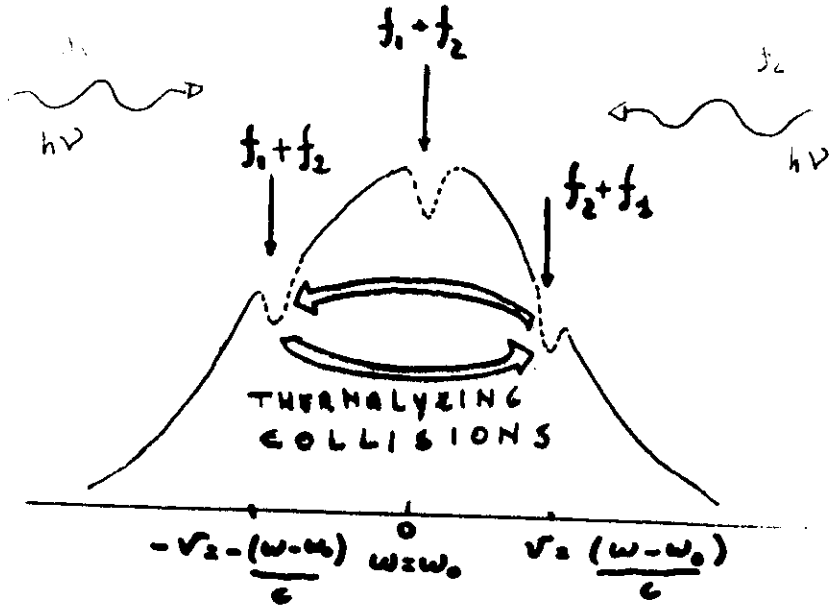

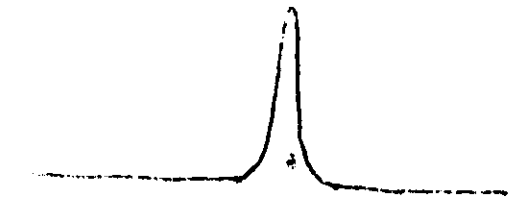

$\mathcal{L}(\omega)$

$G(\omega)$

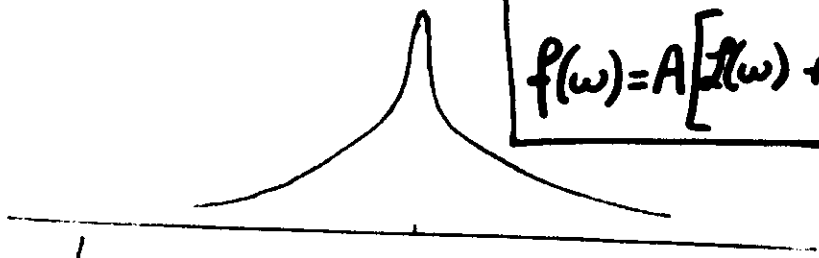

$$f(\omega) = A\left[\mathcal{L}(\omega) + C\ G(\omega)\right]$$

$$C \sim 2\sqrt{\pi}\,\log 2\,\frac{\Gamma_1\,\gamma}{\gamma_2\,\Delta\nu_D^2}$$

VELOCITY CHANGING COLLISIONS

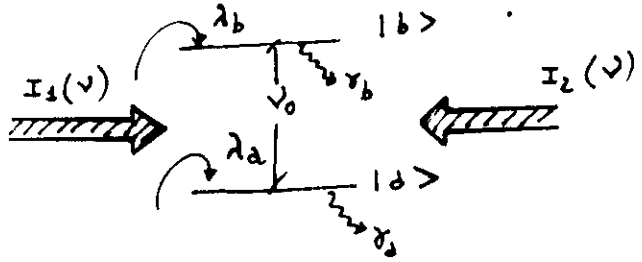

$$n_\alpha(v) = \lambda_\alpha(v) - \gamma_\alpha n_\alpha(v) - [I_1\sigma_1(v) + I_2\sigma_2(v)][n_a - n_b(v)] - \left[\frac{\partial}{\partial t} n_\alpha(v)\right]_{coll} \qquad \alpha = a, b$$

$$\left[\frac{\partial}{\partial t} n_\alpha(v)\right]_{coll.} = -n_\alpha(v)\int \Gamma_\alpha(v,v')\,dv' + \int n_\alpha(v')\,\Gamma_\alpha(v,v')\,dv'$$

- STRONG COLLISIONS $\boxed{\Delta\nu \approx \nu}$
- $\Gamma(\nu',\nu) = \Gamma_\alpha\, G(\nu')$ $\qquad G(\nu') = \frac{1}{\sqrt{\pi}\bar{\nu}}\, e^{-\nu^2/\bar{\nu}^2}$
- WEAK COLLISIONS $\boxed{\Delta\nu \ll \nu}$

$$S_{OC} = A\left\{\frac{\gamma^2}{\gamma^2 + 4\pi(\nu-\nu_0)^2} + C\left[e^{\left[\frac{(\nu-\nu_0)}{\Delta\nu_D}\right]^2}\right]\right\}\left[e^{\left[\frac{\nu-\nu_0}{\Delta\nu_D}\right]^2}\right]$$

$$= A\left\{\mathcal{L}(\nu-\nu_0) + C\,G(\nu-\nu_0)\right\}$$

$\Gamma_\alpha \gg \gamma_0 \gg \tau_\alpha$

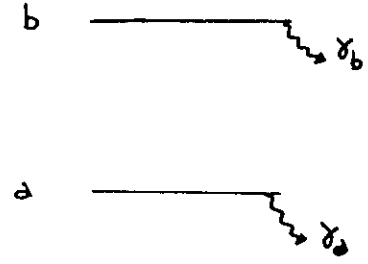

γ decay rates

$$S = A\left[C\cdot G(\omega-\omega_0) + \mathcal{L}(\omega-\omega_0)\right]$$

$$C = 2(\pi\log 2)^{1/2}\cdot\frac{\Gamma_\alpha\,\gamma}{\gamma_a\,\Delta\nu_D} \qquad \gamma_a \ll \gamma_b$$

γ : homogeneous linewidth

γ_a : decay rate $\gamma_a = \gamma_{coll} + \gamma_{diff} + \gamma_{disch} + \gamma_{nat}$

Γ_α : cross-relaxation $\Gamma_\alpha = \Gamma_{ee} + \Gamma_{met}$

So, the Doppler pedestal can gives informations on the collisional physics !!

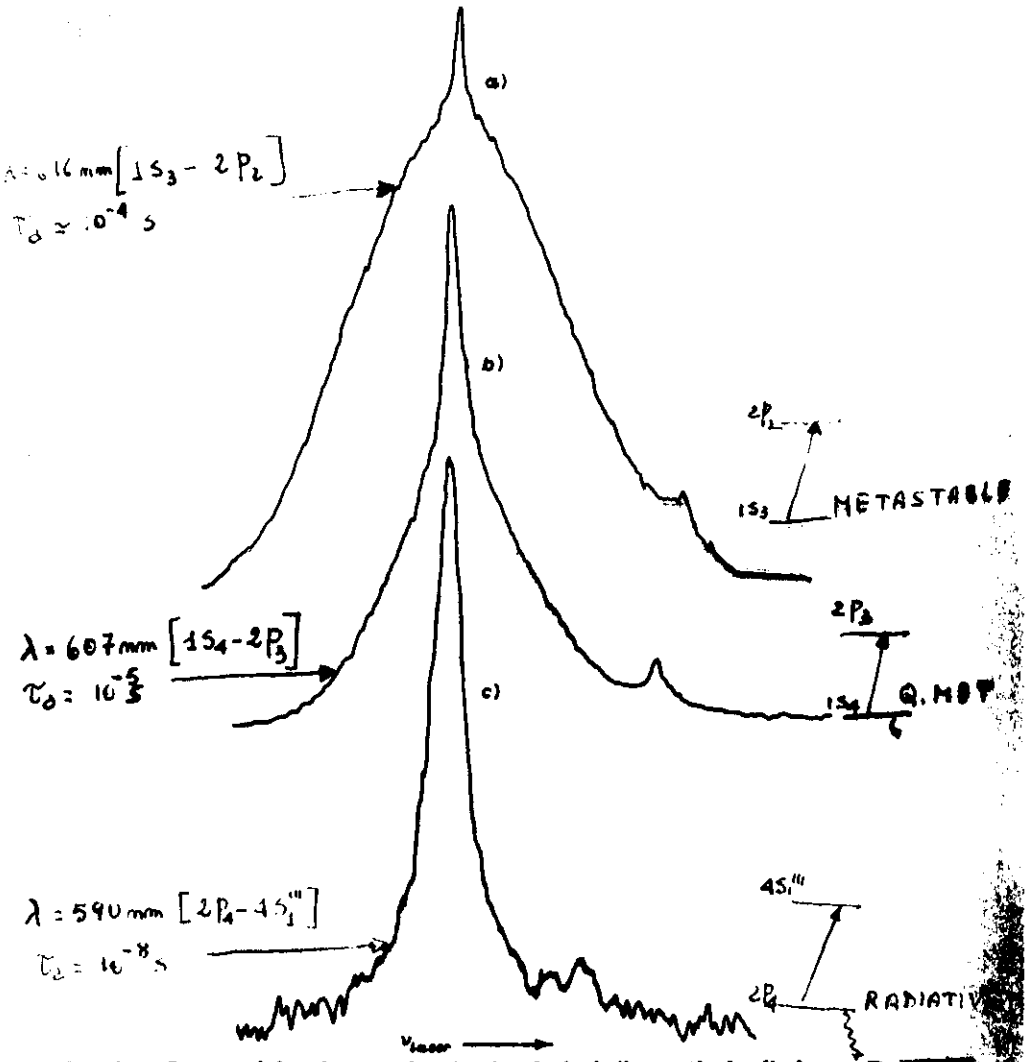

Fig. 3. – Intermodulated optogalvanic signals in hollow-cathode discharges in natural abundance neon. These different transitions are recorded: a) $1s_3 \rightarrow 2p_2$ at 616.4 nm ($p = 1.2$ Torr, $I = 30$ mA, b) $1s_4 \rightarrow 2p_3$ at 607.4 nm ($p = 1.6$ Torr, $I = 40$ mA, c) [illegible] 590.2 nm ($p = 0.6$ Torr, $I = 40$ mA). The change in the lineshapes is caused by [illegible] effective lifetimes of the longer-living (lower) lever of each transition ($\approx 10^{-8}$ in a) 10^{-5} in b) 10^{-4} in c)).

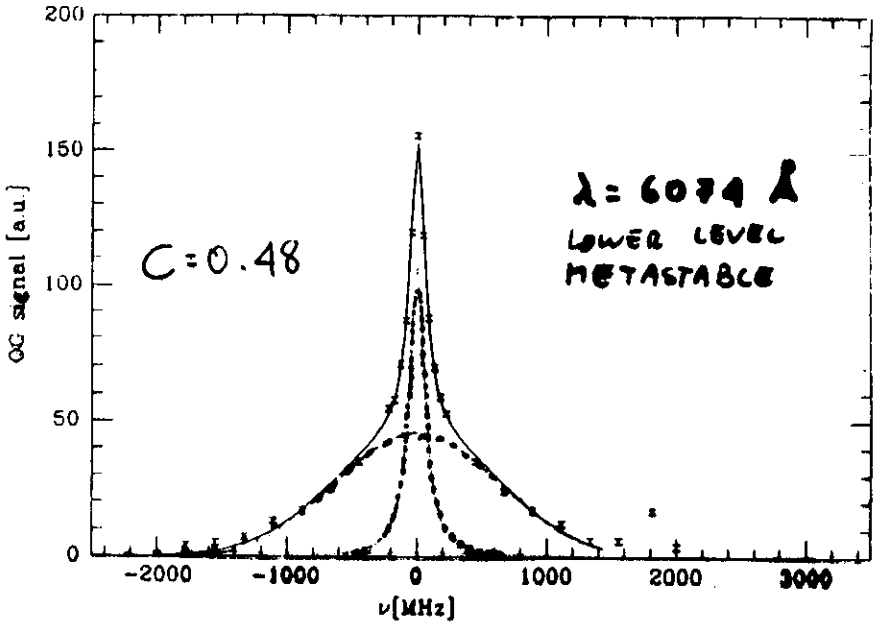

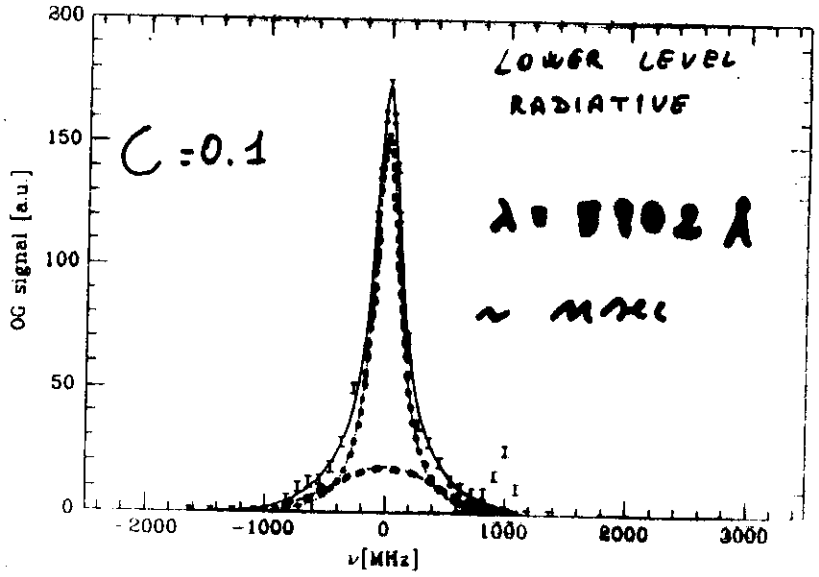

Ne - H mixture

p_{Ne} / p_{He} = 1.02

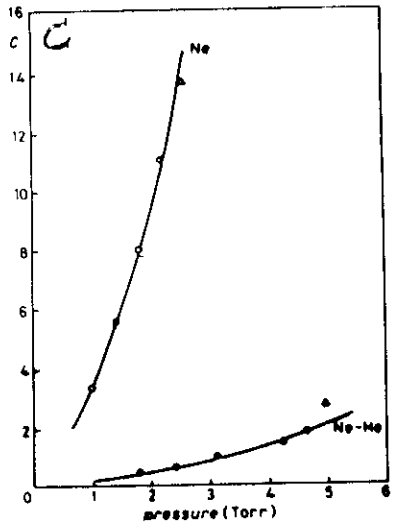

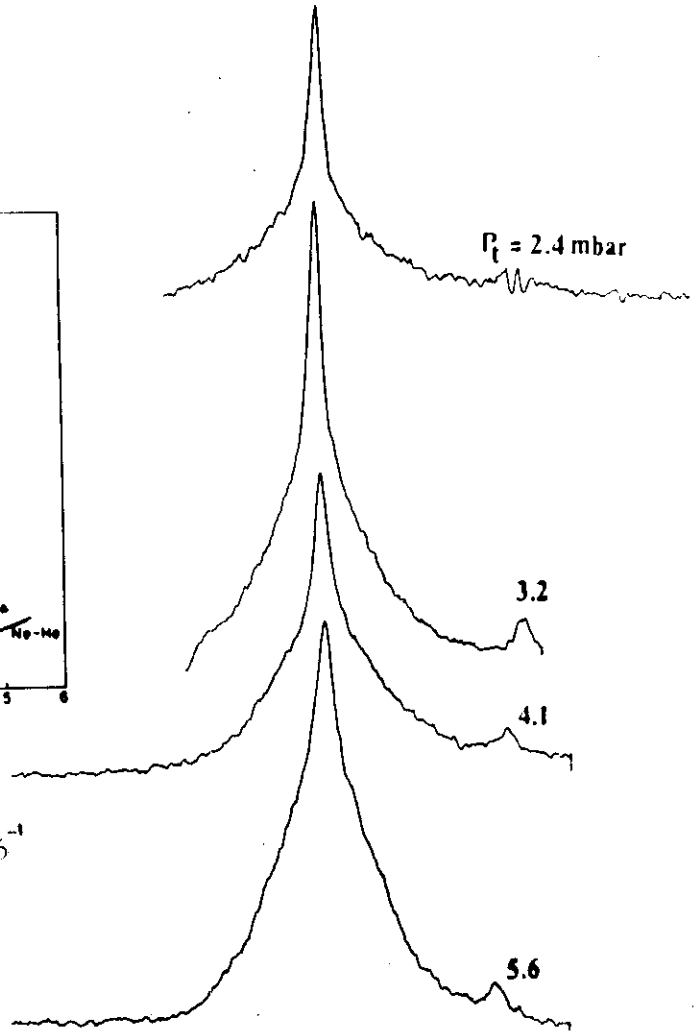

$\Gamma^{met}_{Ne-Ne} = 1.1 \times 10^{7}\ s^{-1}$

$\Gamma^{el.}_{Ne-Ne} = 0.\ldots \times 10^{7}\ s^{-1}$

$C \propto \frac{\Gamma_d \gamma}{\gamma_d \ldots V_p}$

$\Gamma_d = \Gamma_{el} + \Gamma_{met}$

$= n_{Ne} \cdot V_{Ne-Ne} \left(\sigma_{el} + \sigma_{met.}\right)_{Ne} + \ldots$

$n \ldots$

$Ne^{*} + e^{-} \rightarrow Ne + e$

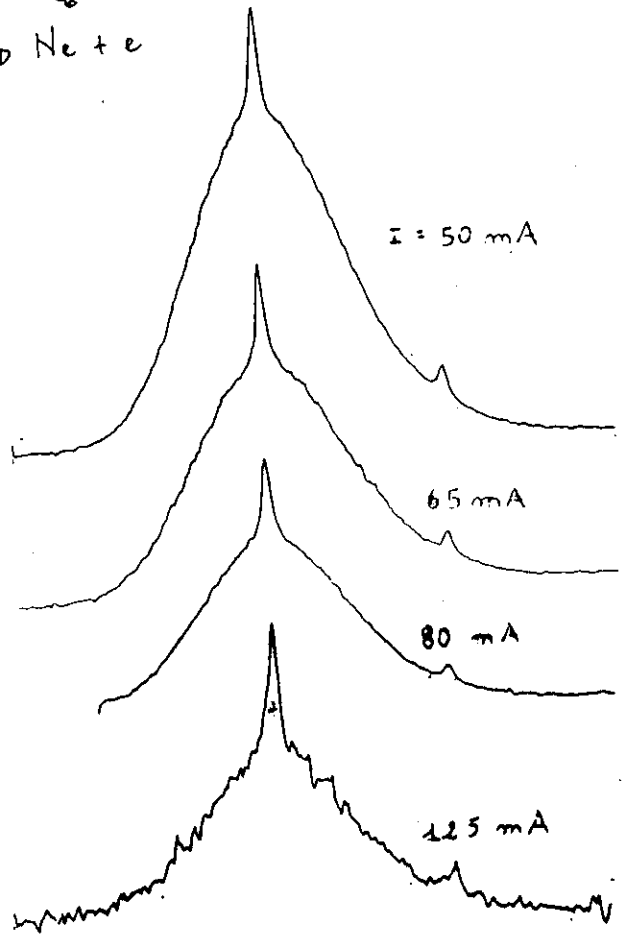

$\ldots_{disch} = 1.5 \times 10^{5}\ s^{-1}$

$C \propto \frac{\Gamma_d \gamma}{\gamma_d \ldots V_p}$

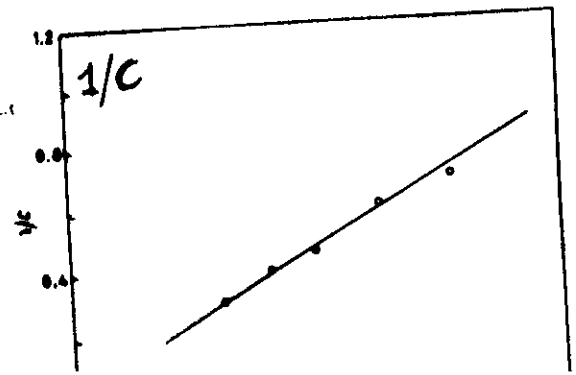

609.6 nm Neon transition

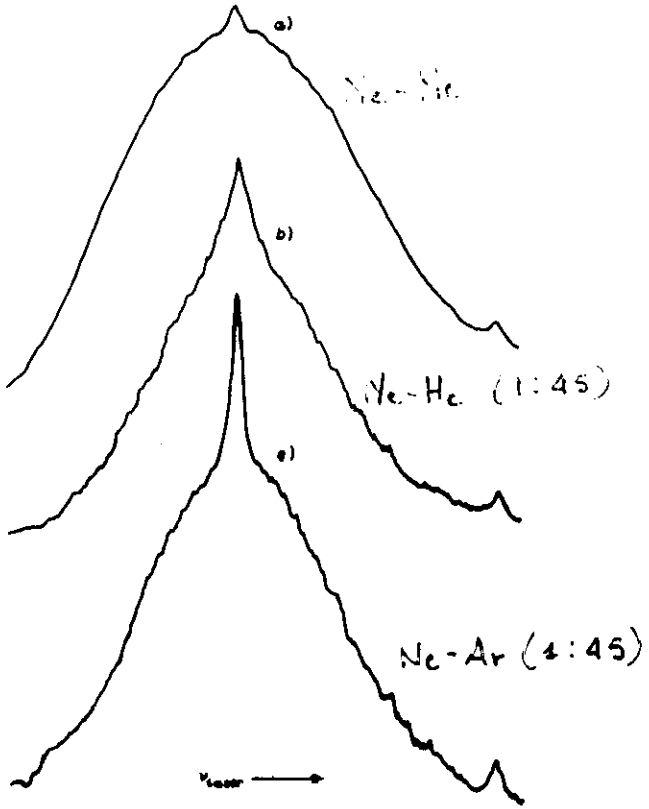

Fig. 8. – Intermodulated radio frequency optogalvanic lineshapes for the 609.6 nm transition: a) refers to a pure neon discharge (p = 5.0 Torr), while b) and c) refer to a 1:45 Ne-He mixture (p_{tot} = 5 Torr) and to a 7:1 Ne-Ar mixture (p_{tot} = 1.5 Torr), respectively. The reduction of the pedestal introduced by the buffer gases is evident.

A. SASSO et al. Nuovo Cim. D 10 921 (1988)

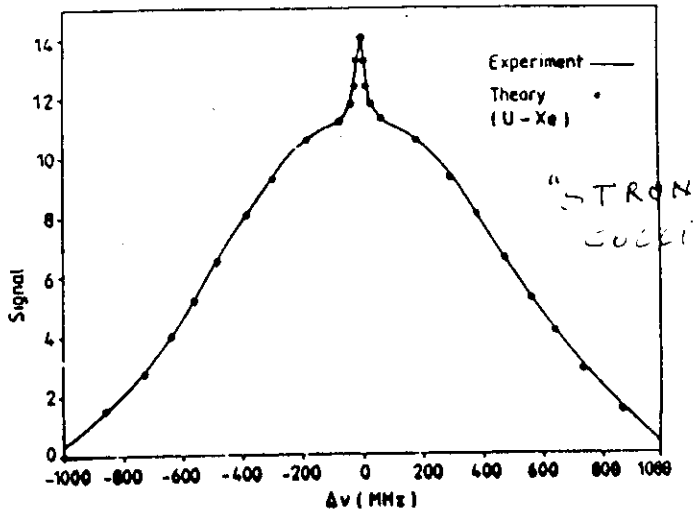

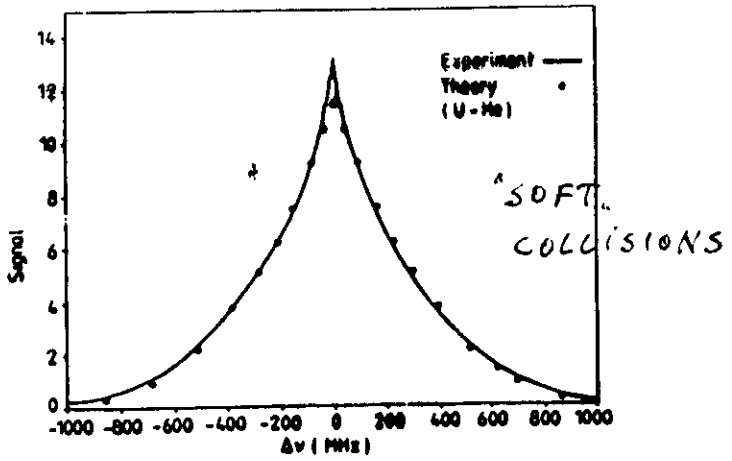

... BERENBAUM et al. J. Phys. B 16, 4513 (1983)

For theory see: P.R. BERMAN Adv. At. Mol. Phys. 13 57 (1978)

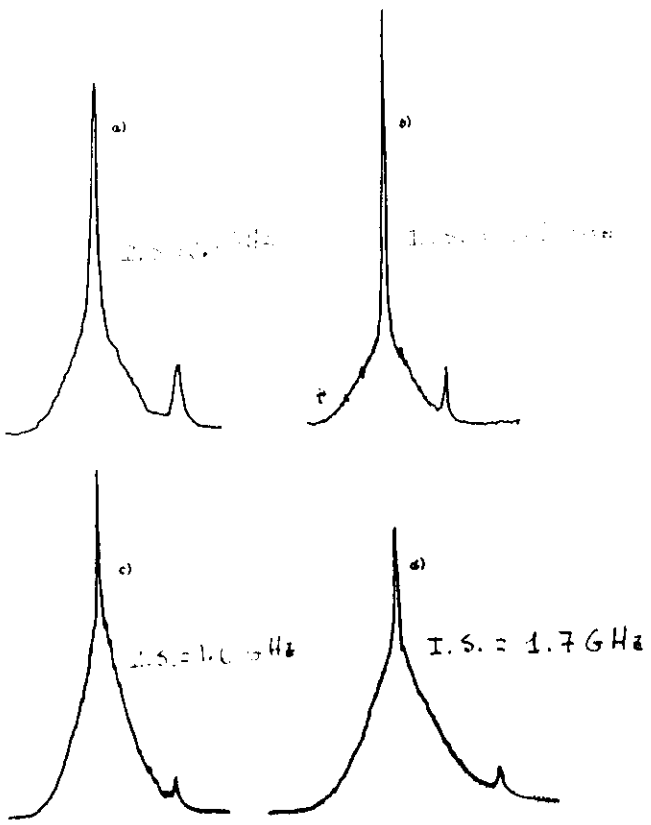

Fig. 22. – Doppler-free intermodulated recordings of natural neon transition involving (lower two) or not (upper two) metastable levels. From [166]. a) [illegible] Å, $1s_5(1)$-$2p_1(0)$, IS : 2.3 GHz; b) 6074.3 Å, $1s_4(1) \rightarrow 2p_2(0)$, IS : 1.7 GHz; c) [illegible] Å, $1s_5(2) \rightarrow 2p_4(2)$, IS : 1.6 GHz; d) 5881.9 Å, $1s_5(2) \rightarrow 2p_2(1)$, IS : 1.7 GHz.

M. INGUSCIO : J. Phys. 7, 44, 217 (1983)

$\lambda = 541.5$ nm

^{235}U

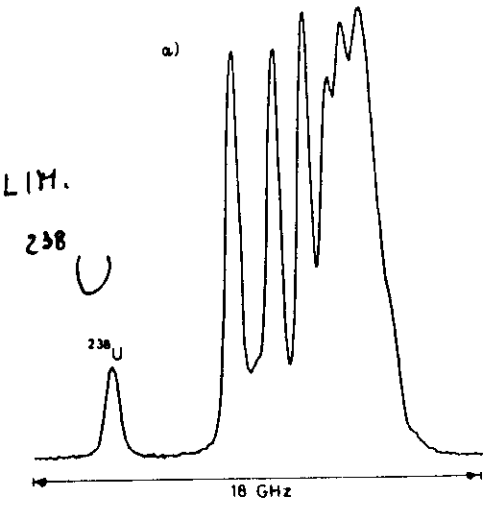

DOPPLER - LIM.

^{238}U

1 MHz

hyperfine structure resolved !

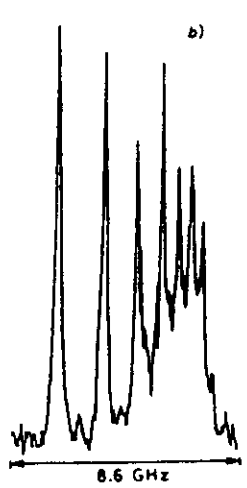

Nuovo Cim. D 4, 17, 1984

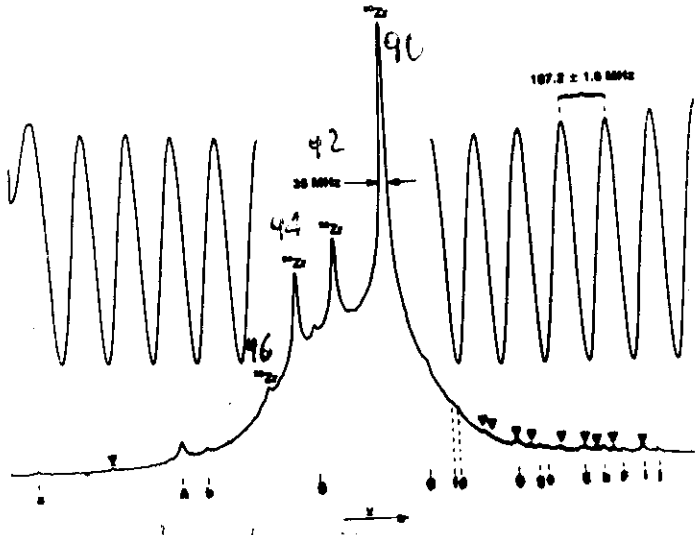

$$W_{JF} = W_J + \frac{C}{2} A_J + B_J \frac{3C(C+1) - 4(J+1)I(J+1)J}{2I(2I-1)J(2J-1)}$$

$C = F(F+1) - J(J+1) + I(I+1)$

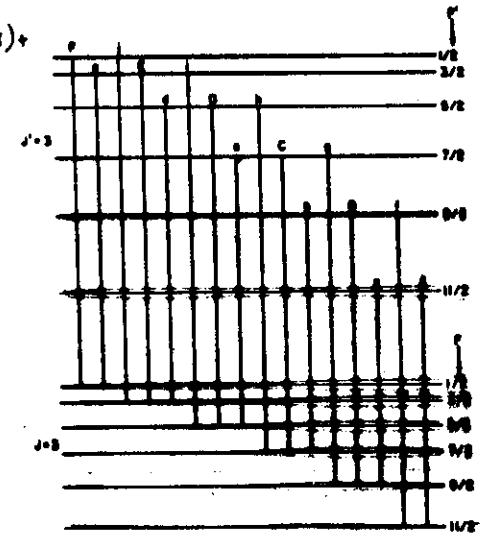

OPTICAL-OPTICAL DOUBLE RESONANCE

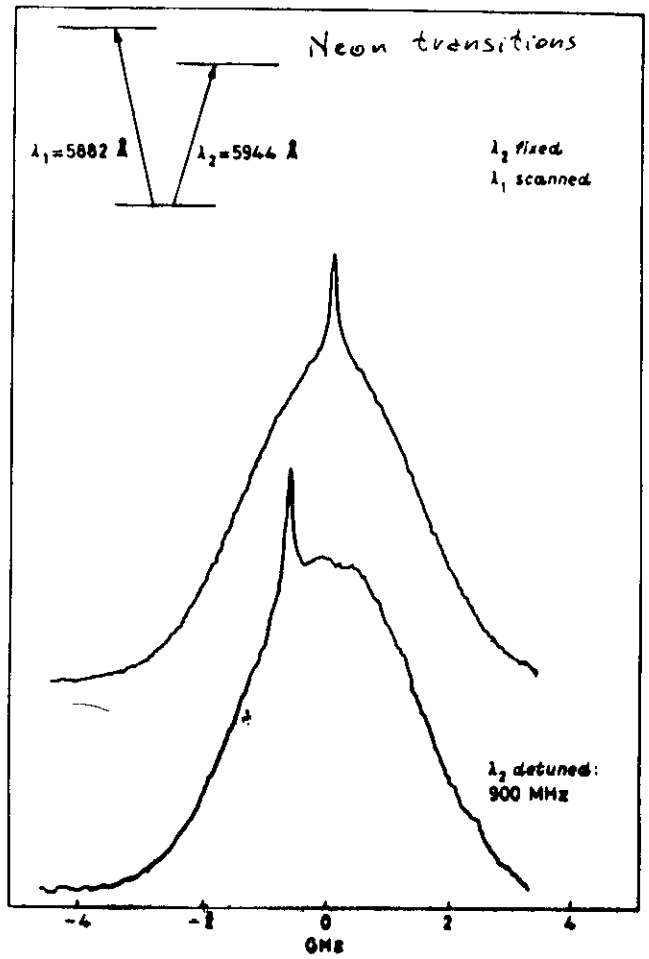

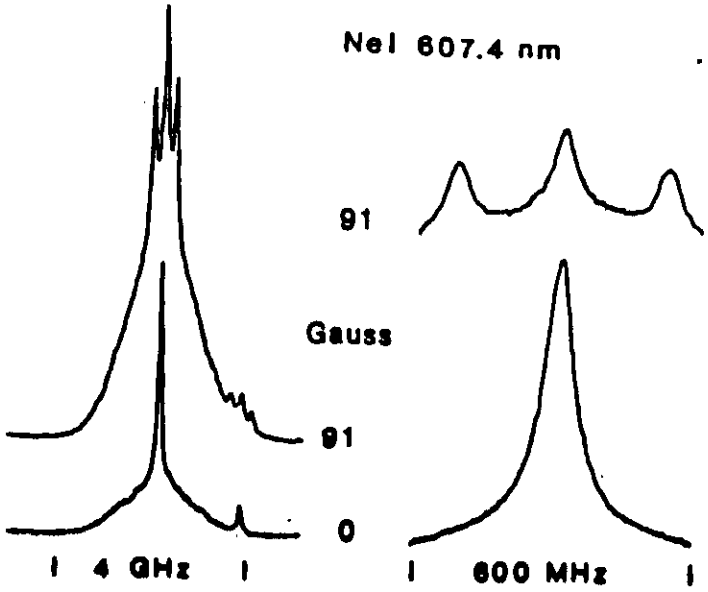

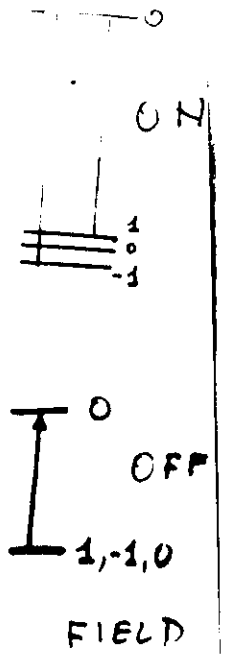

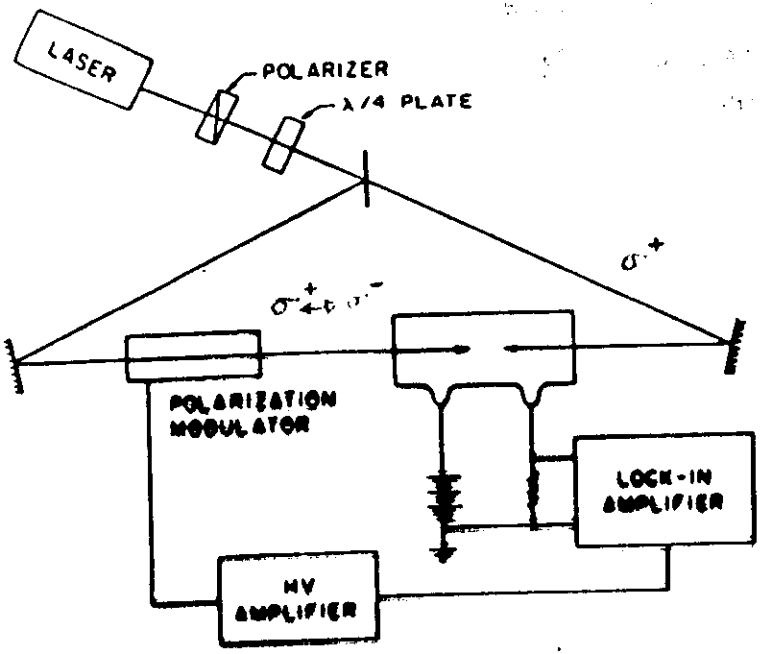

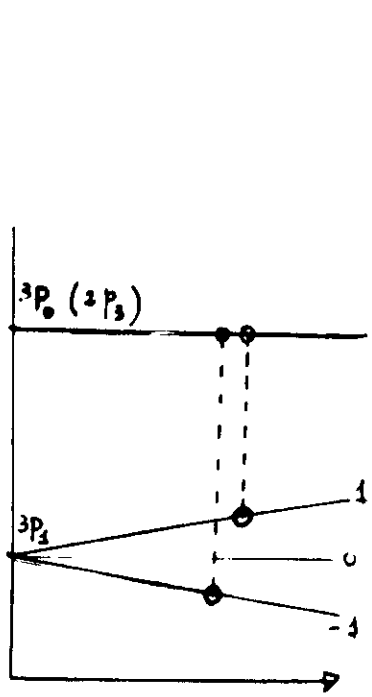

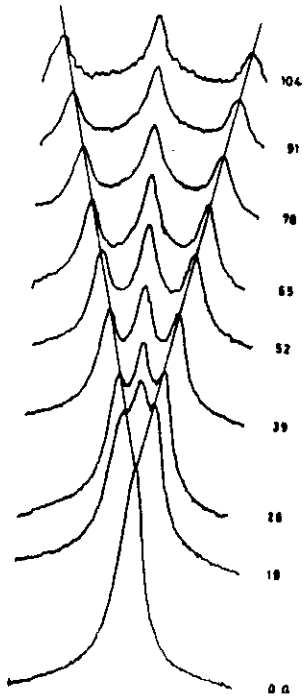

$\Delta\omega = g\,\mu_0 B$

Magnetic field B

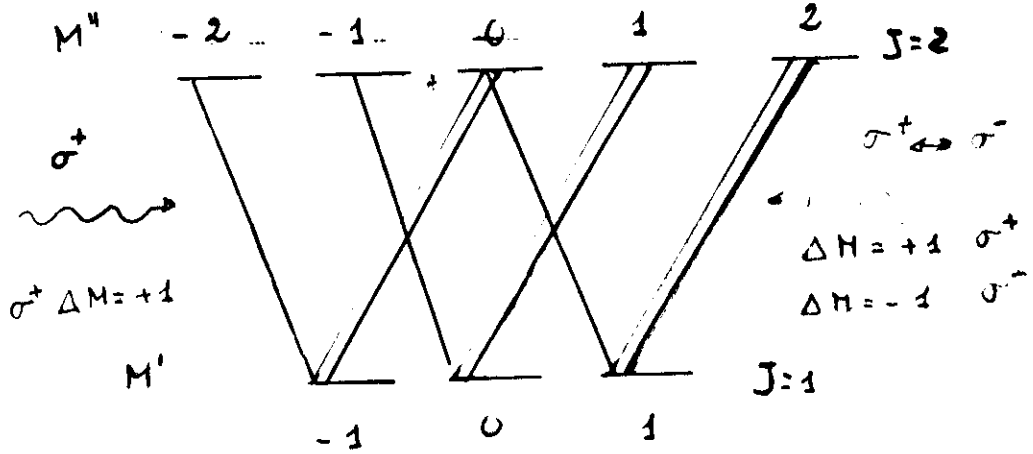

TWO-PHOTON DOPPLER-FREE SPECTROSCOPY

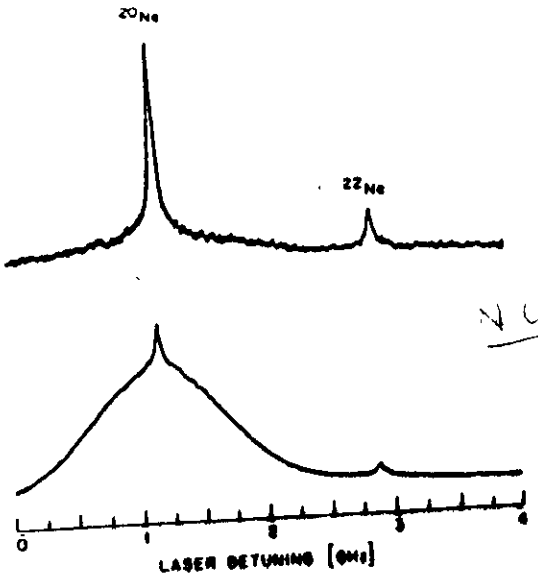

Ne

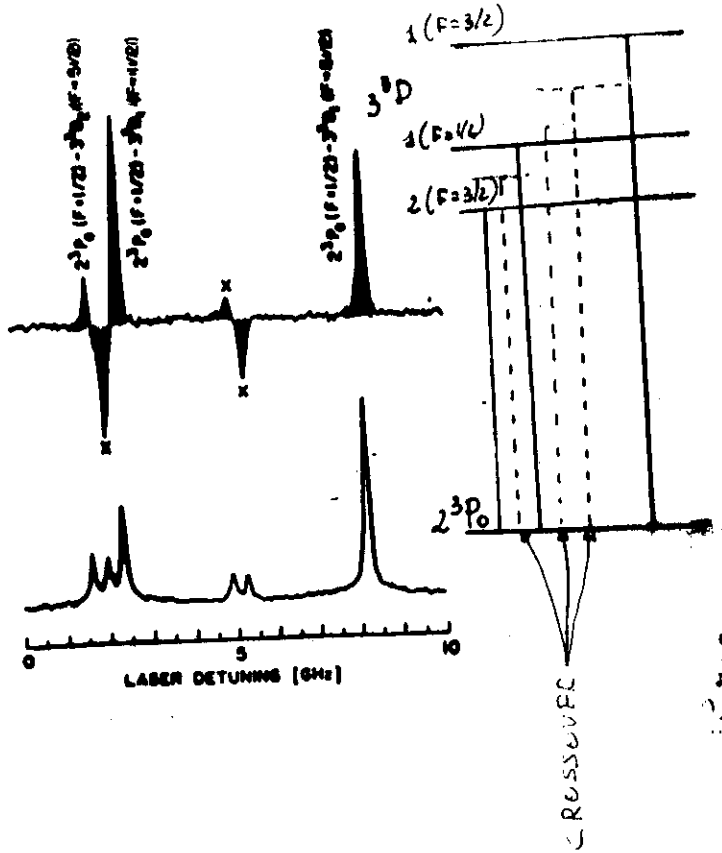

He

PULSED

CROSSOVER

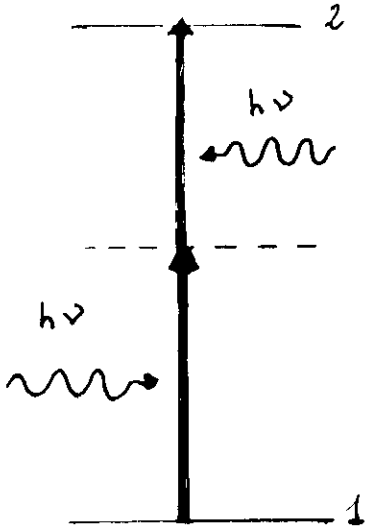

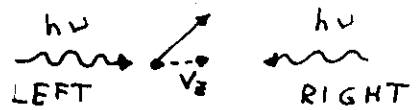

$$\nu_{LEFT} = \nu\left(1 - \frac{V_z}{c}\right)$$

$$\nu_{RIGHT} = \nu\left(1 + \frac{V_z}{c}\right)$$

$$E_2 - E_1 = h\nu_{LEFT} + h\nu_{RIGHT}$$

$$= h\nu\left(1 - \frac{V_z}{c}\right) + h\nu\left(1 + \frac{V_z}{c}\right)$$

$$= 2h\nu$$

^{20}Ne

$3s\,[3/2]\,J=2 - 4d\,[5/2]\,J=2$ $\quad$ $3s\,[3/2]\,J=2 - 4d\,[5/2]\,J=3$

LASER FREQUENCY MODULATION 5KHz : DERIVATIVE RECORDINGS

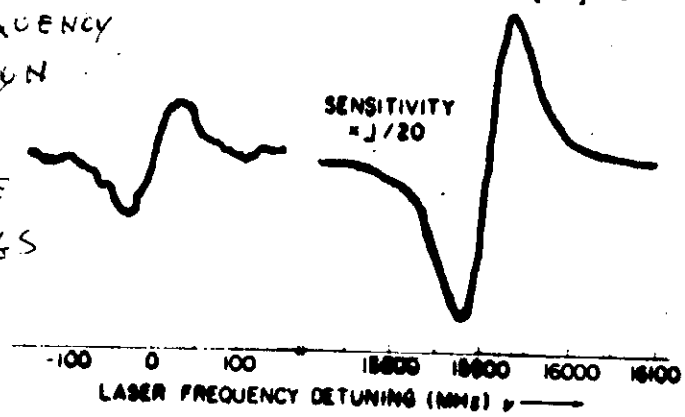

Fig. 2. Experimental traces of the ^{20}Ne transitions used in measuring the $4d[5/2]\,J = 2$–$4d[5/2]\,J = 3$ fine-structure interval.

CO · Lamb-dip Do stabilization

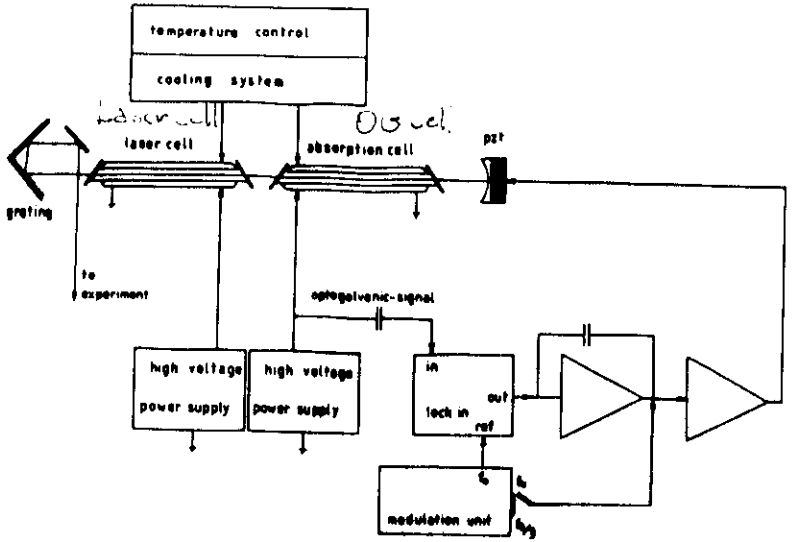

Fig. 1. The laser system. The gain cell is operated at pressures of about 12 Torr. The working pressure in the Lamb dip cell is 1.3 Torr

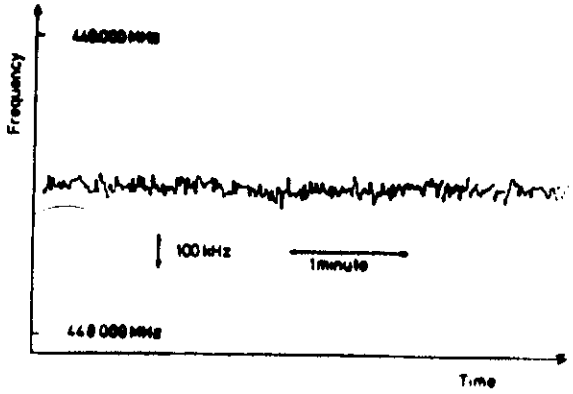

Frequency stability = 100 KHz

M. Schnaiter et al. Appl. Phys. B 44, 241 (1987)

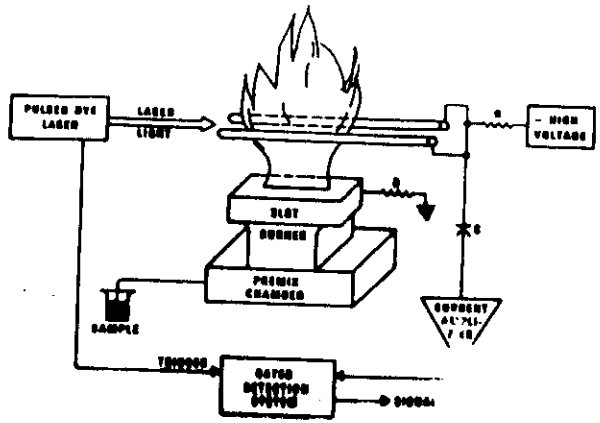

FIG. 1. Schematic diagram of the apparatus.

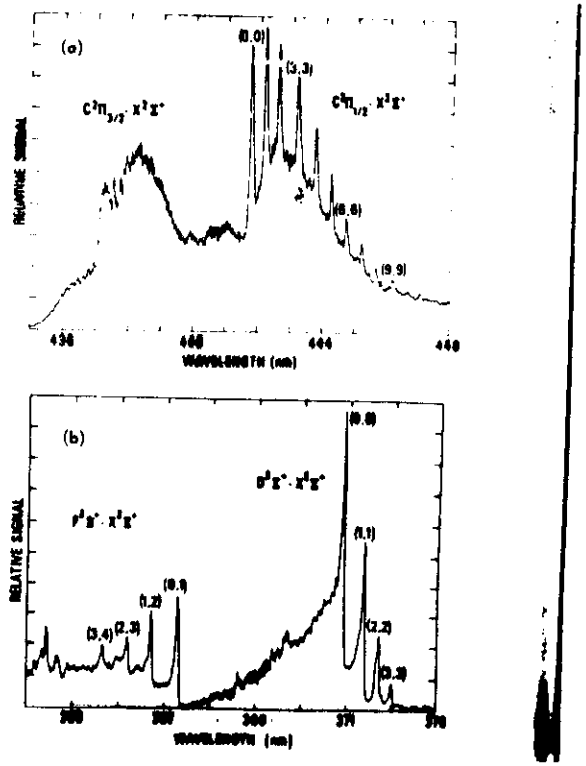

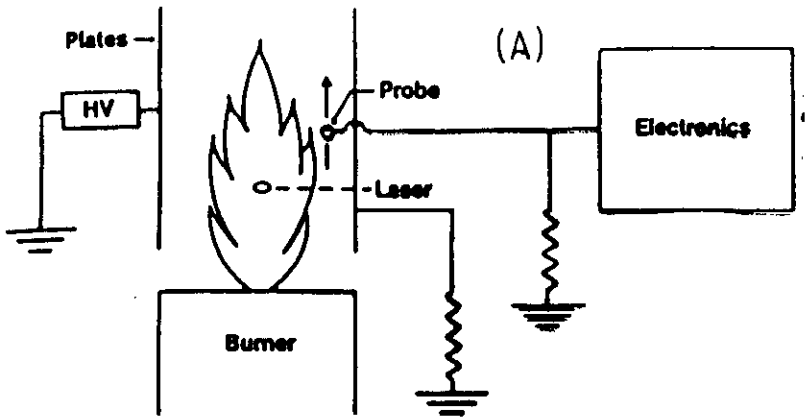

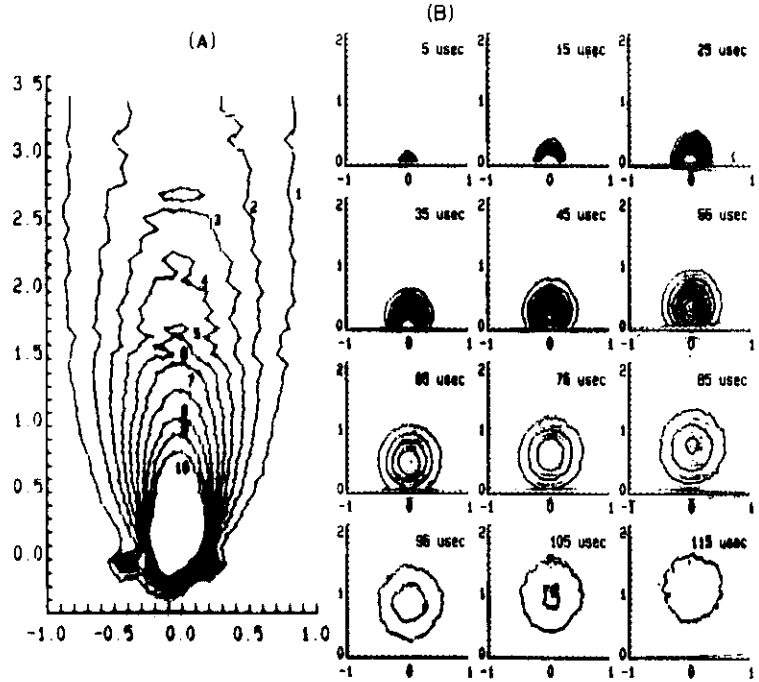

Figure 2. Neutral atom depletion contours (1 percent through 10 percent) for Na in a C_2H_2/air burner. (A) 200 mW laser chopped at 2 kHz (steady state) and (B) time resolved contours following 20 μsec laser pulse.